CHARLES UNIVERSITY IN PRAGUE

2ND FACULTY OF MEDICINE

BIOCHEMISTRY AND PATOBIOCHEMISTRY

MGR. KRISTÝNA BOUŠOVÁ

LOCALIZATION AND CHARACTERIZATION OF BINDING SITES FOR CA^{2+} BINDING PROTEINS AND PHOSPHATIDYLINOSITOL PHOSPHATES ON INTRACELLULAR TERMINI OF TRP CHANNELS

DISSERTATION

SUPERVISOR: ING. JAN TEISINGER CSC.

PRAGUE 2016

UNIVERZITA KARLOVA V PRAZE

2. LÉKAŘSKÁ FAKULTA

BIOCHEMIE A PATOBIOCHEMIE

MGR. KRISTÝNA BOUŠOVÁ

LOKALIZACE A CHARAKTERIZACE VAZEBNÝCH MÍST PRO Ca^{2+} VÁZAJÍCÍ PROTEINY A FOSFATIDYLINOSITOL FOSFÁTY NA INTRACELULÁRNÍCH KONCÍCH TRP KANÁLŮ

DISERTAČNÍ PRÁCE

ŠKOLITEL: ING. JAN TEISINGER CSC.

PRAHA 2016

PROHLÁŠENÍ

Prohlašuji, že jsem závěrečnou práci zpracovala samostatně a že jsem řádně uvedla a citovala všechny použité prameny a literaturu. Současně prohlašuji, že práce nebyla využita k získání jiného nebo stejného titulu

Souhlasím s trvalým uložením elektronické verze mé práce v databázi systému meziuniverzitního projektu Theses.cz za účelem soustavné kontroly podobnosti kvalifikačních prací.

V Praze, 3.6.2016

Kristýna Boušová

IDENTIFIKAČNÍ ZÁZNAM

BOUŠOVÁ, Kristýna. Lokalizace a charakterizace vazebných míst pro Ca^{2+} vázající proteiny a fosfatidylinositol fosfáty na intracelulárních koncích TRP kanálů. Praha, 2016. Počet stran 93, 4 přílohy. Disertační práce (Ph.D.) Univerzita Karlova v Praze, 2. lékařská fakulta.Vedoucí práce Teisinger, Jan.

PODĚKOVÁNÍ

Chtěla bych velmi poděkovat školiteli Ing. Janu Teisingerovi, CSc. za motivaci, vstřícnost, morální podporu a cenné rady během celého mého postgraduálního studia.

Mé poděkování též patří kolegům z Fyziologického Ústavu Akademie Věd České Republiky a z Ústavu Organické Chemie a Biochemie, a to především RNDr. Jiřímu Vondráškovi, Ph.D., díky kterým mohla být tato disertační práce dokončena.

V neposlední řadě děkuji své rodině která mě během studií všestranně podporovala.

ABBREVIATIONS

ARD	ankyrin repeat domain
CaM	calmodulin
CD	circular dichroism
DAG	diacylglycerol
NOMP-C	no mechanoreceptor potential C
IP3	inositol-1,4,5 trisphosphate
PC	phosphatidylcholine
PH	pleckstrin homology domain
PIPs	phosphatidylinositol phosphates
PIP2	phosphatidylinositol 4,5- biphosphate
PIP3	phosphatidylinositol 3,4,5- triphosphate
PI3K	phosphoinositide-3 kinase
PKA	proteinkinase A
PKC	proteinkinase C
PLC	phospholipase C
PX	phox-homology domain
RyR1	rhyanodine receptor
SPR	surface plasmon resonance
S100	S100 proteins
S100A1	S100 calcium-binding protein A1
TRP channels	transient receptor potential channels

CONTENTS

1. INTRODUCTION

1.1. TRANSIENT RECEPTOR POTENTIAL CHANNELS (TRPS)

TRPs are polymodal signal detectors which are important for a wide range of physical and chemical stimuli (Pedersen, Owsianik et al. 2005). They belong to the latest discovered membrane ion receptors - the first transient receptor potential gene was subcloned in 1989 (Montell and Rubin 1989). Then it was followed by molecular identification and functional characterization of all the TRPs members. Nowadays we are probably just at the beginning to get a deeper understanding of the molecular structure, the biophysical properties, the functional role, and the pathophysiological impact of this ion superfamily.

TRPs as a special nociceptive membrane receptors are responsible for the entry of monovalent (K^+, Na^+, Li^+) and divalent (Ca^{2+}, Mg^{2+}, Zn^{2+}) cations into the cell (Gordon-Shaag, Zagotta et al. 2008). They are represented by almost thirty-member family and their variety is demonstrated by dozen of proposed functions: transmission of painful stimuli, modulation of vascular tone, supply of intracellular calcium stores, modulation of cell cycle, calcium oscillations after T cell activation, mechanotransduction, thermosensation, regulation of cell adhesion, etc. (Cortright and Szallasi 2009, Vennekens, Menigoz et al. 2012, Julius 2013, Carlström, Wilcox et al. 2015, Smani, Shapovalov et al. 2015).

1.1.1. TRPS MEMBERS

The mammalian TRP channel superfamily encompasses 28 members subdivided into 7 families based on their protein homology: TRPC (canonical) subfamily, closest homolog of *Drosophila* trp channels; TRPV (vanilloid) subfamily are named after a founding member vanilloid receptor 1 (now TRPV1); TRPM (melastatin) subfamily groups homologs of melastatin-1 (now TRPM1); TRPA (ankyrin) subfamily; TRPPs and TRPMLs include mucolipins and polycystins, respectively; and finally TRPN subfamily named after the 'NO-mechano-potential C' (NOMP-C) channel of *Caenorhabditis elegans* (Voets and Nilius 2003) (Fig.1). In addition, TRP family is also represented in fungi by a single member, *TrpY1* (TRP yeast vacuolar conductance 1), which encodes a vacuolar membrane protein acting as a mechano-sensor of vacuolar osmotic pressure in yeast. The overall protein sequence identity between subfamily members in the same species is usually about 35%, but for duplication pairs (TRPC6 and TRPC7, TRPM4 and TRPM5, or TRPV5 and TRPV6) can reach up to 50 % (Nilius and Owsianik 2011). Intracellular C-terminus and N-terminus regulate channel assembly and function. Number of typical domains like ankyrin repeats, coiled-coil

regions, a TRP signature motif (TRP domain) and others differentiate TRP subfamilies (Voets and Nilius 2003).

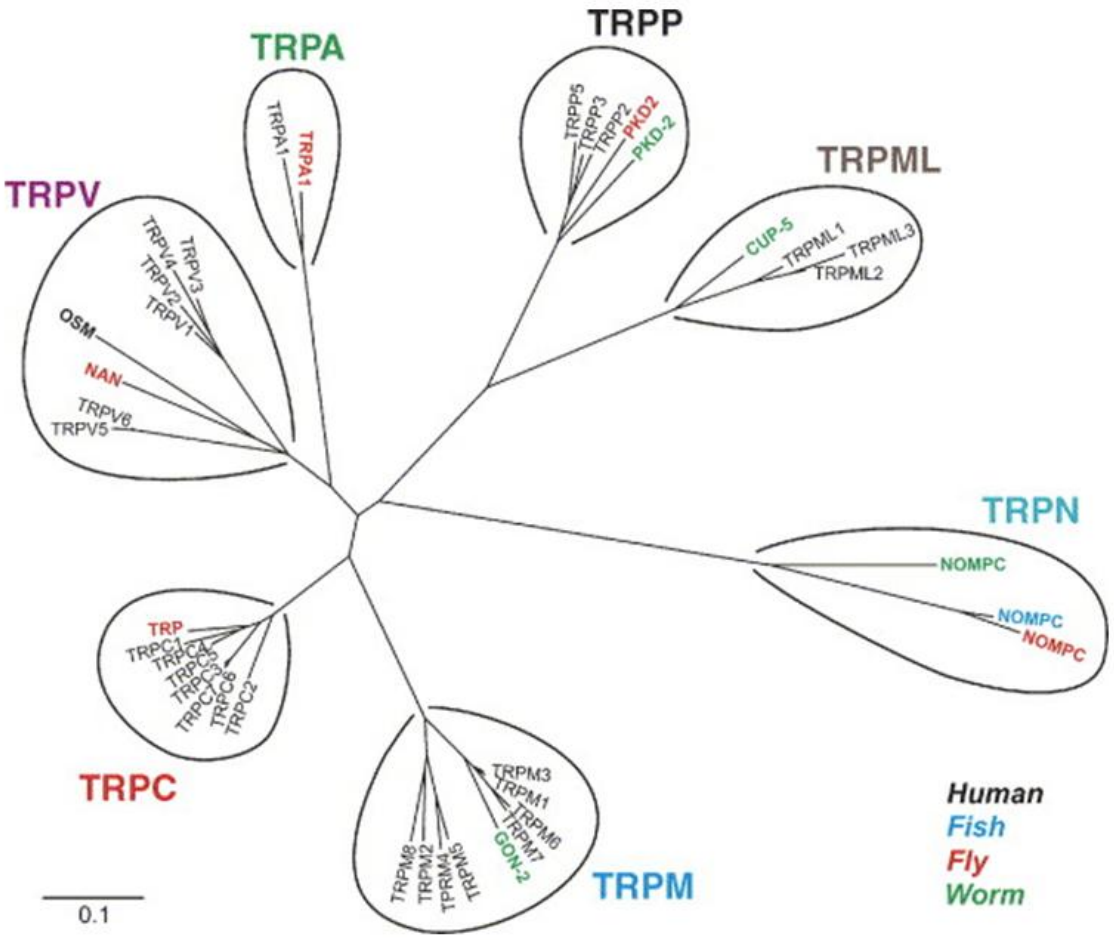

FIGURE 1 Phylogenetic tree of TRPs based on their homology (Pedersen, Owsianik et al. 2005).

1.1.1.1. TRPC

TRPC subfamily was established following the identification and cloning of TRPC1, the first recognized mammalian TRP channel (Prawitt, Enklaar et al. 2000). TRPC channels constitute a group of non-selective cation permeable channels that are activated downstream of Gq/11-coupled receptors, receptor tyrosine kinases or receptor-coupled PIP2 hydrolysis (Plant and Schaefer 2003, Trebak, Lemonnier et al. 2007, Raghu and Hardie 2009). The mammalian members of the TRPC family can by divided into 4 groups on the basis of functional similarities and sequence alignment: TRPC1, TRPC2, TRPC3/6/7, and TRPC4/5. TRPC channels have frequently been proposed to act as store-operated channels activated by depletion of intracellular calcium stores (Ambudkar and Ong 2007) and they are not mechanically gated in physiologically relevant ranges of force.

1.1.1.2. TRPV

Similar to the TRPC family, the TRPV family can be divided into four subfamilies on the basis of structure and function, namely TRPV1/TRPV2, TRPV3, TRPV4, and TRPV5/6 (Nilius, Vennekens et al. 2008). TRPV5 and 6 are the only highly Ca^{2+}-selective channels in the TRP channel family (Nilius, Vennekens et al. 2000, Vennekens, Hoenderop et al. 2000), whereas TRPV1–4 are non-selective cation channels that are activated by temperature and by numerous other stimuli. All channels of the TRPV family contain 3–6 NH_2-terminal ankyrin repeats (Gaudet 2008).

1.1.1.3. TRPM

The genetically and functionally diverse TRPM subfamily is comprised of eight putative members divided into three main groups: TRPM1/3, TRPM4/5, and TRPM6/7; TRPM2 and TRPM8 exhibit low sequence homology and therefore do not seem to warrant grouping. TRPM1 has been suggested that it functions as a tumor suppressor protein in melanocytes, TRPM3 as a hypo-osmolarity and sphingosine-activated channel. TRPM4 and TRPM5 have been described as calcium-activated non-selective cation channels, TRPM6 and TRPM7 as magnesium-permeable and magnesium-modulated cation channels. TRPM2 acts as an ADP-ribose-activated channel of macrophages, and TRPM8 acts as a cold receptor. TRPM2, TRPM6, and TRPM7 are also unique TRPs known for as encoding enzymatically active protein domains fused to their ion channel structures (Kraft and Harteneck 2005, Jiang 2007).

1.1.2. TRPs STRUCTURE

The structure of TRPs was predicted as tetrameric assemblies of six putative transmembrane (TM) domains organized around a central aqueous pore. They can be divided in two building blocks: the sensor, formed by helices S1–S4, and the pore, formed by helices S5 and S6 (Owsianik, Talavera et al. 2006, Li, Yu et al. 2011). TRPs mainly differ in their cytosolic N- and C-terminal domains, which are involved in channel gating and mediating intracellular signalling. Some of TRPs contain specific conserved unique sequences, e.g. TRPC, TRPV and TRPM include proximal C-terminus short hydrophobic stretch so-called TRP domain (Montell 2011) (Fig. 2). This highly specific region contains residues which were demonstrated to be required for binding of small modulatory molecules (e.g. PIPs, Ca^{2+} binding proteins) influencing a channel gating, or it could, under some conditions, serve as a coiled-coil zipper that holds the channel in a closed conformation (Rohács, Lopes et al. 2005). Another well-known sequence present in TRPC, TRPV, TRPN and TRPA members include N-terminal ankyrin repeats, a two-alpha-helices domain mediating protein-protein interactions (Jung, Lee et al. 2002, Mosavi, Minor et al. 2002, Erler, Hirnet et al. 2004). The TRPM2, TRPM6 and TRPM7 proteins have a large extension of the C-terminal

intracellular region beyond the TRP domain encoding an enzymatic catalytic region (Riazanova, Pavur et al. 2000, Perraud, Fleig et al. 2001, Runnels, Yue et al. 2001).

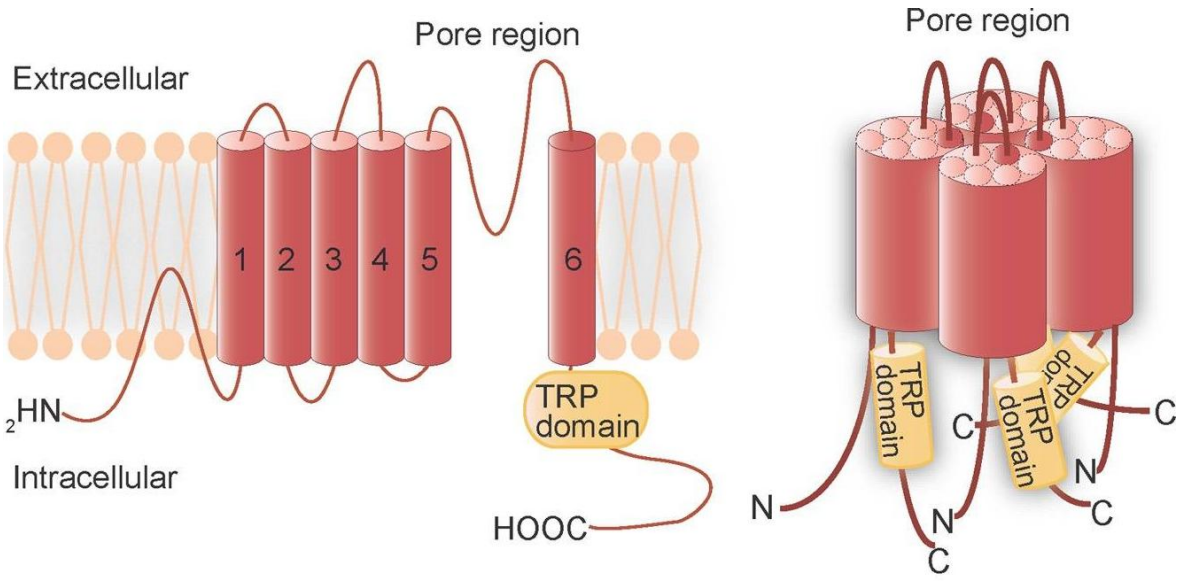

FIGURE 2 Schematic representation of TRPs assembly. (A) Transmembrane topology and the (B) quartenary structure of TRPs. The TRP protein has six putative TM domains, a pore region between the fifth and sixth transmembrane domains, N-terminal and C-terminal (TRP domain) intracellular tails. The TRP protein assembles into homo-tetramers or hetero-tetramers to form ion channels. The pore loop is formed by fifth and sixth TM domain of each monomer unit (Takahashi, Kozai et al. 2013).

The structure of TRPs was unknown for a long time. Whereas that obtaining crystals for membrane proteins, particularly of mammalian origin, is generally challenging, perhaps especially so for TRP channels, which respond to diverse stimuli (chemical and physical) and are therefore believed to be conformationally dynamic. Despite numerous crystallization attempts, the structures of several examples have been determined only by cryo-electron microscopy (CryoEM) measurements at ~ 4Å resolutions in the past few years. These include the transmembrane part of TRPV1 (Liao, Cao et al. 2013), the whole TRPA1 (Paulsen, Armache et al. 2015) and TRPV2 (Zubcevic, Herzik Jr et al. 2016).

Recent CryoEM studies revealed several similarities between TRPV1 and TRPA1 probably representing common TRPs features (Fig.3). Both channels assemble as homotetramers that exhibit domain swapping within the transmembrane core, and possess an ion permeation pathway. Additional modes of intersubunit interactions are facilitated by discrete substructures within the cytoplasmic domain, although the exact nature of these contacts is protein-specific (for example, β-strand–ARD interactions, coiled-coil –TRP domain, etc.). These cytoplasmic intersubunit interactions may regulate channel assembly and/or facilitate concerted conformational changes after co-

factor binding or agonist-evoked gating. Additionally, α-helix subsequent to S6 (TRP domain) probably operates as a conserved allosteric regulatory structure that engages in extensive interactions with pore-forming domains (Liao, Cao et al. 2013, Huynh, Cohen et al. 2014, Paulsen, Armache et al. 2015). The last published CryoEM study about TRPV2 joined this channel to the general dogma about TRPs, because confirmed the predicted transmembrane topology with quartenary assembly (Zubcevic, Herzik Jr et al. 2016).

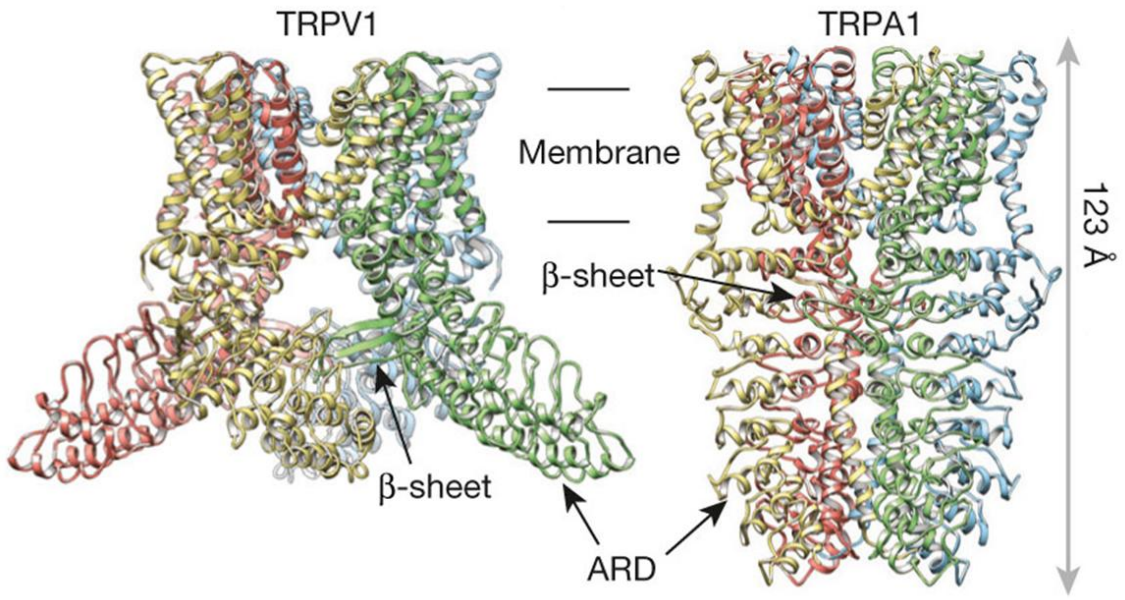

FIGURE 3 Structural information in ribbon diagrams of TRPV1 in comparison with TRPA1 atomic models obtained by CryoEM. Both channels are composed of S1–S6 helices (membrane part) and intracellular N- and C- termini containing beta-sheets and ankyrin repeats (ARD). Diagrams are shown in (A) side and view with 123 A° dimension (Paulsen, Armache et al. 2015).

1.1.3. TRPs ACTIVATION

The sensitivity of TRP channels to polymodal activation suggests that the physiologically relevant stimulus for any given TRP will be managed by the specifics of cellular context (phosphorylation, lipid environment, interacting proteins, and concentrations of relevant ligands). Moreover, cooperativity intrinsic to TRP channels may result in allosteric coupling of different activation stimuli, blurring the definition of activator versus modulator. The activation of TRP channels may be divided into three classes (Ramsey, Delling et al. 2006):

- *Receptor activation*: G protein–coupled receptors and receptor tyrosine kinases that activate phospholipases C (PLCs) can modulate TRP channel activity with subsequent release of Ca^{2+} from intracellular stores in at least three ways: (a)

hydrolysis of phosphatidylinositol-4,5 bisphosphate (PIP2), (b) production of diacylglycerol (DAG), or (c) production of inositol (1,4,5) trisphosphate (IP3).

- *Ligand activation*: Ligands activating TRPs can be exogenous small organic molecules, including synthetic compounds and natural products (capsaicin, icilin, 2-APB); endogenous lipids or products of lipid metabolism (diacylglycerols, phosphoinositides, eicosanoids, anandamide); purine nucleotides and their metabolites; or inorganic ions (mainly Ca^{2+} and Mg^{2+}).
- *Direct activation*: Ligands activating TRPs can be also intracellular ligands (i.e. Ca^{2+}, calcium binding proteins like calmodulin or S100A1, etc); or channels can be also activated through changes in ambient temperature which are strongly coupled to the opening of some TRP members, but the mechanisms is still poorly understood. Other putative direct activators include mechanical stimuli, conformational coupling to IP3 receptors, and channel phosphorylation. Heating and cell swelling may also act indirectly to activate TRPs through second messengers or other unidentified mechanisms.

1.1.4. TRPs AND HUMAN DISEASES

The discovery of TRPs has revolutionized our understanding of many sensory and general physiological processes. TRPs generally act in concert with other ion channels and proteins. Given that, in many cases, these mechanisms are evolutionarily conserved from invertebrates to humans. It is not surprising that inherited impairments of TRPs functions lead to disease. Several TRP genes has been found to participate in a wide range of human diseases (Hsu, Hoenderop et al. 2007, Nilius 2007, Kang, Shin et al. 2012, Takada, Numata et al. 2013, Entin-Meer, Levy et al. 2014). These fall under group of the 'channelopathies' defined as diseases caused by disorder channel functions, resulting from either mutations in the encoding gene or an acquired mechanism, such as autoimmunity (Nilius and Owsianik 2011). Supportive example of disorder channel functions showed us that mutations in the TRPM4 gene have been associated with cardiac conduction disorders (Kruse, Schulze-Bahr et al. 2009),

The important role of some TRPs members in cancer was also described. Expression of TRPM8 is associated with androgen-dependent prostate cancer cells (Tsavaler, Shapero et al. 2001), regulation of cell proliferation and apoptosis (Prevarskaya, Skryma et al. 2007). Expression of TRPV6 is increased in prostate cancer (Fixemer, Wissenbach et al. 2003), TRPM1 is highly expressed in early stage melanomas but its expression declines with increases in the degree of aggressiveness of the melanoma (Duncan, Deeds et al. 1998). TRPV1 is expressed in neurones involved in sensing cancer pain, and is a potential target for pharmacological inhibition of cancer pain in bone metastases, pancreatic cancer and most likely in other cancers (Dömötör, Peidl et al. 2005, Hartel, Di Mola et al. 2006).

Many TRPs members have been implicated in human diseases, however in no case the functional link between channel activity and the disease process is clearly known. Undoubtedly, the modulation of TRPs is strictly interrelated system which could have relevant applications in important therapeutic areas of inflammation, pain, cancer, etc. Nevertheless, the clinical translation of the 20-year research activity on the most examined channel TRPV1 is still in its infancy (Morelli, Amantini et al. 2013).

1.2. Intracellular modulatory molecules of TRPs

1.2.1. Calcium binding proteins

Calcium-binding proteins participate in calcium cell signalling pathways, contribute to the control of calcium concentration in the cytosol and participate in numerous cellular functions by acting as calcium transporters across cell membranes or as calcium-modulated sensors (Kretsinger 1976). The role of calcium as a key and pivotal second messenger in cells depends largely on a wide number of heterogeneous so-called calcium binding proteins, which have the ability to bind this ion in specific binding motif (Goodman, Pechére et al. 1979). This motif called EF-hand is composed of two alpha helices (E and F) connected by a Ca^{2+}-binding loop. EF-hands have been identified in numerous calcium-binding proteins by similarity of amino acid sequence and confirmed in some crystal structures (Senguen and Grabarek 2012, Dunlap, Guo et al. 2014, Lin, van den Bedem et al. 2016). Functional EF-hands seem always to occur in pairs. To date, the EF-hand homologous family contains more than 160 different calcium-modulated proteins which have a broad range of functions. Among them there are the calmodulin (Chin and Means 2000), the S-100 proteins (Marenholz, Heizmann et al. 2004), troponin C (Li and Hwang 2015), myosin regulatory light chain (Kitazawa, Gaylinn et al. 1991), parvalbumin (Cates, Berry et al. 1999), and calbindins (Kojetin, Venters et al. 2006).

1.2.1.1. Calmodulin (CaM)

CaM is a ubiquitous, highly conserved 17 kDa Ca^{2+} binding protein (148 amino acids) functional as a monomer. It comprises of two globular domains connected by eight-turn α-helix flexible linker that allows CaM to adopt different conformations (Barbato, Ikura et al. 1992). In crystal structure, the N-terminal domain forms two EF-hand motifs (I and II) as does the C-terminal domain (III and IV) (Saimi and Kung 2002). Isolated CaM binds Ca^{2+} at the physiological concentration range ($Kd = 5 \times 10^{-7}$ to 5×10^{-6} M), but its Ca^{2+} affinity is much higher when complexed with other protein (Jurado, Chockalingam et al. 1999). CaM becomes more extended with each pair of EF-hands upon Ca^{2+} binding exposing a hydrophobic patch that is available to interact with a target protein (Wriggers, Mehler et al. 1998). The X-ray and NMR studies revealed that

the both CaM domains bind the target protein by combination of hydrophobic and by van der Waals interactions, with the glutamate residues in the Ca^{2+} coordinating loop in each of the EF hands (Ikura, Clore et al. 1992, Meador, Means et al. 1992). Similarly, the known primary sequence of binding sites of target proteins are often amphipatic α-helices with a hydrophobic side and a highly positively charged side (Fig.4) (Rhoads and Friedberg 1997, Yap, Kim et al. 2000). Most of the CaM interacting proteins have recognizable CaM-binding motifs (hydrophobic amino acids in positions: 1-5-10 and 1-8-14) (Yap, Kim et al. 2000), but these features do not strictly dictate specific binding to CaM. As much as half of CaM is associated with membranes, the rest remains soluble in the cytoplasm and inside the nucleus (Santella and Carafoli 1997, Toutenhoofd and Strehler 2000).

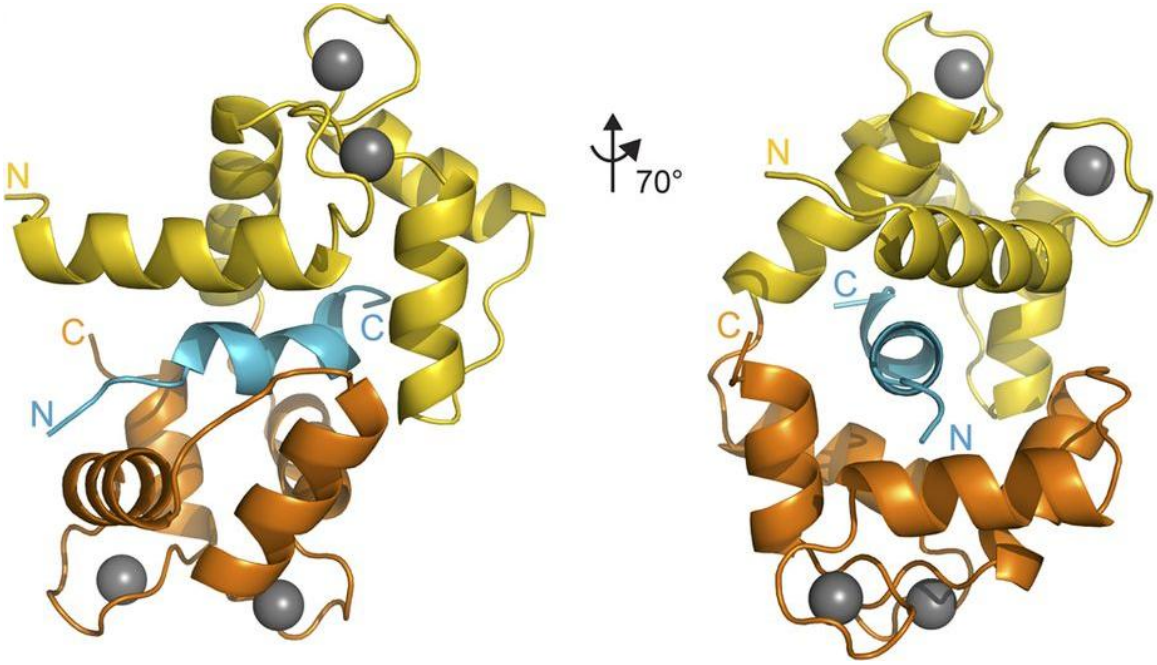

FIGURE 4 Structure of a basic amphipathic α-helix in complex with Ca^{2+}–CaM. Ribbon diagrams of amphipathic α-helix (cyan; example of TRPV1-CT binding domain in this case) bound to Ca^{2+}–CaM, shown in two different orientations; the view on the right is rotated 70° around the vertical axis with respect to the one on the left. The CaM N-lobes and C-lobes are yellow and orange, respectively, and the calcium ions are gray (Lau, Procko et al. 2012).

1.2.1.1.1. CaM modulation of TRPs

Nowadays, TRPs are a giant family of Ca^{2+}-permeable cation channels of diverse functions and distributions. Ca^{2+} play an important role for TRPs as intermediator of the interactions with CaM, which has been shown as its modulator. In most cases, the regulation is achieved through direct binding of CaM on the intracellular N- or C-termini. Multiple CaM binding sites were identified on different TRP proteins. There

are many differences among various CaM-binding sites in terms of affinities to CaM, as well as the precise conformations and the regions of CaM that are bound to these sites.

CaM bindig sites were identified for all three main subfamilies TRPC, TRPV and TRPM. The first connection between CaM and TRPC subfamily is dated in 1992 (Phillips, Bull et al. 1992), later was demonstrated that TRPL is regulated by calcium in a CaM-dependent manner (Chevesich, Kreuz et al. 1997). Some mammalian TRPC have also been shown to bind CaM. The protein–protein interaction of TRPC4 with CaM has been demonstrated in calmodulin-binding studies (Niemeyer, Bergs et al. 2001, TROST, BERGS et al. 2001). In functional studies the consequences of CaM binding to TRPC4 revealed inhibition affect on channel function, as well as for TRPC3 (Zhu 2005). In vaniloid superfamily is CaM involved in the desensitization of TRPV1 channels (Numazaki, Tominaga et al. 2003). In TRPV4 there were four described CaM binding site on N- and C- termini, respectively (Strotmann, Schultz et al. 2003). Multiple CaM-binding sites were also identified for TRPV6 (Niemeyer, Bergs et al. 2001, Lambert, Drews et al. 2011). A CaM binding site found in human TRPV6 has been shown to mediate Ca^{2+}-dependent channel inactivation. CaM binding at this site is competitively regulated by the phosphorylation of a threonine residue by protein kinase C. It was described that Ca^{2+} entering through TRPM2 enhances interaction of CaM with TRPM2 at the binding motif in the N terminus, providing decisive positive feedback for channel activation (Tong, Zhang et al. 2006). CaM binding site together shared with S100A1 and PIP2 binding sites was identified in the TRPM3 N-terminus (Holakovska, Grycova et al. 2012, Holendova, Grycova et al. 2012). Hereafter, studies with deletion mutants of TRPM4 suggest that the CaM bindig sites on C-terminus are important for the Ca^{2+}-induced activation. For instance, CaM is involved in inhibiting the kinase activity of TRPM7 (Ryazanova, Dorovkov et al. 2004). It appears that CaM exerts multiple regulatory roles on TRPs, this can activate and/or inhibit channel function via different mechanisms. One can anticipate that more CaM binding sites will be identified in different TRP proteins and the functional implications of these interactions will be very complex.

1.2.1.2. S100A1

S100 proteins are calcium binding proteins that use calcium influx to control a variety of cellular processes such as cell differentiation and survival, cell growth and mobility, regulation of cell cycle, modulation of enzyme activity, calcium homeostasis (Duarte-Costa, Castro-Ferreira et al. 2014). S100A1, the most abundant representative of this protein family, is formed into symmetric homodimer. The both monomer subunits are composed from four helices containing two EF-hand calcium-binding loops. (Ritterhoff and Most 2012). The solution structures of Apo- and calcium-S100A1 were determined by NMR (Rustandi, Baldisseri et al. 2002, Wright, Varney et al. 2005). Upon binding of Ca^{2+}, the 3rd helix of S100A1 undergoes a large reorientation and shifts from being

almost anti-parallel to being perpendicular to the 4th helix. This conformational change reveals a large hydrophobic cleft that interacts with target proteins (Tong, Zhang et al. 2006). Correspondingly, the known primary sequence of binding sites of target proteins (binding partners of S100A1) is usually interpreted as basic amphipathic α-helices with a hydrophobic sides and a highly positively charged sides (Fig.5) These specific domains conforming to primary sequence of its S100A1 binding sites are often amphipathic α-helices with a hydrophobic amino acids consensus of the CaM recognition motifs 1-5-10 or 1-8-14 (Zhu 2005). Additionally, it was confirmed that basic amino acid residues in CaM recognition receptor motif are also involved in the interactions with other calcium-binding proteins. There were also described some shared or overlapped calcium-binding proteins interaction sites (Zhu 2005, Prosser, Wright et al. 2008, Wright, Prosser et al. 2008, Rezvanpour and Shaw 2009, Friedlova, Grycova et al. 2010, Prosser, Hernández-Ochoa et al. 2011, Holakovska, Grycova et al. 2012, Holendova, Grycova et al. 2012, Bily, Grycova et al. 2013, Grycova, Holendova et al. 2014).

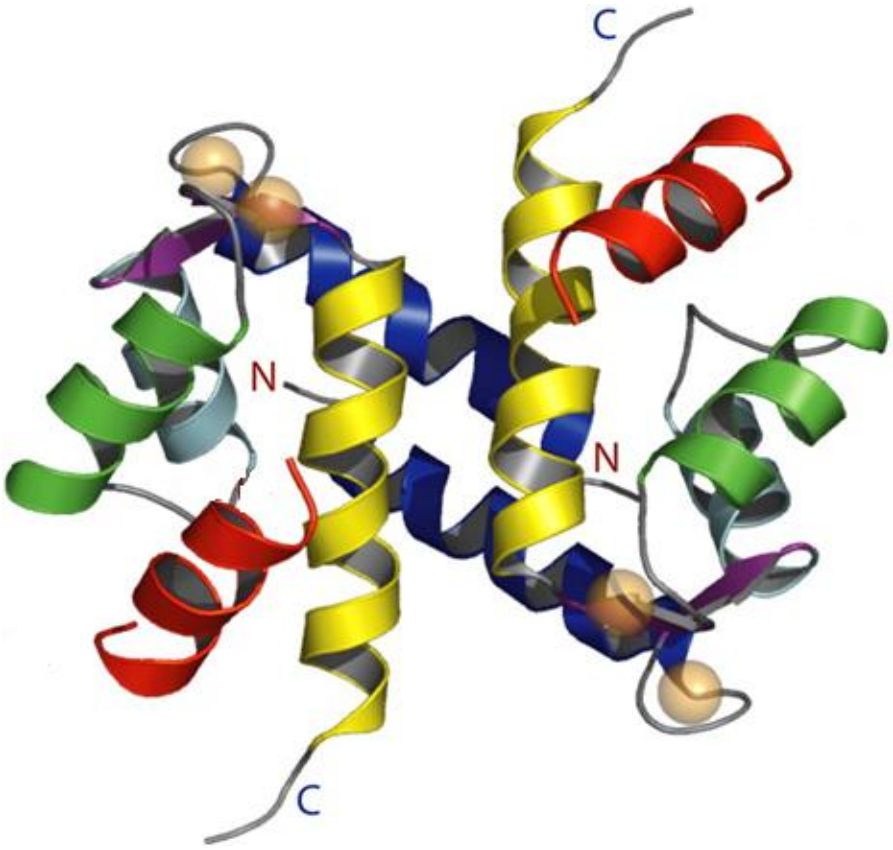

FIGURE 5 The three-dimensional structure of the basic amphipathic α-helix with S100A1 dimer. Ribbon diagram of amphipathic α-helix (red; example of Ca^{2+}-S100A1-RyRP12 complex in this case) bound to Ca^{2+}–S100A1 (other colores) shown in upper orientation, and the calcium ions are transparently orange (Wright, Prosser et al. 2008).

1.2.1.2.1. S100A1 MODULATION OF TRPS

Calcium ions were previously shown to participate in the regulation of TRP channels through interactions with calcium-binding proteins like CaM or S100A1 (Tong, Zhang et al. 2006, Kwon, Hofmann et al. 2007, Rohacs 2013). S100A1 binding site is mostly shared with CaM binding site and recognize the same interaction motif. These common calcium binding proteins domains were reported in the N- and C- termini tails of TRPM3 and TRPC6 (Friedlova, Grycova et al. 2010, Holakovska, Grycova et al. 2012, Bily, Grycova et al. 2013). The interaction of the vanilloid family TRP channels TRPV5 and TRPV6 with the S100A10/AnexinA2 complex, that mediates trafficking to the plasma membrane, was also reported (van de Graaf, Hoenderop et al. 2003, Rezvanpour and Shaw 2009). Given that S100A1 modulation of TRPs is still not well described and understood, the best known and described interaction mechanism of S100A1 is with ryanodine receptor (RyR), a calcium permeable channel present in sarcoplasma (Prosser, Wright et al. 2008). It was shown that S100A1 and CaM can compete for a binding site within the ryanodine receptor 1 where they function as activators (Prosser, Wright et al. 2008, Wright, Prosser et al. 2008, Prosser, Hernández-Ochoa et al. 2011).

1.2.2. PHOSPHATIDYLINOSITOL PHOSPHATES (PIPS)

PIPs are widely present in the inner leaflet of the cell and are frequently involved in membrane trafficking and signaling cell pathways. They are relatively variable in their structure and can exist in one of eight molecular species, via phosphorylation at the 3, 4 or 5 position of the inositol head-group. Polyphosphoinositides are enzymatically generated by a series of specifically phosphorylation or dephosphorylation reactions via phosphoinositide kinases and phosphatases (Bridges and Saltiel 2015). The most abundant representative PIP in signalling pathways - phosphatidylinositol-4, 5 bisphosphate (PIP2), was thought to be synthesized exclusively by phosphorylation of phosphatidylinositol-4 phosphate at the 5th position of the inositol ring. It is the substrate for phospholipase C (PLC), thus the precursor of the two classical second messengers inositol-1,4,5 trisphosphate (IP3) and diacylglycerol (DAG). It is also a substrate for phosphoinositide-3 kinase (PI3K) to generate phosphatidylinositol-3,4,5 trisphosphate (PIP3). In most cells, PIP3 is the lowest abundance PIPs, and is generated primarily by phosphorylation of PIP2 on 3rd position of the inositol ring by PI3K (Wymann and Schneiter 2008). PIP3 as well as its analogue PIP2 are membrane phospholipids that function in a number of crucial cellular processes, such as membrane trafficking, plasma membrane-cytoskeleton linkages, second messenger signalling, cell adhesion and motility and the regulation of proteins involved in phospholipids metabolism (Rohacs 2014, Hille, Dickson et al. 2015).

PIPs in many cases serves as a membrane anchor for cytoplasmic proteins which bind its via various lipid binding domains (Rosenhouse-Dantsker and Logothetis 2007). PIP2 regulates a wide variety of ion channels, including inwardly rectifying Kir and voltage gated K^+ and Ca^{2+} channels, epithelial Na^+ channels (Suh and Hille 2005, Suh

and Hille 2008) and as will be discussed here, TRP channels. Out of the many described phospholipid-binding proteins, a number of different domain structures have been defined that exhibit stereospecific recognition of specific phosphoinositide head groups in the context of cellular membrane surfaces. These include the pleckstrin homology (PH) and Phox-homology (PX) domains (Lemmon, Ferguson et al. 1995). The common hypothesis to explain the binding of PIP2 is that positively charged residues present in the binding domain of channel are responsible for the ligand-dependent modulation of the channel activity through their binding of PIP2 negatively charged phosphate groups (Suh and Hille 2005). The best explanation of the PIP2 interaction mode with channel has been elucidated using crystal structure of Kir2.2 channel with bounded PIP2 (Fig.6). This provided the first atomic resolution description of a molecular mechanism by which PIP2 regulates channel activity and how it induces large conformation changes in the protein (Hansen, Tao et al. 2011).

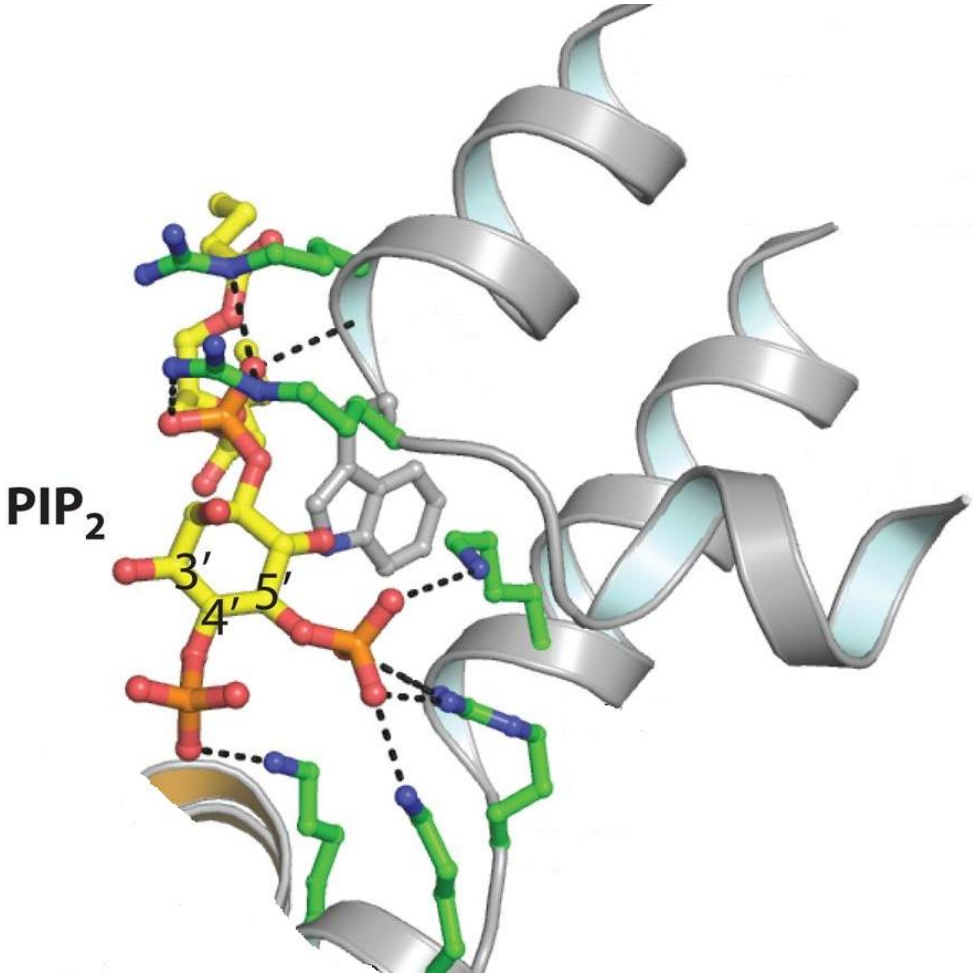

FIGURE 6 A detailed view of the PIP_2-binding site in Kir2.2 channel. Ball and sticks diagram of PIP2 (coloured according to atom type: carbon, yellow; phosphorous, orange; and oxygen, red) in the interaction with PH domain of Kir2.2 channel (grey). Basic amino acid residues involved in the PIP2 binding are colored green (nitrogen, blue). (Hansen, Tao et al. 2011)

1.2.2.1. PIPs MODULATION OF TRPs

The history of PIPs studies in the TRP field started in the late 1990s (Chyb, Raghu et al. 1999, Hwang, Cho et al. 2000) and knowledge has thus far expanded to cover various aspects such as ligand binding, bilayer-protein interactions, sensitivity shift, upstream metabotropic signaling. Nowadays, more than 50 endogenous lipids and lipid-like molecules have been identified as direct activators or inhibitors of TRPs and the most studied are PIPs (Nilius, Owsianik et al. 2008, Raghu and Hardie 2009, Rohacs 2014).

The picture of PIP2 regulation is probably best understood among the major TRP channel sub-families on TRPM channels (Steinberg, Lespay-Rebolledo et al. 2014). For almost all of the members have been identified PIP2 binding sites and for some of them was confirmed PIP2 positive or negative modulation of TRPM channels. Recently has been identified PIP2 binding site in N-terminal distal part of poorly examined TRPM1 (Jirku, Bumba et al. 2015). A shared binding domain for PIP2, CaM and S100A1 was found in the TRPM3 N-terminus and was confirmed that these ligands can compete to each other (Holakovska, Grycova et al. 2012, Holendova, Grycova et al. 2012). In the TRP domain of TRPM4 intracellular C-terminus another PIP2 binding site was described (Nilius, Mahieu et al. 2006). It was demonstrated that PIP2 enhances the activity of TRPM4 Ca^{2+} - activated cation channels by decreasing Ca^{2+} sensitivity, shifting their voltage dependence, and provided evidence that these effects require an intact C-terminal PH domain. Shared binding site for PIP2 and PIP3 in the proximal part of the first TRPM4 TM domain described recently confirmed two identical arginine residues involved in the interaction with both ligands (Bousova, Jirku et al. 2015). Further, PIP2 promotes the gating of TRPM5 channel, which, after desensitization, was activated by lower concentrations of Ca^{2+} (Liu and Liman 2003). The hydrolysis of PIP2 by phospholipase C -coupled hormones may represent an important pathway for TRPM6 gating (Xie, Sun et al. 2011). Negative reagulation caused by PIP2 has been reported for TRPM7, in which PIP_2 hydrolysis by PLCs inhibits channel activation (Runnels, Yue et al. 2002). The breakdown of PIP2 also appears to underlie the desensitization of TRPM8 (Yudin, Lukacs et al. 2011). Whereas the PIP2 is degraded by PLC, its action may also underly the response of some TRPs to the stimulation of PLC-coupled plasma membrane receptors (Runnels, Yue et al. 2002).

From other TRP subfamilies, it has been reported that TRPV1 is inhibited by PIP2 (Chuang, Prescott et al. 2001), and another PIP2 binding sites were revealed using biophysical methods on both N- and C- termini of the channel (Grycova, Holendova et al. 2012). TRPV5 on the other hand was reported to be activated by PIP2 (Lee, Cha et al. 2005). PIP2 inhibit the Drosophila TRPL, which is a homolog of the mammalian TRPC channels (Estacion, Sinkins et al. 2001). TRPC and their non-mammalian homologues are activated by G protein coupled receptors that activate PLC and hydrolyze PIP2. TRPC3, TRPC6 and TRPC7 were shown to be activated by DAG (Hofmann, Obukhov et al. 1999). It was also found that PIP3 binds TRPC6 directly with

the highest potency (Kwon, Hofmann et al. 2007). An effect of PIP2 on mammalian TRPCs was not yet published, but clearly, relief from PIP2 inhibition is an attractive hypothesis that is worth testing. It is also possible that DAG and relief from PIP2 inhibition together lead to full activation as proposed (Hardie and Minke 1992).

2. AIMS OF THE STUDY

TRP channels represent superfamily of important mediators which play critical roles in sensory physiology: contributions to taste, olfaction, vision, hearing, touch and thermo- and osmo- sensation. Many of these special ion transporters are activated by a variety of different stimuli and function as signal integrators. The variety of functions to which TRP channels contribute and the polymodal character of their activation predict that failures in correct channel gating or permeation will likely contribute to complex pathophysiological mechanisms.

The principal roles of this work are:

- to identify and characterize binding domain to the calcium binding protein S100A1 in the intracellular C- terminal part of TRPC6:
  - determine basic amino acid residues playing important role in the interaction with S100A1
  - characterize secondary structural composition of S100A1 binding domain in TRPC6

- to identify and characterize S100A1 binding site in integrative binding site of the intracellular C- terminal part of TRPV1:
  - confirm whether are basic amino acid residues playing important role in the interaction with CaM and PIP2 also involved in the interaction with S100A1
  - demonstrate calcium-dependency of TRPV1/S100A1 interaction

- to identify and characterize multiple PIPs binding site in the proximal part of the intracellular N-terminus of TRPM4:
  - determine basic amino acid residues in potential PH domain playing crucial role in the interaction with PIP2 and PIP3
  - characterize secondary structure composition of the TRPM4 identified by binding domain facilitating the interaction with PIP2 or PIP3
  - delineate the potential interaction mechanism of TRPM4/PIPs complexes using *De Novo* molecular modeling approach

- to identify and characterize PIP2 binding site in the distal part of intracellular N-terminus of TRPM1:
  - determine basic amino acid residues which are involved in the interaction with PIP2
  - specify secondary structure composition of PIP2 binding domain in TRPM1, determine secondary structural changes in TRPM1/PIP2 complex

- describe the potential binding interface of TRPM1/PIP2 using *de novo* molecular modeling approach

3. MATERIALS AND METHODS

3.1. SUBCLONING AND SITE-DIRECTED MUTAGENESIS OF TRPS SEGMENTS

Complementary DNA of constructs encoding the selected TRP channel regions was subcloned into the pET_32b expression vector (Novagen, Madison, WI, USA). Mutagenesis of the appropriate DNA constructs was performed using Pfu Ultra High-fidelity DNA polymerase according to the manufacturer´s protocol (Stratagene, Santa Clara, CA, USA). Selected hydrophobic and basic amino acid residues were replaced to get amino acids with different features in order to abolish the protein-protein (protein-lipid) interactions. The integrity of the encoding sequences was verified by DNA sequencing.

3.2. PROTEIN EXPRESSION AND PURIFICATION

3.2.1. TRPS SEGMENTS

Recombinant TRP protein was expressed as fusion with thioredoxin (to improve protein solubility) on N-terminus and 2x His-tag anchors on N- and C- termini. The protein expression was induced by isopropyl-1-thio-β-D-galactopyranoside (0.5 mM) for approximately 20 hours at 25°C and purified from *E. coli* Rosetta cells using chelating Sepharose fast flow columns (Amersham Biosciences, Little Chalfont, United Kingdom) with bound Ni^{2+} ions. The fusion TRP segment was obtained by eluting with a buffer containing 10 mM PBS (pH depends on specific protein sequence; PBS composition: 1.36 M NaCl, 0.027 M KCl, 0.0177 M KH_2PO_4, 0.05 Na_2HPO_4 . 2 H_2O), 500 mM NaCl, 2 mM β-Mercaptoethanol, and 400 mM imidazol. The second purification step was gel permeation chromatography on Superdex 75 column (Amersham Biosciences, Little Chalfont, United Kingdom). Protein was eluted with a buffer containing 25 mM HEPES or Tris-HCl (pH depends on specific protein sequence), 250 mM NaCl, 2 mM β-MerkaptoEtOH, 0.1% Tween and 10% glycerol. The identity and purity of protein were verified using 15% SDS-polyacrylamide gel electrophoresis (PAGE). Protein concentration was measured by UV absorption at 280 nm. Proteins were stored at -80°C for a maximum of 6 months.

3.2.2. CAM, S100A1

The S100A1 was subcloned into the pET_28b expression vector; CaM was subcloned into the pET_3a expression vector. The proteins were expressed in *E. coli* BL21 cells by inducing with isopropyl-1-thio-β-D-galactopyranoside (0.5 mM) for 12 h at 25 °C, then they were purified using affinity chromatography (5 mM $CaCl_2$ was added to the

supernatant) on Phenyl Sepharose CL4B (Amersham Biosciences, Little Chalfont, United Kingdom) and eluted using a buffer containing 50 mM Tris-HCl (pH 7.5), 1.5 mM EDTA and 100 mM NaCl. The second purification step was performed using gel permeation chromatography and Superdex 75 columns (Amersham Biosciences, Little Chalfont, United Kingdom). Proteins were eluted with a buffer that contained 50 mM Tris-HCl (pH 7.0), 250 mM NaCl, 2 mM $CaCl_2$, 2 mM β-mercaptoethanol, and 10% glycerol. The identity and purity of protein were verified using 15% SDS-polyacrylamide gel electrophoresis (PAGE). Protein concentration was measured by UV absorbtion at 280 nm. Proteins were stored at -80°C for a maximum of 6 months.

3.3. PROTEIN SEQUENCE VERIFICATION BY MASS SPECTROMETRY

The identities of proteins were verified by MALDI-TOF. Mass spectra were obtained using an Ultra-FLEX III mass spectrometer (Bruker-Daltonics, Bremen, Germany). Protein bands from SDS-PAGE gels were digested with trypsin endoprotease (Promega, Madison, WI, United States) in the gel after destaining. The protein mixture was extracted and loaded onto the MALDI-TOF/TOF target with a matrix of α-cyano-4-hydroxycinnamic acid. Peptide sequences were verified by manual interpretation of the MS/MS tandem mass spectra of selected *m/z* signals.

3.4. LIPOSOME PREPARATION

The lipids L-a-phosphatidylinositol-4,5-bisphosphate (PIP2), 1,2-dioleoyl-*sn*-glycero-3-phospho-(1'-myo-inositol-3',4',5'-trisphosphate) (PIP3) and 1,2-dimyristoyl-sn-glycero-3-phosphocholine (PC) were obtained from Avanti Polar Lipids, Inc (Alabaster, AL, USA). A stock solutions of PIP2 and PIP3 were prepared in a chloroform: methanol: H_2O (20:9:1) mixture, a stock solution of PC only in chloroform. Liposomes of the following compositions were prepared: PC, PC/PIP2 50/50% and PC/PIP3 50/50%. After being dried under N2 stream, lipid films were hydrated with Hank´s Balanced Salt Solution (HBSS) buffer (25 mM HEPES, 250 mM NaCl) followed by extrusion 21 times through a polycarbonate membrane with Nuclepore Track-Etched membranes with 100 nm pore diameter (Avanti Lipids, Alabaster, AL, USA). The liposomes obtained were then centrifuged (50 000 g) for 30 min at 4°C. The vesicles were diluted on 100 µg/ml concentration in HBSS buffer.

3.5. SURFACE PLASMON RESONANCE

Surface Plasmon resonance (SPR) measurements were performed at 25 °C using a liposome-coated NLC sensor chip (Bio-Rad, Hercules, CA, USA) mounted on a ProteOn XPR36 Protein Interaction Array System (Bio-Rad, Hercules, CA, USA). The liposomes were prepared as above however the hydrated lipids were incubated with

oligonucleotide modified at the 3' end with cholesterol (Generi Biotech, Hradec Kralove, Czech Republic). The mixture was extruded through a 100-nm polycarbonate membrane (Avanti Lipids, Alabaster, AL, USA) and the freshly-formed liposomes were incubated with 8 mM anti-sense oligonucleotide modified at the 3' end with biotin (Generi Biotech, Hradec Kralove, Czech Republic). The pelleted vesicles were resuspended to a final concentration of 100 µg/ml in HBSS buffer and immediately immobilized on the streptavidin-coated NLC chip surface. All SPR experiments were carried out in HBSS buffer at a flow rate of 30 µl/min for association and dissociation phases of the sensograms, respectively. The proteins were serially diluted in the running buffer and injected in parallel over the immobilized liposome surfaces. Surfaces were typically regenerated with 100 µl of 50 mM NaOH and 150 mM NaCl. The sensograms were corrected for sensor background by interspot referencing and double referenced by subtraction of analyte using a "blank" injection. The data were analyzed using a ProteOn software (Bio-Rad, Hercules, CA, USA) and fitted with a 1:1 Langmuir-type and heterogeneous binding models to determine association (*ka*) and dissociation (*kd*) rate constants. The Langmuir-type model assumes the interaction between liposomes (L) and protein (P) resulting in a direct formation of the final complex (LP)

$$L + P \underset{kd}{\overset{ka}{\rightleftharpoons}} LP$$

where *ka* and *kd* are the association and the dissociation rate constants, respectively. The heterogeneous binding models assumes two binding sites on the ligand

$$L1 + P \underset{kd1}{\overset{ka1}{\rightleftharpoons}} L1P; \quad L2 + P \underset{kd2}{\overset{ka2}{\rightleftharpoons}} L2P$$

where L1 and L2 are two separate binding sites on the ligand and P is the analyte protein. Note that there are two separate sets of association and dissociation rate constants (*ka1/kd1* and *ka2/kd2*) to describe each binding event. The binding response of a sensorgram from a heterogeneous ligand then, is the sum of the binding response of two separate binding events. An apparent equilibrium dissociation constant, *KD* was determined as *kd/ka*.

3.6. LABELING OF CALCIUM BINDING PROTEINS

For fluorescence labelling, CaM or S100A1 were dialyzed overnight into 10 mM $NaHCO_3$ (pH 10.0) at 4 °C. After dialysis, the protein was mixed with a 0.6 M dansyl chloride (DNS) solution (Sigma-Aldrich, St. Louis, Missouri, United States) at a molar ratio of 1:1.5 and incubated at RT for 3 h. Then the mixture was dialyzed overnight at 4°C against 20 mM Tris-HCl (pH 7.5), 250 mM NaCl and 2 mM $CaCl_2$ to remove free DNS. The labeled protein was checked by measuring the ratio of the fluorescence intensities of the bound and unbound states (excitation at 340 nm, emission at 510 nm).

3.7. STEADY-STATE FLUORESCENT ANISOTROPY

Steady-state fluorescence anisotropy measurements were performed at 25°C on an ISS PC1TM photon counting spectrofluorometer. TRP/Ca^{2+}-binding-protein binding assay was performed at RT in 20 mM Tris-HCl (pH depends on specific protein segment), 250 mM NaCl and 2 mM $CaCl_2$ buffer with DNS-labeled CaM or S100A1. Sample was titrated with increasing amounts of TRP protein about appropriate concentration. At each TRP concentration, the steady-state fluorescence anisotropy of CaM-DNS/S100A1-DNS was recorded (excitation at 340 nm, emission at 510 nm). The fraction of bound TRP protein segment (F_B) was calculated from Equation 1 (Boura, Silhan et al. 2007)

$$F_B = (r_{obs} - r_{min}) / [(r_{max} - r_{obs})Q + (r_{obs} - r_{min})] \qquad \text{(Eq. 1)}$$

where Q represents the quantum yield ratio of the bound to the free form of the protein and was estimated by the ratio of the intensities of the bound to the free DNS fluorophore. The parameter r_{max} is the anisotropy at saturation, r_{obs} is the observed anisotropy for any TRP segment concentration, and r_{min} is the minimum observed anisotropy for the free CaM-DNS/S100A1-DNS. F_B was plotted against TRP protein concentration and fitted using Equation 2 (Kohler and Schepartz 2001) to determine the equilibrium dissociation constant (K_D) for TRP/Ca^{2+}-binding protein formation.

$$F_B = \frac{K_D + [P1] + [P2] - \sqrt{(K_D + [P1] + [P2])^2 - 4[P1][P2]}}{2[P1]} \qquad \text{(Eq. 2)}$$

[*P1*] represents the CaM-DNS/S100A1-DNS concentration and [*P2*] is the TRP protein concentration. Nonlinear data fitting was performed using the program SigmaPlot 12.0. All experiments were performed at least three times. Control experiments were performed to show that thioredoxine is not involved in binding to CaM or S100A1 in the TRP fusion protein. To assess the role of Ca^{2+} in binding of the TRP channel segments to CaM or S100A1, we added 2 mM $CaCl_2$ to the buffer (20 mM Tis-HCl [pH depends on specific protein segment] and 250 mM NaCl) after purification. EDTA (10 mM) was then used to chelate all calcium ions in the buffer for verification of decoupling of Ca^{2+} dependent interaction of TRP and Ca^{2+} binding proteins.

3.8. CIRCULAR DICHROISM

The circular dichroism (CD) spectra of TRP protein segments were measured on a Jasco J-815 CD spectrometer (Jasco Corporation, Tokyo, Japan) over a spectral range of 200-300 nm using a quartz cell with a 0.05 cm path length at RT. The experimental setup was usually as follows: 0.5 nm step resolution, 5 nm/min speed, 16 s response time, 2 accumulations and 1 nm bandwidth. TRP samples were kept in 25 mM HEPES (pH:

depends on specific TRP segment), 2 mM $CaCl_2$ and 150 mM NaCl. After baseline correction, the final spectra were expressed in terms of molar elipticity θ ($deg.cm^2.dmol^{-1}$) per residue (Whitmore and Wallace 2008). The secondary structure content of TRP and its mutants was determined by CD analysis using CDPro software and the Contill algorithm (standard deviation between 0.02 and 0.05) (Provencher and Gloeckner 1981).

3.9. MOLECULAR MODELING

The molecular models of selected TRP channel binding domains were generated *de novo* using the I-Tasser, Robeta and Psi-Pred prediction servers (Kim, Chivian et al. 2004, Buchan, Minneci et al. 2013, Yang, Yan et al. 2015). The final 3D models of TRP channel binding regions were carefully selected based on the specific requirement on interacting amino acid residues to be exposed into the solvent, and also on geometric constraints imposed on the ligand binding sites. The quality of the resulting structures were assessed using STING Milenium (Neshich, Togawa et al. 2003) and ProSA-web (Wiederstein and Sippl 2007). 3D refine freeware (Bhattacharya and Cheng 2013) was used for hydrogen bonding network optimization and atomic-level energy minimization. Ligand docking of PIP2 (3SPI) and PIP3 (1W1G) was performed in Molecular Operating Environment (MOE) with the Induced Fit protocol (Deeth, Fey et al. 2005). The docking of S100A1 protein into specific TRP molecular model was performed using the pyDockWeb (pyDockRST) program (Jiménez-García, Pons et al. 2013). The optimal binding modes were selected based on interaction energy. The schematic representations of the TRP/ligand complexes were generated using Chimera freeware (Pettersen, Goddard et al. 2004).

4. RESULTS

4.1. DESIGN OF POTENTIAL PIPS BINDING SITES IN TRPM4

For designing of potential PIPs binding sites in intracellular tails of TRPM4 channel we searched PH domain (Fig.7) (Lemmon, Ferguson et al. 1995), which is abundant on cluster of basic amino acids and demonstrably interacts with negatively charged phosphate groups of PIPs (Suh and Hille 2005).
According to the secondary structure prediction of whole TRPM4 channel (Lu, Slominski et al. 2010, Yang, Yan et al. 2015), we chose a region meeting requirements for secondary structure formation of selected protein segment. This selection together with localization of potential ligand binding site has provided us a proposal of specific protein segment. Selected TRPM4 (E733-W772) segment has 186 amino acids and molecular weight 20.012 kDa (Mw predicted in ProtParam tool, (Gasteiger, Hoogland et al. 2005). Protein segment was recombinantly expressed and purified (Fig.8) in sufficient yield and purity and it was used for binding assays with PIPs ligands and for *in silico* experiments.

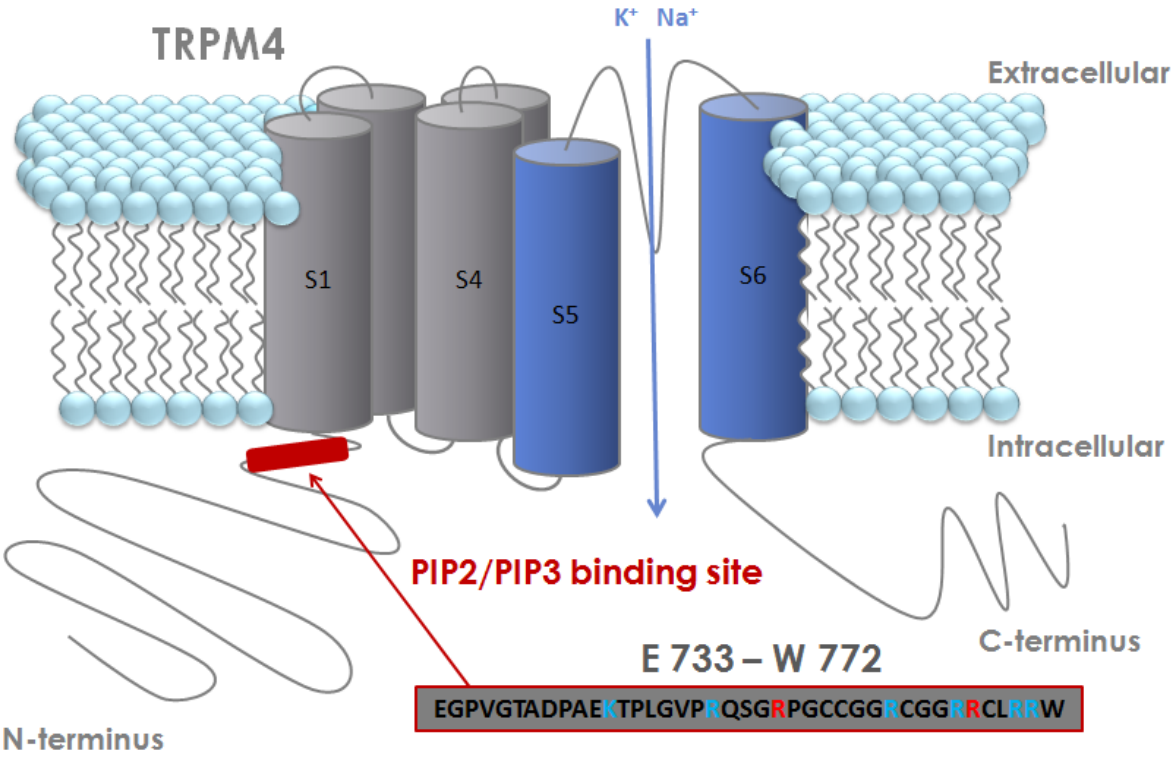

FIGURE 7 Prediction of potential PIP2/PIP3 binding domain based on pleckstrin homology domain presence. Predicted transmembrane topology of the TRPM4 channel: receptor has six putative transmembrane helices, a pore region between the fifth and sixth transmembrane domains for transporting monovalent ions and

intracellular N- and C-termini. The red block shows the potential PIP2/PIP3 binding site in the proximal region of the TRPM4 N-terminus. The selected sequence of TRPM4 (E733-W772) segment based on secondary structure prediction is represent in red frame. Basic amino acid residues (Lys and Arg) proposed to participate in the interaction with PIP2/PIP3 are indicated by blue. The red highlighted arginines (R755 and R767) were confirmed as important partners for complex formation with PIP2 and PIP3.

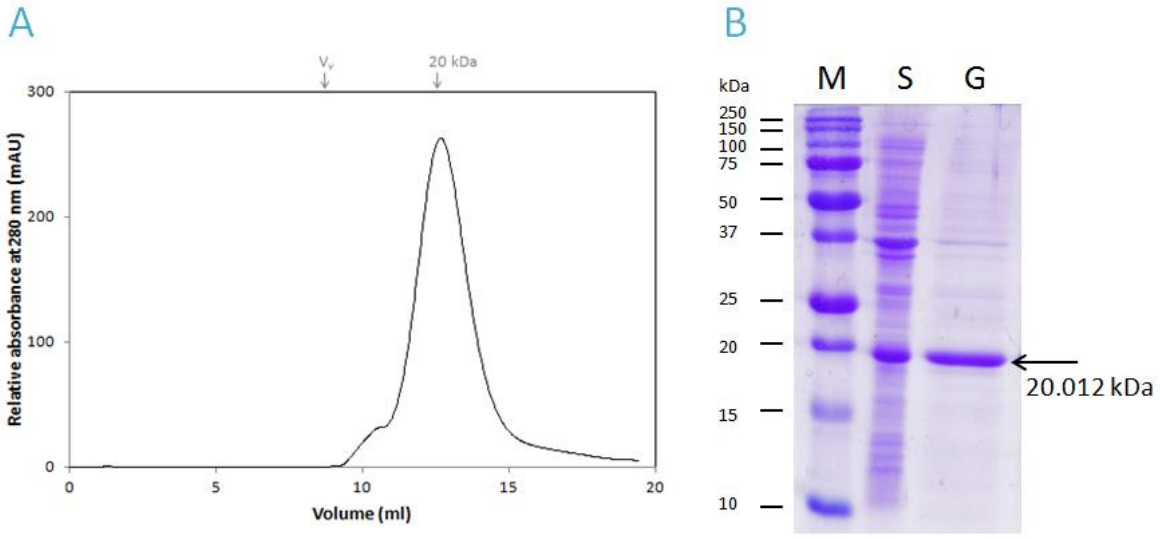

FIGURE 8 The purification of TRPM4 (E733-W772) segment about 20.012 kDa; (A) gel permeation chromatography on Superdex 75 column, (B) SDS-PAGE of protein in sonicate - S and after gel permeation chromatography –G. Molecular weight of standard – M.

4.2. CHARACTERIZATION OF PIPS BINDING SITE IN TRPM4 N-TERMINUS

To kinetically characterize the interaction of TRPM4 (E733-W772) with PIP2 and PIP3, we utilized surface plasmon resonance (SPR) measurements. The liposomes containing PIP2 and PIP3 were immobilised on a chip surface and conduction with TRPM4 fusion proteins (wild type and mutants) were tested in running buffer at concentrations ranging from 0 to 10 μM. Real time interaction of serially-diluted TRPM4 (E733-W772) with lipid surfaces revealed typical concentration-dependent binding curves (Fig. 9). Binding of the thioredoxin fusion was exclusively mediated through the TRPM4 segments, since thioredoxin itself did not bind the lipid surface.

Figure 9 shows the experimental binding curves for the interaction of TRPM4 (E733-W772) with liposomes made from PC and PC enriched by PIP2/PIP3. The data showed a close fit to a heterogeneous ligand model. The heterogeneous ligand model assumes that analyte TRPM4 (E733-W772) binds two separate binding sites on the ligand (liposomes) and each ligand sites bind the analyte independently with different set of rate constants. The calculated association and dissociation rate constants (*ka1*, *ka2*, *kd1*,

and *kd2*) as well as *KD1* and *KD2* for the interaction are listed in Table 1. The data analysis revealed that the affinities of TRPM4 (E733-W772) to PIP2 and PIP3-enriched liposomes were comparable and found to be *KD1* = 0.3 μM and *KD2* = 5.5 μM for PIP2, and *KD1*= 0.5 μM and *KD2* = 5.4 μM for PIP3, respectively. In view of the fact that the heterogeneous ligand model assumes TRPM4 (E733-W772) binding at two distinct sites with the binding affinity being approximately ten times higher for the first than for the second site and simultaneously TRPM4 (E733-W772) interacts non-specifically with liposome membranes made from PC alone. Thus, the heterogeneous ligand model is the most likely model of the interaction of TRPM4 (E733-W772) with PIP2- and PIP3-enriched vesicles.

Specificity of TRPM4 (E733-W772) to PIP2 and PIP3 was further analyzed on a double-mutant carrying substitution of two arginine residues (R775 and R767) within a putative motif of PH domain. In agreement with the wild-type construct, the binding curves for the interaction of the TRPM4 (E733-W772) - R755A/R767A mutant with lipid vesicles were fitted to the heterogeneous ligand model (Fig.9). The calculated association and dissociation constants of double-mutant are also listed in Table 1. Overall comparison of *KD* values revealed significant decrease in the binding affinity for the double-mutant. Moreover, the kinetics of interaction of the double-mutant did not prove any significant differences between binding to PC and PIP2- and PIP3-enriched vesicles indicating a complete loss of PIP2 and PIP3 specificity. Thus, the TRPM4 (E733-W772) segment interacts specifically with PIP2 or PIP3 on the membrane surface and the R755 and R767 residues the important participants in complex formation.

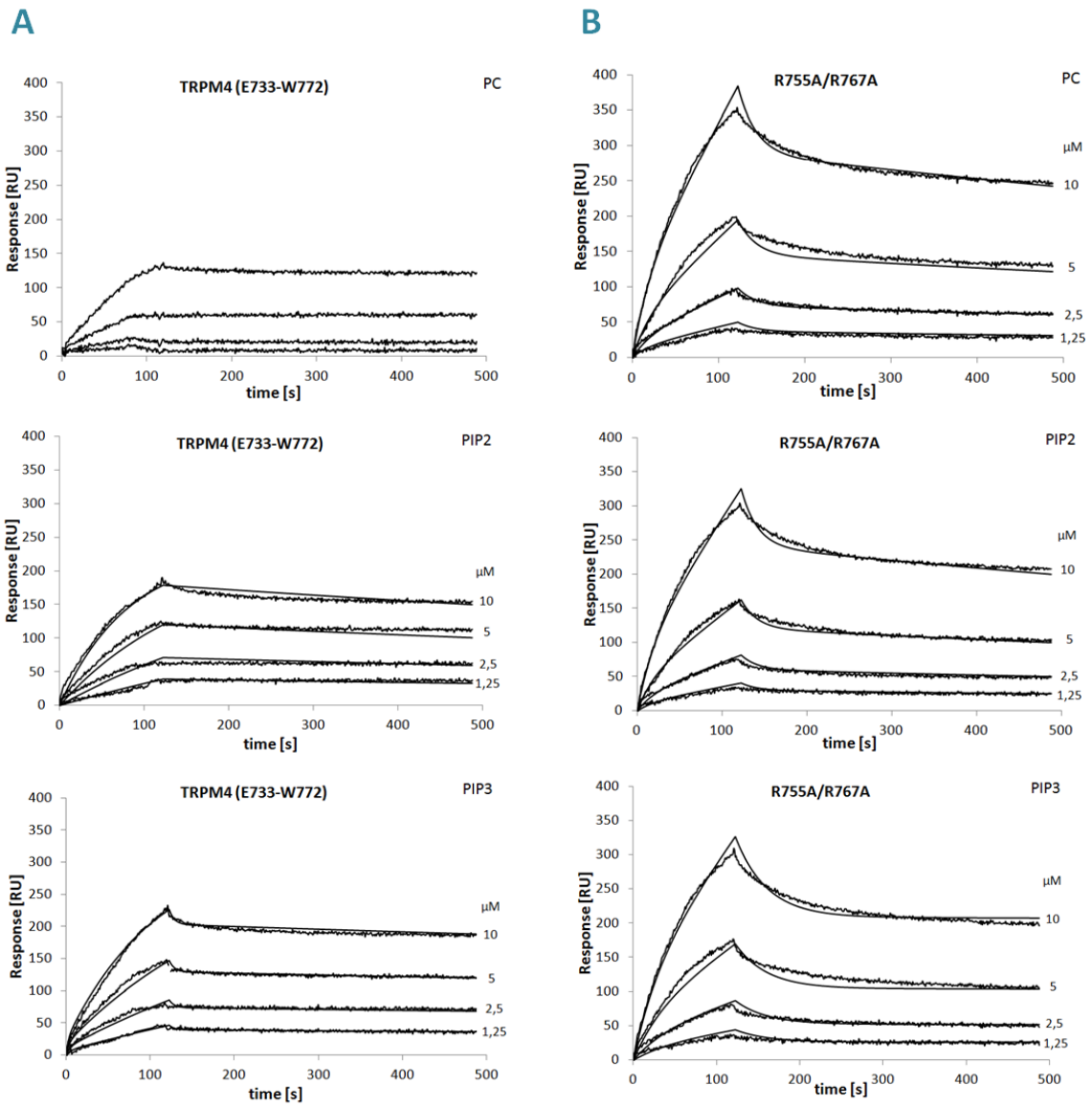

FIGURE 9 SPR kinetic binding analysis of the interaction between TRPM4 (E733-W772) **and lipid vesicles.** One-shot kinetic analysis of the interaction of TRPM4 (E733-W772) (A) and its double mutant TRPM4 (E733-W772) - R755A/R767A (B) with PC, PIP2 and PIP3 enriched lipid vesicles. Serially diluted proteins were injected in parallel over the sensor chip coated with 100-nm lipid vesicles and left to associate (120 s) and dissociate at constant flow rate of 30 µl/min. Apart from the interaction of TRPM4 (E733-W772) with PC, which could not be fitted to any of the binding models. Kinetic data were globally fitted by using a heterogeneous ligand model. Fitted curves are superimposed as black lines on top of the sensograms.

TABLE 1 Kinetic and binding affinity constants for the interactions of TRPM4 (E733-W772) with PC, PIP2 and PIP3 enriched lipid vesicles.

		ka1×10^3 [$M^{-1}.s^{-1}$][a]	kd1×10^{-4} [s^{-1}]	KD1 [µM][b]	ka2×10^4 [$M^{-1}.s^{-1}$]	kd2×10^{-1} [s^{-1}]	KD2 [µM]
TRPM4 (E733-W772) R755/R767	PC	-	-	-	-	-	-
	PIP2	1.5 ± 0.4	4.6 ± 1.1	0.3 ± 0.1	3.8 ± 0.8	2.1 ± 0.5	5.5 ± 1.4
	PIP3	1.2 ± 0.3	6.5 ± 2.1	0.5 ± 0.2	3.3 ± 0.7	1.8 ± 0.4	5.4 ± 1.3
	PC	0.3 ± 0.1	9.8 ± 2.5	3.3 ± 0.9	4.1 ± 1.2	0.6 ± 0.2	1.5 ± 0.4
	PIP2	0.2 ± 0.1	10.1 ± 3.1	5.1 ± 1.4	5.2 ± 1.7	0.7 ± 0.2	1.3 ± 0.3
	PIP3	0.2 ± 0.1	9.9 ± 2.9	4.9 ± 1.5	3.2 ± 0.9	0.6 ± 0.2	1.9 ± 0.3

[a] Results are means ± S.D. from the analysis of two independent measurements.

[b] The equilibrium dissociation constants (KD1 and KD2) was determined as kd1/ka1 and kd2/ka2, respectively.

4.3. TRPM4 (E733-W772) SECONDARY STRUCTURE CONTENT

The secondary structure of the TRPM4 (E733-W772) fusion protein was studied by CD spectroscopy. Whereas the structure of cytosolic regions of TRPM4 is still unknown, the secondary structural composition of TRPM4 (E733-W772) with thioredoxin was determined as to be mostly disordered (Fig.10, Tab.2). CD spectra TRPM4 (E733-W772) fusion confirmed that protein is mostly unstructured, which is in a good agreement with the theoretical prediction based on its primary structure. According to CD spectra, TRPM4 (E733-W772) in presence of liposomes formed by PC alone or PC containing PIP2/PIP3 (50/50%) does not change its secondary structure content (Fig.10, Tab.2). This suggests that binding PIP2 or PIP3 to TRPM4 (E733-W772) has no significant influence on its structure.

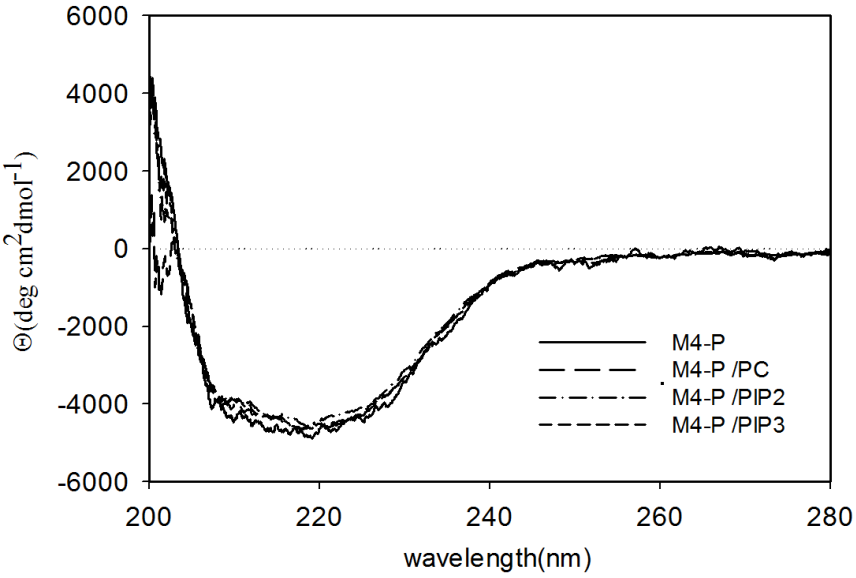

FIGURE 10 CD spectra of TRPM4 (E733-W772) [M4-P in figure] in presence of liposomes. The interaction of TRPM4 (E733-W772) with PC, PIP2 and PIP3 enriched liposomes shows that the secondary structural content of TRPM4 (E733-W772) was not changed during the complex formation. CD spectra were expressed as molar elipticity Q (deg.cm^2.dmol^{-1}) per residue.

TABLE 2 Calculated incidence (%) of TRPM4 (E733-W772) secondary structure content alone and of protein in complexes with PIP2 and PIP3 determined by CD spectroscopy in 25mM HEPES (pH=8.0), 250 mM NaCl.

	Helix	Anti-parallel	Parallel	β-turn	Random coil
TRPM4 (E733-W772)	17	13	13	17	40
TRPM4 (E733-W772)/PC	15	13	13	18	41
TRPM4(E733 W772)/PIP2	15	11	14	17	42
TRPM4 (E733-W772)/PIP3	17	13	13	17	40

4.4. IN SILICO EXPERIMENTS

To predict the interactions of the PIPs binding site of TRPM4 N-termini with PIP2/PIP3 ligands, we created 3D model of the corresponding TRPM4 (E733-W772) in fusion construct with thioredoxin. Model of human TRPM4 fusion protein segment was generated using the I-Tasser prediction server. The thioredoxin structure was deleted from the model and potential PIP2/PIP3 binding site was assigned by MOE. Eventually,

PIP2 and PIP3 ligands were docked into the assigned binding site (Fig.11). To orient PIP2/PIP3 ligands properly, we utilized structural information from the literature – in particular the interaction of PIP2 with the proximal region of the intracellular tails of potassium ion channels (Hansen, Tao et al. 2011) which is well characterized. For the models of TRPM4-PIP2/PIP3 complexes we assumed that the interaction is accomplished by an arginine/lysine cluster interacting with the phosphate groups of PIP2 (PIP3). Positively charged amino acids are frequent in vicinity of the inner plasma membrane leaflet where binding sites for regulatory molecules such as phosphatidylinositol phosphates are expected to be abundant. Their mutation to alanine residues causes a replacement of their charged - side chains in the binding site, which makes it less favorable for interaction with PIP2 (Khelashvili, Galli et al. 2012, Bodhinathan and Slesinger 2013, Pattnaik, Tokarz et al. 2013).

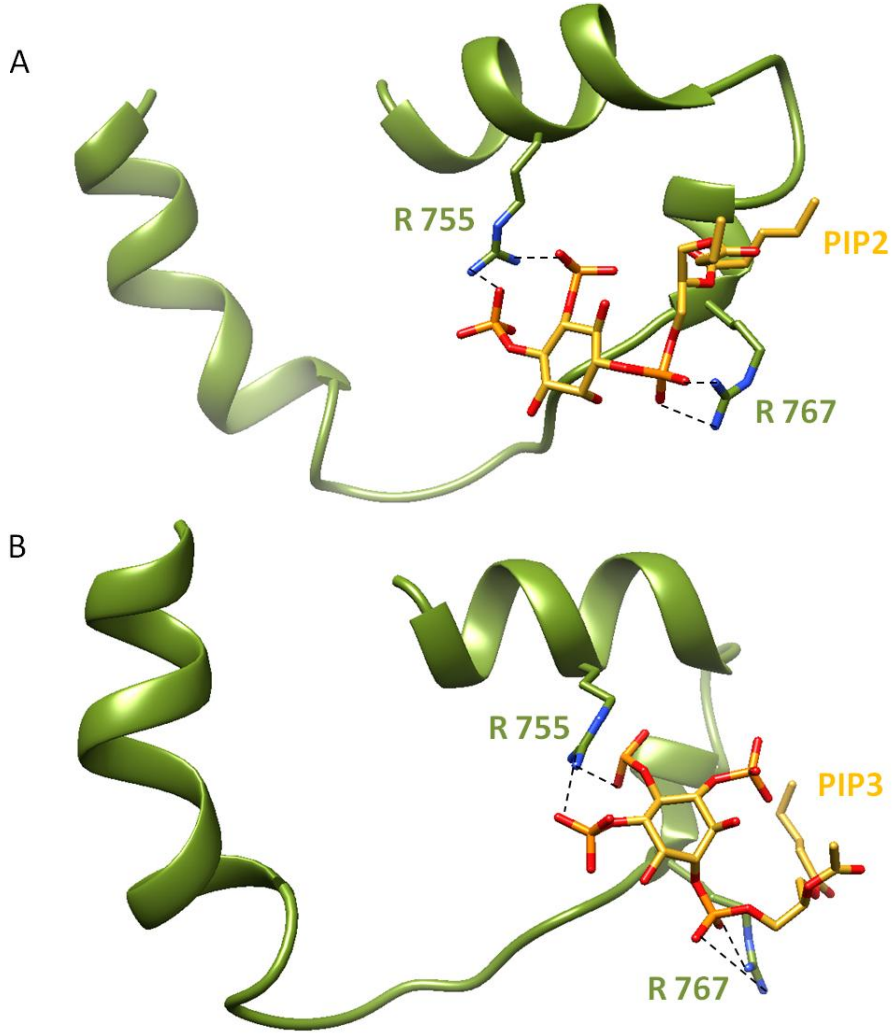

FIGURE 11 TRPM4 (E733-W772) domain binds PIP2 and PIP3. Schematic view of TRPM4 peptide interacts with (A) PIP2 and (B) PIP3. Important arginine residues bonded (dashed lines) to PIP2/PIP3 are colored green (R755 and R767). We used the following color convention: green - protein backbone of the TRPM4 (E733-W772), yellow - carbon atoms of PIP2, oxygen (O_2) - red, nitrogen (N) - blue, phosphorus (P) - orange.

5. DISCUSSION TO THE INDIVIDUAL PUBLICATIONS

5.1. CHARACTERIZATION OF THE S100A1 PROTEIN BINDING SITE ON TRPC6 C-TERMINUS

The TRPC6 channel is permeable for Ca^{2+} in eukaryotic cells, including sensory receptor cells which response to external signals. Its activity is modulated by multiple factors. Previously was shown that CaM acts as an important mediator of Ca^{2+} - dependent regulation (Zhu 2005, Kwon, Hofmann et al. 2007) and its binding site was described (Friedlova, Grycova et al. 2010). S100A1 behaves similarly in terms of mediating the activity of other ion channels (Wright, Varney et al. 2005, Prosser, Wright et al. 2008, Wright, Prosser et al. 2008). To find out whether CaM binding site is also available for another Ca^{2+} binding protein S100A1, we tested the binding of the S100A1 protein to TRPC6 C-terminus (801–878) (below as TRPC6-CT).

Using site-directed mutagenesis of the predicted basic amino acid residues of TPRC6-CT in combination with steady-state fluorescence anisotropy measurements, we characterized S100A1 binding site. Fluorescence measurements showed that dissociation constant for S100A1/TRPC6-CT (*Kd* 0.31 μM) interaction is in the same range as well as for CaM/TRPC6-CT (*Kd* 0.31 μM) (Friedlova, Grycova et al. 2010) and ligand binding sites are overlapping. As the amino acid residues important for CaM binding are known, it was tested their role in S100A1 interaction. Although the TRPC6 WT binding affinities to both ligands CaM and S100A1 are almost the same, according to the results we obtained it seems that different residues are involved in the binding. The mutations of K856A and R864A had the most striking effect which leaded to an up to 3-fold decrease in the binding affinity to S100A1. According to our results, interaction of both binding partners is similar but not exactly the same, because different residues are essential for the interaction.

Numerical analysis of the experimental CD spectra enabled estimation of the relative abundance of the various secondary structure elements. The α-helical conformation (66%) was found to be the major component of the S100A1 protein, which is in good agreement with the conformation found in its native state. The CD spectra analysis confirmed the theoretical prediction, suggesting that the TRPC6 protein construct has adopted its native form. The CD experiment was also used to observe changes in the secondary structural elements during the TRPC6/S100A1 complex formation, we suggest that the changes in the secondary structure of TRPC6 (801–878) have no significant effect on its binding to S100A1.

Since S100A1 is a Ca^{2+}-binding protein and Ca^{2+} play a crucial role in TRPC6 activity regulation, the role of Ca^{2+} in S100A1 binding to TRPC6-CT was assessed.

Fluorescence measurements suggest that the binding is Ca^{2+}-dependent. The same behaviour has been revealed for the CaM/TRPC6– CT (Friedlova, Grycova et al. 2010).

5.2. Ca^{2+} BINDING PROTEIN S100A1 COMPETES WITH CaM AND PIP2 FOR BINDING SITE ON THE C-TERMINUS OF THE TPRV1 RECEPTOR

TRPV1 serve as important and the most examined nociceptor from TRP superfamily. Regulation of its activity is proposed to be mediated through interactions with activating agents as e.g. PIP2 (Liu, Zhang et al. 2005, Lishko, Procko et al. 2007, Lukacs, Thyagarajan et al. 2007) or inhibiting agents as e.g. CaM (Lishko, Procko et al. 2007). In previous reports, we found the C-terminal region of TRPV1 (TRPV1-CT) harbouring the integrative binding site for CaM and PIP2 (Rosenbaum, Gordon-Shaag et al. 2004, Grycova, Lansky et al. 2008, Grycova, Holendova et al. 2012). Since a family of the Ca^{2+}-binding S100 proteins was shown to interact with similar binding motifs like CaM (Wright, Prosser et al. 2008) we sought to explore whether TRPV1-CT also shares binding site for the S100A1 protein.

S100A1/TRPV1-CT complex formation was determined using SPR measurement. The kinetic parameters of the S100A1/TRPV1-CT interactions revealed that the rates of complex formation are similar for both S100A1 and CaM, however the stability of the complexes is significantly higher for S100A1, the binding affinity of TRPV1-CT to S100A1 is about two times higher for ligand than for CaM. Based on the residues identified in the TRPV1-CT/CaM complex as the most important, it was investigated alanine scanning mutagenesis of the TRPV1-CT followed by SPR analysis to assess the contribution of individual residues in kinetics of the interaction and stability of the TRPV1-CT/S100A1complex. The results showed that TRPV1-CT bears the binding site for both S100A1 and CaM. However, the binding of S100A1 is more specific than for CaM.

In order to determine whether S100A1 competes with CaM for the same binding site on the TRPV1-CT, CaM was mixed with TRPV1-CT in a molar ratio of 1:1 and the capacity of the prepared TRPV1-CT/CaM complex to bind S100A1 was analyzed using SPR. The binding of the TRPV1-CT/CaM complex was reduced to about 50% as compared to TRPV1-CT alone, indicating that S100A1 and CaM compete for the same binding site within TRPV1-CT. In view of the fact that CaM shares the TRPV1-CT binding site with PIP2, we examined whether S100A1 is also able to compete with PIP2 for TRPV1-CT binding. The measurements suggested that the S100A1 binding site overlaps with the PIP2-binding site on TRPV1-CT. In conclusion, it was shown competition between S100A1 with CaM and PIP2 for identical TRPV1-CT binding site. While CaM participates in TRPV1 desensitization the physiological role of S1000A1 in TRPV1 activity modulation is still elusive.

5.3. PIP2 AND PIP3 INTERACT WITH N-TERMINUS REGION OF TRPM4 CHANNEL

The regulation of TRPM channels by PIP2 has been widely demonstrated in last decade (Steinberg, Lespay-Rebolledo et al. 2014). Similarly, TRPM4 channel also contain intracellular domain clusters we have identified as potential PIPs binding pockets (Lemmon, Ferguson et al. 1995, Suh and Hille 2005). To confirm presence of new PIPs binding sites in intracellular regions of TRPM4 we utilized biophysical and bioinformatics approaches. Our findings could improve understanding of the regulation of the TRPM4 by lipid ligands (PIP2/PIP3).

Concretely, we used SPR to directly study the binding affinity and specificity of PIP2 and PIP3 to TRPM4 selected regions. We proposed the putative PIPs binding site of TRPM4 (E733-W772) in close proximity of the first TM domain based on its abundant presence on positive charge residues willingly interact with negative charged phosphates of PIPs. SPR demonstrated that TRPM4 (E733-W772) can interact with lipid bilayer (induced by PC in our experiments) and binds both PIPs specifically. Dissociation constants for TRPM4 (E733-W772)-PIP2/PIP3 complexes were in the similar micro molar range suggested on high affinity bonds in the interaction. A similar binding affinity for PIP2 (PIP3) was observed previously with the TRP family members (Grycova, Holendova et al. 2012, Holendova, Grycova et al. 2012). Using alanine scanning mutagenesis it was found that two residues R755 and R767 are important in the N-termini PIP2/PIP3 binding domain. Their mutation caused complete loss of specificity for PIP2/PIP3 binding.

Intracellular tails of TRPs are highly heterologous across the whole superfamily. Whereas the structural data about TRPM4 are still missing, we decided to obtain knowledge about secondary structure of TRPM4 PIPs binding site by circular dichroism measurements. In effect, the secondary structure of TRPM4 (E733-W772) fusion protein was determined to be mostly disordered. In complexes of TRPM4 (E733-W772)-PIP2/PIP3 no changes of the protein structure during interaction has been detected.

3D model of the TRPM4 (E733-W772) interacting with PIP2/PIP3 suggests the phosphate head groups of PIP2 and PIP3 form ionic interactions with positively charged arginines R755 and R767. According to the data from SPR, the binding affinity for TRPM4 (E733-W772) - PIP2/PIP3 complexes is very similar. The molecular model with PIP3 confirmed our SPR data, because specific one extra phosphate group of PIP3 does not have a particularly large influence on the strength of the interaction.

Surely, PIPs are the important regulators of TRPs and it is very likely that they could regulate TRPM4 channel via binding its intracellular N-terminus in the same way as was reported for other members of the TRPM family (Runnels, Yue et al. 2002, Liu and

Liman 2003, Grycova, Holendova et al. 2012). Notwithstanding functional studies are needed to elucidate the role of PIP2 and PIP3 in TRPM4 gating and regulation.

5.4. Characterization of the part of N-terminal PIP2 binding site of the TRPM1 channel

The last publication reported about the first identified interaction of PIP2 with TRPM1 channel. As was described previously, the selection of potential interaction site was choosen based on presence of positively charged residues cluster in the intracellular tails of TRPM1. Thus, we have characterized the capacity of a N-terminal segment of the TRPM1 channel (TRPM1-NT), encompassing residues A451 to N566, to interact with PIP2 using biophysical and bioinformatic tools. Neutralizing the positive charges in these regions usually results in a reduction of binding affinity of PH domains for PIP2, indicating a direct interaction between the cytoplasmic regions of TRPM channels with PIPs (Lemmon, Ferguson et al. 1995, Suh and Hille 2008, Grycova, Holendova et al. 2012).

At first, fluorescence measurements provide strong evidence for the interaction of TRPM1-NT with soluble PIP2 (labeled by fluorescent probe Bodipy). After, the SPR measurements confirmed the TRPM1-NT/PIP2 binding and provided us kinetic data during the association and dissociation of the complex. We found that the binding affinity of TRPM1-NT is almost three-times higher for PIP2 than for PC (membrane suplement during SPR measurement), indicating a higher specificity of TRPM1-NT for PIP2 on the membrane surface. Moreover, the K_D value of TRPM1-NT for PIP2 is in the micromolar range, which corresponds well to previous PIPx/receptor complex characterization (Hansen, Tao et al. 2011, Holendova, Grycova et al. 2012, Bousova, Jirku et al. 2015). To find concrete amino acids(s) involved in the interaction, we performed alanin scanning mutagenesis. This suggested the basic side chain of lysine residue at position 464 of TRPM1-NT mediates electrostatic interactions with the negatively charged phosphate group(s) of PIP2 at the membrane surface. Additionally, using CD measurements it has been discovered that TRPM1-NT/PIP2 complex formation is accompanied by significant changes in the secondary structure content of the protein. The 3D molecular model confirmed that the interaction is mediated through the negatively charged phosphate groups of PIP2, which are coordinated by a patch of positively charged residues on the TRPM1 surface.

Although we determined a possible PIP2 binding interface to the intracellular N-terminus of the TRPM1 fragment, the question of whether this interaction is mediated straightly by the N-terminus of the TRPM1 fragment remains unanswered. According to structural data, potassium channels possess four PIP2 binding sites in the $K_{ir}6.2$ tetramer, one per subunit, with both the N- and C-termini domains of the K_{ir} channels contributing to the PIP2 binding sites (Hansen, Tao et al. 2011, Whorton and MacKinnon 2011). Specific intracellular portions of the channel are attracted to the

plasma membrane due to direct interactions with the phospholipid. PIP2 exerts a tangential force on the N- and C-termini to open the channel. The PIP2-binding site for K_{ir}6.2 lies at the interface between the N- and C-termini regions between two neighboring subunits(Whorton and MacKinnon 2011). According to the tetramer assembly and with respect to the close proximity of the N- and C-terminal regions of TRPs (Liao, Cao et al. 2013, Paulsen, Armache et al. 2015, Zubcevic, Herzik Jr et al. 2016), we postulate that this pattern may occur for TRPM1. However, structural findings concerning TRP channel intracellular regions, which are essential for understanding the mechanism of the channel function will require further investigation.

6. CONCLUSIONS

TRP channels respond to multiple activation triggers and therefore serve as polymodal signal detectors. With respect to the complexity of the of TRPs function it is still a needed to devote an effort to understand the complex regulation mechanisms of TRPs function. The presented thesis is a summary of our results contributing to the description and characterization of four independent binding sites for regulatory molecules in the most important members of TRPs.

In the first publication the interaction of the Ca^{2+} -binding protein S100A1 with the TRPC6-CT conserved region (position 801–878) was investigated. It was found that this domain binds S100A1 with high affinity and the binding is Ca^{2+} -dependent. This work confirmed that there are more Ca^{2+} -binding proteins interacting with TRPC6-CT conserved region, as it follows from identification of the same domain for another Ca^{2+} dependent protein - CaM. The interaction of S100A1 and CaM with TRPC6 is similar in many ways but does not have exactly the same binding topology as was shown by identification of different basic residues essential for the binding of Ca^{2+} -dependent proteins.

The earlier studies dealt with interactability of TRPV1-CT (position 712-838) domain have revealed CaM and PIP2 common binding site. We succeeded to characterize the region in the TRPV1-CT responsible for the interaction with previously mentioned S100A1 protein using biophysical methods. We have shown that this domain overlaps with CaM and PIP2 binding sites and that S100A1 again competes in binding with these two ligands. Similarly to the S100A1 binding in TRPC6 –CT, several positively charged residues of this domain were identified as the most important in S100A1 binding. The interaction of S100A1/TRPV1-CT was shown to be again Ca^{2+} -dependent. Data obtained from steady-state fluorescent anisotropy and surface plasmon resonance measurements provided a clue to a mechanism of the mutual PIP2, S100A1 and CaM regulation in TRPV1.

We succeeded to identify important multiple PIPs binding site for TRPM subfamily, particularly at the proximal part of TRPM4 N- terminus (position E733-W772). By combination of experimental and theoretical methods we identified two positively charged amino acids - R755 and R767 at the TRPM4-NT crucial for the interaction with PIP2 and PIP3. Simultaneous mutation of these residues caused a total loss of binding affinity to both PIPs. We also experimentally proved that the TPRM4 domain can bind PIP2 and PIP3 with a similar binding affinity to the binding domain. One can assume that PIP2 and PIP3 binding site is the same for both ligands but this mechanism has to be confirmed in future. Due to lack of structural information about TRPM4 channel we decided to map secondary structure content of the selected TRPM4 intracellular binding domain. The data from secondary structure prediction and CD spectroscopy revealed

that the peptide terminus appears as mostly disordered and the binding of PIP2/PIP3 has no significant influence on its folding. To visualize TRPM4-PIP2/PIP3 binding interfaces we utilized *de novo* molecular modeling methods.

The last study presented in this thesis was focused on the identification of new PIP2 binding site in the distal part of TRPM1 N-terminus. We have characterized that the A451-N566 region of the TRPM1 interacts with PIP2, and we identified the lysine residue K464 participating in the PIP2 binding. This is the first report showing that PIP2 interacts with member of TRPM1 subfamily. In the contrary to the previously identified PIPs binding region in TRPM4, the characterization of TRPM1 binding domain revealed high content of secondary structure elements and we also observed significant increase of secondary structure elements upon PIP2 binding to the TRPM1. To structurally characterize the TRPM1/PIP2 interaction mode we used molecular modeling and docking methods similarly as for the TRPM4-PIP2/PIP3 complexes.

Results published in this thesis extend our knowledge about the existing binding sites for important signal integrators in TRPs. Their documented large structural and functional variability allows further characterization of not yet identified binding sites for common modulatory molecules whose regulatory functions have already been demonstrated on other TRPs subfamilies. Newly provided receptor-ligand characteristics drive us to better understanding of regulation complexity for TRPs members. To summarize our achievements – we documented features of four independent ligand binding domains localized in 3 main families of TRPs – TRPC, TRPV and TRPM. Based on that, we can constitute a few noticeable general characteristics of this binding. First, the interaction of proteins with TRPs is Ca^{2+} dependent and often realized via intracellular regions of TRPs enriched by positively charged amino acids arginine and lysine. Second, the interaction of PIP2 and PIP3 utilizes very similar binding interface as identified for another TRPs partners. We can hypothesize that PIPs interaction could be facilitating in large extent by the same of the positively charged residues. Last but not least, the process of any ligand binding to TRPs can induce conformational changes of their rather unstructured characters and increase a secondary structural content contributing to the binding selectivity.

These findings raising awareness about potential modulation of TRP receptors, which can lead further to cation transport and consequently to possible treatment of human diseases linked with disorders in TRPs. On the other hand, the overall functional role of TRPs within physiological processes such as hormonal cellular control, nociception or cellular calcium homeostasis is still not clear as these extensive processes often involve multi-cooperation of protein complexes. Deeper and comprehensive understanding of the molecular structure, biophysical properties, functional and pathophysiological roles of the TRPs is therefore more needed than ever before.

7. REFERENCES

Ambudkar, I. S. and H. L. Ong (2007). "Organization and function of TRPC channelosomes." Pflügers Archiv-European Journal of Physiology **455**(2): 187-200.

Barbato, G., et al. (1992). "Backbone dynamics of calmodulin studied by nitrogen-15 relaxation using inverse detected two-dimensional NMR spectroscopy: the central helix is flexible." Biochemistry **31**(23): 5269-5278.

Bhattacharya, D. and J. Cheng (2013). "3Drefine: Consistent protein structure refinement by optimizing hydrogen bonding network and atomic-level energy minimization." Proteins: Structure, Function, and Bioinformatics **81**(1): 119-131.

Bily, J., et al. (2013). "Characterization of the S100A1 protein binding site on TRPC6 C-terminus." PLoS One **8**(5): e62677.

Bodhinathan, K. and P. A. Slesinger (2013). "Alcohol modulation of G-protein-gated inwardly rectifying potassium channels: from binding to therapeutics." Frontiers in physiology **5**: 76-76.

Boura, E., et al. (2007). "Both the N-terminal loop and wing W2 of the forkhead domain of transcription factor Foxo4 are important for DNA binding." Journal of Biological Chemistry **282**(11): 8265-8275.

Bousova, K., et al. (2015). "PIP2 and PIP3 interact with N-terminus region of TRPM4 channel." Biophys Chem **205**: 24-32.

Bridges, D. and A. R. Saltiel (2015). "Phosphoinositides: Key modulators of energy metabolism." Biochimica et Biophysica Acta (BBA)-Molecular and Cell Biology of Lipids **1851**(6): 857-866.

Buchan, D. W., et al. (2013). "Scalable web services for the PSIPRED Protein Analysis Workbench." Nucleic acids research **41**(W1): W349-W357.

Carlström, M., et al. (2015). "Renal autoregulation in health and disease." Physiological reviews **95**(2): 405-511.

Cates, M. S., et al. (1999). "Metal-ion affinity and specificity in EF-hand proteins: coordination geometry and domain plasticity in parvalbumin." Structure **7**(10): 1269-1278.

Cortright, D. N. and A. Szallasi (2009). "TRP channels and pain." Current pharmaceutical design **15**(15): 1736-1749.

Cuajungco, M. P., et al. (2006). "PACSINs bind to the TRPV4 cation channel PACSIN 3 modulates the subcellular localization of TRPV4." Journal of Biological Chemistry **281**(27): 18753-18762.

D'hoedt, D., et al. (2008). "Stimulus-specific modulation of the cation channel TRPV4 by PACSIN 3." Journal of Biological Chemistry **283**(10): 6272-6280.

Deeth, R. J., et al. (2005). "DommiMOE: An implementation of ligand field molecular mechanics in the molecular operating environment." Journal of computational chemistry **26**(2): 123-130.

Dömötör, A., et al. (2005). "Immunohistochemical distribution of vanilloid receptor, calcitonin-gene related peptide and substance P in gastrointestinal mucosa of patients with different gastrointestinal disorders." Inflammopharmacology **13**(1): 161-177.

Duarte-Costa, S., et al. (2014). "S100A1: a major player in cardiovascular performance." Physiol Res.

Duncan, L. M., et al. (1998). "Down-regulation of the novel gene melastatin correlates with potential for melanoma metastasis." Cancer Research **58**(7): 1515-1520.

Dunlap, T. B., et al. (2014). "Stoichiometry of the Calcineurin Regulatory Domain–Calmodulin Complex." Biochemistry **53**(36): 5779-5790.

Entin-Meer, M., et al. (2014). "The transient receptor potential vanilloid 2 cation channel is abundant in macrophages accumulating at the peri-infarct zone and may enhance their migration capacity towards injured cardiomyocytes following myocardial infarction." PLoS One **9**(8).

Erler, I., et al. (2004). "Ca2+-selective transient receptor potential V channel architecture and function require a specific ankyrin repeat." Journal of Biological Chemistry **279**(33): 34456-34463.

Estacion, M., et al. (2001). "Regulation of Drosophila transient receptor potential-like (TrpL) channels by phospholipase C-dependent mechanisms." The Journal of physiology **530**(1): 1-19.

Fixemer, T., et al. (2003). "Expression of the Ca2+-selective cation channel TRPV6 in human prostate cancer: a novel prognostic marker for tumor progression." Oncogene **22**(49): 7858-7861.

Friedlova, E., et al. (2010). "The interactions of the C-terminal region of the TRPC6 channel with calmodulin." Neurochemistry international **56**(2): 363-366.

Gasteiger, E., et al. (2005). Protein identification and analysis tools on the ExPASy server, Springer.

Gaudet, R. (2008). "A primer on ankyrin repeat function in TRP channels and beyond." Molecular BioSystems **4**(5): 372-379.

Goodman, M., et al. (1979). "Evolutionary diversification of structure and function in the family of intracellular calcium-binding proteins." Journal of molecular evolution **13**(4): 331-352.

Gordon-Shaag, A., et al. (2008). "Mechanism of Ca2+-dependent desensitization in TRP channels." Channels **2**(2): 125-129.

Grycova, L., et al. (2012). "Integrative binding sites within intracellular termini of TRPV1 receptor." PLoS One **7**(10): e48437.

Grycova, L., et al. (2014). "Ca2+ Binding Protein S100A1 Competes with Calmodulin and PIP2 for Binding Site on the C-Terminus of the TPRV1 Receptor." ACS chemical neuroscience **6**(3): 386-392.

Grycova, L., et al. (2008). "Ionic interactions are essential for TRPV1 C-terminus binding to calmodulin." Biochemical and biophysical research communications **375**(4): 680-683.

Hansen, S. B., et al. (2011). "Structural basis of PIP2 activation of the classical inward rectifier K+ channel Kir2. 2." Nature **477**(7365): 495-498.

Hardie, R. C. and B. Minke (1992). "The trp gene is essential for a light-activated Ca 2+ channel in Drosophila photoreceptors." Neuron **8**(4): 643-651.

Hartel, M., et al. (2006). "Vanilloids in pancreatic cancer: potential for chemotherapy and pain management." Gut **55**(4): 519-528.

Hille, B., et al. (2015). "Phosphoinositides regulate ion channels." Biochimica et Biophysica Acta (BBA)-Molecular and Cell Biology of Lipids **1851**(6): 844-856.

Hofmann, T., et al. (1999). "Direct activation of human TRPC6 and TRPC3 channels by diacylglycerol." Nature **397**(6716): 259-263.

Holakovska, B., et al. (2012). "Calmodulin and S100A1 protein interact with N terminus of TRPM3 channel." Journal of Biological Chemistry **287**(20): 16645-16655.

Holendova, B., et al. (2012). "PtdIns (4, 5) P 2 interacts with CaM binding domains on TRPM3 N-terminus." Channels **6**(6): 479-482.

Hsu, Y.-J., et al. (2007). "TRP channels in kidney disease." Biochimica et Biophysica Acta (BBA)-Molecular Basis of Disease **1772**(8): 928-936.

Huynh, K. W., et al. (2014). "Structural insight into the assembly of TRPV channels." Structure **22**(2): 260-268.

Hwang, S. W., et al. (2000). "Direct activation of capsaicin receptors by products of lipoxygenases: endogenous capsaicin-like substances." Proceedings of the National Academy of Sciences **97**(11): 6155-6160.

Chevesich, J., et al. (1997). "Requirement for the PDZ domain protein, INAD, for localization of the TRP store-operated channel to a signaling complex." Neuron **18**(1): 95-105.

Chin, D. and A. R. Means (2000). "Calmodulin: a prototypical calcium sensor." Trends in cell biology **10**(8): 322-328.

Chuang, H.-h., et al. (2001). "Bradykinin and nerve growth factor release the capsaicin receptor from PtdIns (4, 5) P2-mediated inhibition." Nature **411**(6840): 957-962.

Chyb, S., et al. (1999). "Polyunsaturated fatty acids activate the Drosophila light-sensitive channels TRP and TRPL." Nature **397**(6716): 255-259.

Ikura, M., et al. (1992). "Solution structure of a calmodulin-target peptide complex by multidimensional NMR." Science **256**(5057): 632-638.

Jiang, L.-H. (2007). "Subunit interaction in channel assembly and functional regulation of transient receptor potential melastatin (TRPM) channels." Biochemical Society Transactions **35**(1): 86-88.

Jiménez-García, B., et al. (2013). "pyDockWEB: a web server for rigid-body protein-protein docking using electrostatics and desolvation scoring." Bioinformatics: btt262.

Jirku, M., et al. (2015). "Characterization of the part of N-terminal PIP2 binding site of the TRPM1 channel." Biophysical chemistry **207**: 135-142.

Julius, D. (2013). "TRP channels and pain." Annual review of cell and developmental biology **29**: 355-384.

Jung, J., et al. (2002). "Agonist recognition sites in the cytosolic tails of vanilloid receptor 1." Journal of Biological Chemistry **277**(46): 44448-44454.

Jurado, L. A., et al. (1999). "Apocalmodulin." Physiological reviews **79**(3): 661-682.

Kang, S. S., et al. (2012). "Human skeletal dysplasia caused by a constitutive activated transient receptor potential vanilloid 4 (TRPV4) cation channel mutation." Experimental & molecular medicine **44**(12): 707-722.

Khelashvili, G., et al. (2012). "Phosphatidylinositol 4, 5-biphosphate (PIP2) lipids regulate the phosphorylation of syntaxin N-terminus by modulating both its position and local structure." Biochemistry **51**(39): 7685-7698.

Kim, D. E., et al. (2004). "Protein structure prediction and analysis using the Robetta server." Nucleic acids research **32**(suppl 2): W526-W531.

Kitazawa, T., et al. (1991). "G-protein-mediated Ca2+ sensitization of smooth muscle contraction through myosin light chain phosphorylation." Journal of Biological Chemistry **266**(3): 1708-1715.

Kohler, J. J. and A. Schepartz (2001). "Kinetic Studies of Fos⊙ Jun⊙ DNA Complex Formation: DNA Binding Prior to Dimerization." Biochemistry **40**(1): 130-142.

Kojetin, D. J., et al. (2006). "Structure, binding interface and hydrophobic transitions of Ca2+-loaded calbindin-D28K." Nature Structural & Molecular Biology **13**(7): 641-647.

Kraft, R. and C. Harteneck (2005). "The mammalian melastatin-related transient receptor potential cation channels: an overview." Pflügers Archiv **451**(1): 204-211.

Kretsinger, R. H. (1976). "Calcium-binding proteins." Annual review of biochemistry **45**(1): 239-266.

Kruse, M., et al. (2009). "Impaired endocytosis of the ion channel TRPM4 is associated with human progressive familial heart block type I." The Journal of clinical investigation **119**(9): 2737-2744.

Kwon, Y., et al. (2007). "Integration of phosphoinositide-and calmodulin-mediated regulation of TRPC6." Molecular cell **25**(4): 491-503.

Lambert, S., et al. (2011). "Transient receptor potential melastatin 1 (TRPM1) is an ion-conducting plasma membrane channel inhibited by zinc ions." Journal of Biological Chemistry **286**(14): 12221-12233.

Lau, S.-Y., et al. (2012). "Distinct properties of Ca2+–calmodulin binding to N-and C-terminal regulatory regions of the TRPV1 channel." The Journal of general physiology **140**(5): 541-555.

Lee, J., et al. (2005). "PIP2 activates TRPV5 and releases its inhibition by intracellular Mg2+." The Journal of general physiology **126**(5): 439-451.

Lemmon, M. A., et al. (1995). "Specific and high-affinity binding of inositol phosphates to an isolated pleckstrin homology domain." Proceedings of the National Academy of Sciences **92**(23): 10472-10476.

Li, M., et al. (2011). Structural biology of TRP channels. Transient Receptor Potential Channels, Springer**:** 1-23.

Li, M. X. and P. M. Hwang (2015). "Structure and function of cardiac troponin C (TNNC1): Implications for heart failure, cardiomyopathies, and troponin modulating drugs." Gene **571**(2): 153-166.

Liao, M., et al. (2013). "Structure of the TRPV1 ion channel determined by electron cryo-microscopy." Nature **504**(7478): 107-112.

Lin, J., et al. (2016). "Atomic resolution experimental phase information reveals extensive disorder and bound 2-methyl-2, 4-pentanediol in Ca2+-calmodulin." Acta Crystallographica Section D: Structural Biology **72**(1): 83-92.

Lishko, P. V., et al. (2007). "The ankyrin repeats of TRPV1 bind multiple ligands and modulate channel sensitivity." Neuron **54**(6): 905-918.

Liu, B., et al. (2005). "Functional recovery from desensitization of vanilloid receptor TRPV1 requires resynthesis of phosphatidylinositol 4, 5-bisphosphate." The Journal of neuroscience **25**(19): 4835-4843.

Liu, D. and E. R. Liman (2003). "Intracellular Ca2+ and the phospholipid PIP2 regulate the taste transduction ion channel TRPM5." Proceedings of the National Academy of Sciences **100**(25): 15160-15165.

Lu, S., et al. (2010). "The correlation of TRPM1 (Melastatin) mRNA expression with microphthalmia-associated transcription factor (MITF) and other melanogenesis-related proteins in normal and pathological skin, hair follicles and melanocytic nevi." Journal of cutaneous pathology **37**(s1): 26-40.

Lukacs, V., et al. (2007). "Dual regulation of TRPV1 by phosphoinositides." The Journal of neuroscience **27**(26): 7070-7080.

Marenholz, I., et al. (2004). "S100 proteins in mouse and man: from evolution to function and pathology (including an update of the nomenclature)." Biochemical and biophysical research communications **322**(4): 1111-1122.

Meador, W. E., et al. (1992). "Target enzyme recognition by calmodulin: 2.4 A structure of a calmodulin-peptide complex." Science **257**(5074): 1251-1255.

Minke, B., et al. (1975). "Induction of photoreceptor voltage noise in the dark in Drosophila mutant." Nature **258**(5530): 84-87.

Montell, C. (2001). "Physiology, phylogeny, and functions of the TRP superfamily of cation channels." Science Signaling **2001**(90): re1-re1.

Montell, C. (2011). "The history of TRP channels, a commentary and reflection." Pflügers Archiv-European Journal of Physiology **461**(5): 499-506.

Montell, C. and G. M. Rubin (1989). "Molecular characterization of the Drosophila trp locus: a putative integral membrane protein required for phototransduction." Neuron **2**(4): 1313-1323.

Morelli, M. B., et al. (2013). "TRP channels: new potential therapeutic approaches in CNS neuropathies." CNS & Neurological Disorders-Drug Targets (Formerly Current Drug Targets-CNS & Neurological Disorders) **12**(2): 274-293.

Mosavi, L. K., et al. (2002). "Consensus-derived structural determinants of the ankyrin repeat motif." Proceedings of the National Academy of Sciences **99**(25): 16029-16034.

Neshich, G., et al. (2003). "STING Millennium: A web-based suite of programs for comprehensive and simultaneous analysis of protein structure and sequence." Nucleic acids research **31**(13): 3386-3392.

Niemeyer, B. A., et al. (2001). "Competitive regulation of CaT-like-mediated Ca2+ entry by protein kinase C and calmodulin." Proceedings of the National Academy of Sciences **98**(6): 3600-3605.

Nilius, B. (2007). "TRP channels in disease." Biochimica et Biophysica Acta (BBA)-Molecular Basis of Disease **1772**(8): 805-812.

Nilius, B., et al. (2006). "The Ca2+-activated cation channel TRPM4 is regulated by phosphatidylinositol 4, 5-biphosphate." The EMBO journal **25**(3): 467-478.

Nilius, B. and G. Owsianik (2011). "The transient receptor potential family of ion channels." Genome Biol **12**(3): 218.

Nilius, B., et al. (2008). "Transient receptor potential channels meet phosphoinositides." The EMBO journal **27**(21): 2809-2816.

Nilius, B., et al. (2008). "Vanilloid transient receptor potential cation channels: an overview." Current pharmaceutical design **14**(1): 18-31.

Nilius, B., et al. (2000). "Whole-cell and single channel monovalent cation currents through the novel rabbit epithelial Ca2+ channel ECaC." The Journal of physiology **527**(2): 239-248.

Numazaki, M., et al. (2003). "Structural determinant of TRPV1 desensitization interacts with calmodulin." Proceedings of the National Academy of Sciences **100**(13): 8002-8006.

Owsianik, G., et al. (2006). "Permeation and selectivity of TRP channels." Annu. Rev. Physiol. **68**: 685-717.

Pattnaik, B. R., et al. (2013). "Snowflake vitreoretinal degeneration (SVD) mutation R162W provides new insights into Kir7. 1 ion channel structure and function." PLoS One **8**(8): e71744.

Paulsen, C. E., et al. (2015). "Structure of the TRPA1 ion channel suggests regulatory mechanisms." Nature.

Pedersen, S. F., et al. (2005). "TRP channels: an overview." Cell calcium **38**(3): 233-252.

Perraud, A.-L., et al. (2001). "ADP-ribose gating of the calcium-permeable LTRPC2 channel revealed by Nudix motif homology." Nature **411**(6837): 595-599.

Pettersen, E. F., et al. (2004). "UCSF Chimera—a visualization system for exploratory research and analysis." Journal of computational chemistry **25**(13): 1605-1612.

Phillips, A. M., et al. (1992). "Identification of a Drosophila gene encoding a calmodulin-binding protein with homology to the trp phototransduction gene." Neuron **8**(4): 631-642.

Plant, T. D. and M. Schaefer (2003). "TRPC4 and TRPC5: receptor-operated Ca 2+-permeable nonselective cation channels." Cell calcium **33**(5): 441-450.

Prawitt, D., et al. (2000). "Identification and characterization of MTR1, a novel gene with homology to melastatin (MLSN1) and the trp gene family located in the BWS-WT2 critical region on chromosome 11p15. 5 and showing allele-specific expression." Human Molecular Genetics **9**(2): 203-216.

Prevarskaya, N., et al. (2007). "Ion channels in death and differentiation of prostate cancer cells." Cell Death & Differentiation **14**(7): 1295-1304.

Prosser, B. L., et al. (2011). "S100A1 and calmodulin regulation of ryanodine receptor in striated muscle." Cell calcium **50**(4): 323-331.

Prosser, B. L., et al. (2008). "S100A1 binds to the calmodulin-binding site of ryanodine receptor and modulates skeletal muscle excitation-contraction coupling." Journal of Biological Chemistry **283**(8): 5046-5057.

Provencher, S. W. and J. Gloeckner (1981). "Estimation of globular protein secondary structure from circular dichroism." Biochemistry **20**(1): 33-37.

Raghu, P. and R. C. Hardie (2009). "Regulation of Drosophila TRPC channels by lipid messengers." Cell calcium **45**(6): 566-573.

Ramsey, I. S., et al. (2006). "An introduction to TRP channels." Annu. Rev. Physiol. **68**: 619-647.

Rezvanpour, A. and G. S. Shaw (2009). "Unique S100 target protein interactions." Gen Physiol Biophys **28**(Spec No Focus): F39-46.

Rhoads, A. R. and F. Friedberg (1997). "Sequence motifs for calmodulin recognition." The FASEB Journal **11**(5): 331-340.

Riazanova, L., et al. (2000). "[Novel type of signaling molecules: protein kinases covalently linked to ion channels]." Molekuliarnaia biologiia **35**(2): 321-332.

Ritterhoff, J. and P. Most (2012). "Targeting S100A1 in heart failure." Gene therapy **19**(6): 613-621.

Rohacs, T. (2013). "Advances in Biological Regulation."

Rohacs, T. (2014). Phosphoinositide regulation of TRP channels. Mammalian Transient Receptor Potential (TRP) Cation Channels, Springer**:** 1143-1176.

Rohács, T., et al. (2005). "PI (4, 5) P2 regulates the activation and desensitization of TRPM8 channels through the TRP domain." Nature neuroscience **8**(5): 626-634.

Rosenbaum, T., et al. (2004). "Ca2+/calmodulin modulates TRPV1 activation by capsaicin." The Journal of general physiology **123**(1): 53-62.

Rosenhouse-Dantsker, A. and D. E. Logothetis (2007). "Molecular characteristics of phosphoinositide binding." Pflügers Archiv-European Journal of Physiology **455**(1): 45-53.

Runnels, L. W., et al. (2001). "TRP-PLIK, a bifunctional protein with kinase and ion channel activities." Science **291**(5506): 1043-1047.

Runnels, L. W., et al. (2002). "The TRPM7 channel is inactivated by PIP2 hydrolysis." Nature cell biology **4**(5): 329-336.

Rustandi, R. R., et al. (2002). "Three-dimensional solution structure of the calcium-signaling protein apo-S100A1 as determined by NMR." Biochemistry **41**(3): 788-796.

Ryazanova, L. V., et al. (2004). "Characterization of the protein kinase activity of TRPM7/ChaK1, a protein kinase fused to the transient receptor potential ion channel." Journal of Biological Chemistry **279**(5): 3708-3716.

Saimi, Y. and C. Kung (2002). "Calmodulin as an ion channel subunit." Annual review of physiology **64**(1): 289-311.

Santella, L. and E. Carafoli (1997). "Calcium signaling in the cell nucleus." The FASEB Journal **11**(13): 1091-1109.

Senguen, F. T. and Z. Grabarek (2012). "X-ray structures of magnesium and manganese complexes with the N-terminal domain of calmodulin: insights into the mechanism and specificity of metal ion binding to an EF-hand." Biochemistry **51**(31): 6182-6194.

Smani, T., et al. (2015). "Functional and physiopathological implications of TRP channels." Biochimica et Biophysica Acta (BBA)-Molecular Cell Research **1853**(8): 1772-1782.

Steinberg, X., et al. (2014). "A structural view of ligand-dependent activation in thermoTRP channels." Front. Physiol **5**: 171.

Strotmann, R., et al. (2003). "Ca2+-dependent potentiation of the nonselective cation channel TRPV4 is mediated by a C-terminal calmodulin binding site." Journal of Biological Chemistry **278**(29): 26541-26549.

Suh, B.-C. and B. Hille (2005). "Regulation of ion channels by phosphatidylinositol 4, 5-bisphosphate." Current opinion in neurobiology **15**(3): 370-378.

Suh, B.-C. and B. Hille (2008). "PIP2 is a necessary cofactor for ion channel function: how and why?" Annual review of biophysics **37**: 175.

Takada, Y., et al. (2013). "Targeting TRPs in neurodegenerative disorders." Current topics in medicinal chemistry **13**(3): 322-334.

Takahashi, N., et al. (2013). "TRP channels: sensors and transducers of gasotransmitter signals." Gasotransmitters: novel regulators of ion channels and transporters: 21.

Tong, Q., et al. (2006). "Regulation of the transient receptor potential channel TRPM2 by the Ca2+ sensor calmodulin." Journal of Biological Chemistry **281**(14): 9076-9085.

Toutenhoofd, S. and E. Strehler (2000). "The calmodulin multigene family as a unique case of genetic redundancy: multiple levels of regulation to provide spatial and temporal control of calmodulin pools?" Cell calcium **28**(2): 83-96.

Trebak, M., et al. (2007). Phospholipase C-coupled receptors and activation of TRPC channels. Transient Receptor Potential (TRP) Channels, Springer**:** 593-614.

TROST, C., et al. (2001). "The transient receptor potential, TRP4, cation channel is a novel member of the family of calmodulin binding proteins." Biochemical Journal **355**(3): 663-670.

Tsavaler, L., et al. (2001). "Trp-p8, a novel prostate-specific gene, is up-regulated in prostate cancer and other malignancies and shares high homology with transient receptor potential calcium channel proteins." Cancer Research **61**(9): 3760-3769.

van de Graaf, S. F., et al. (2003). "Functional expression of the epithelial Ca2+ channels (TRPV5 and TRPV6) requires association of the S100A10–annexin 2 complex." The EMBO journal **22**(7): 1478-1487.

Vennekens, R., et al. (2000). "Permeation and gating properties of the novel epithelial Ca2+ channel." Journal of Biological Chemistry **275**(6): 3963-3969.

Vennekens, R., et al. (2012). TRPs in the brain. Reviews of Physiology, Biochemistry and Pharmacology, Vol. 163, Springer**:** 27-64.

Voets, T. and B. Nilius (2003). "TRPs make sense." The Journal of membrane biology **192**(1): 1-8.

Whitmore, L. and B. A. Wallace (2008). "Protein secondary structure analyses from circular dichroism spectroscopy: methods and reference databases." Biopolymers **89**(5): 392-400.

Whorton, M. R. and R. MacKinnon (2011). "Crystal structure of the mammalian GIRK2 K+ channel and gating regulation by G proteins, PIP 2, and sodium." Cell **147**(1): 199-208.

Wiederstein, M. and M. J. Sippl (2007). "ProSA-web: interactive web service for the recognition of errors in three-dimensional structures of proteins." Nucleic acids research **35**(suppl 2): W407-W410.

Wriggers, W., et al. (1998). "Structure and dynamics of calmodulin in solution." Biophysical journal **74**(4): 1622-1639.

Wright, N. T., et al. (2008). "S100A1 and calmodulin compete for the same binding site on ryanodine receptor." Journal of Biological Chemistry **283**(39): 26676-26683.

Wright, N. T., et al. (2005). "The three-dimensional solution structure of Ca 2+-bound S100A1 as determined by NMR spectroscopy." Journal of molecular biology **353**(2): 410-426.

Wymann, M. P. and R. Schneiter (2008). "Lipid signalling in disease." Nature Reviews Molecular Cell Biology **9**(2): 162-176.

Xie, J., et al. (2011). "Phosphatidylinositol 4, 5-bisphosphate (PIP2) controls magnesium gatekeeper TRPM6 activity." Scientific reports **1**.

Yang, J., et al. (2015). "The I-TASSER Suite: protein structure and function prediction." Nature methods **12**(1): 7-8.

Yap, K. L., et al. (2000). "Calmodulin target database." Journal of structural and functional genomics **1**(1): 8-14.

Yudin, Y., et al. (2011). "Decrease in phosphatidylinositol 4, 5-bisphosphate levels mediates desensitization of the cold sensor TRPM8 channels." The Journal of physiology **589**(24): 6007-6027.

Zhu, M. X. (2005). "Multiple roles of calmodulin and other Ca2+-binding proteins in the functional regulation of TRP channels." Pflügers Archiv **451**(1): 105-115.

Zubcevic, L., et al. (2016). "Cryo-electron microscopy structure of the TRPV2 ion channel." Nature Structural & Molecular Biology.

8. LIST OF PUBLICATIONS

Appendix 1

Bily J, Grycova L, Holendova B, Jirku M, Janouskova H, **Bousova K**, Teisinger J., Characterization of the S100A1 protein binding site on TRPC6 C-terminus. PLoS One. 2013, 3;8(5):e62677. doi: 10.1371/journal.pone.0062677.

Appendix 2

Grycova L, Holendova B, Lansky Z, Bumba L, Jirku M, **Bousova K**, Teisinger J., Ca(2+) binding protein S100A1 competes with calmodulin and PIP2 for binding site on the C-terminus of the TPRV1 receptor. ACS Chem Neurosci. 2015, 18;6(3):386-92. doi: 10.1021/cn500250r.

Appendix 3

Bousova K, Jirku M, Bumba L, Bednarova L, Sulc M, Franek M, Vyklicky L, Vondrasek J, Teisinger J., PIP2 and PIP3 interact with N-terminus region of TRPM4 channel. Biophys Chem. 2015, 205:24-32. doi: 10.1016/j.bpc.2015.06.004.

Appendix 4

Jirku M, Bumba L, Bednarova L, Kubala M, Sulc M, Franek M, Vyklicky L, Vondrasek J, Teisinger J, **Bousova K**, Characterization of the part of N-terminal PIP2 binding site of the TRPM1 channel. Biophys Chem. 2015, 207:135-42. doi: 10.1016/j.bpc.2015.10.005.

APPENDIX 1

Bily J, Grycova L, Holendova B, Jirku M, Janouskova H, **Bousova K**, Teisinger J., Characterization of the S100A1 protein binding site on TRPC6 C-terminus. PLoS One. 2013, 3;8(5):e62677. doi: 10.1371/journal.pone.0062677.

OPEN ACCESS Freely available online

PLOS ONE

Characterization of the S100A1 Protein Binding Site on TRPC6 C-Terminus

Jan Bily, Lenka Grycova, Blanka Holendova, Michaela Jirku, Hana Janouskova, Kristyna Bousova, Jan Teisinger*

Department of Protein Structures, Institute of Physiology, Academy of Sciences of the Czech Republic, Prague, Czech Republic

Abstract

The transient receptor potential (TRP) protein superfamily consists of seven major groups, among them the ''canonical TRP'' family. The TRPC proteins are calcium-permeable nonselective cation channels activated after the emptying of intracellular calcium stores and appear to be gated by various types of messengers. The TRPC6 channel has been shown to be expressed in various tissues and cells, where it modulates the calcium level in response to external signals. Calcium binding proteins such as Calmodulin or the family of S100A proteins are regulators of TRPC channels. Here we characterized the overlapping integrative binding site for S100A1 at the C-tail of TRPC6, which is also able to accomodate various ligands such as Calmodulin and phosphatidyl-inositol-(4,5)-bisphosphate. Several positively charged amino acid residues (Arg852, Lys856, Lys859, Arg860 and Arg864) were determined by fluorescence anisotropy measurements for their participation in the calcium-dependent binding of S100A1 to the C terminus of TRPC6. The triple mutation Arg852/Lys859/Arg860 exhibited significant disruption of the binding of S100A1 to TRPC6. This indicates a unique involvement of these three basic residues in the integrative overlapping binding site for S100A1 on the C tail of TRPC6.

Citation: Bily J, Grycova L, Holendova B, Jirku M, Janouskova H, et al. (2013) Characterization of the S100A1 Protein Binding Site on TRPC6 C-Terminus. PLoS ONE 8(5): e62677. doi:10.1371/journal.pone.0062677

Editor: Mark J. van Raaij, Centro Nacional de Biotecnologia - CSIC, Spain

Received January 21, 2013; **Accepted** March 24, 2013; **Published** May 3, 2013

Funding: This work was supported by grant 301/10/1159 of the Grant Agency of the Czech Republic, grant P205/10/P308 of the Grant Agency of the Czech Republic and from institutional project of the Institute of Physiology (RVO: 67985823) and institutional project of the Institute of Microbiology, Academy of Sciences of the Czech Republic (RVO: 61388971). The funders had no role in study design, data collection and analysis, decision to publish, or preparation of the manuscript.

Competing Interests: The authors have declared that no competing interests exist.

* E-mail: teisingr@biomed.cas.cz

Introduction

TRPC6 is a member of a large group of transient receptor potential (TRP) channels, a diverse group of cation-permeable channels. This family includes more than 30 proteins that play critical roles in various biological processes [1]. They are widely expressed in the nervous system and non-excitable cells. TRP channels are involved in many physiological processes, they are important regulators of cation homeostasis in cells and many of them serve as biological sensors for the detection of various environmental stimuli [2]. TRP channels can be divided into seven subfamilies (C - canonical, V - vanilloid, M - melastatin, ML - mucolipin, P - polycystin, A – ankyrin, N – no mechanoreceptor potential C) on the basis of sequence homology [3]. TRP channels contain six putative transmembrane domains, a pore region between domain 5 and 6, and amino- and carboxy- intracellular termini [3,4]. Many conserved domains have been identified within the intracellular termini, and they serve as important interaction sites for various regulatory molecules [2].

Members of the TRPC subfamily (TRPC1-TRPC7) typically contain 3–4 ankyrin repeats on their N-terminus and a conserved region called TRP box at the C-terminus, also present in TRPVs and TRPMs. These channels are non-selectively permeable to cations, nevertheless their selectivity for calcium over sodium varies among their members. It has been proposed that TRPC channels can be activated by the stimulation of phospholipase C, but a number of different modulators such as signaling proteins, cytoskeletal elements, scaffold molecules and also other ion channels have been reported to modulate their activity. All TRPC channels have been described as store-operated channels (SOCs), that are activated when intracellular Ca^{2+} stores become depleted [5].

TRPC6 was reported to be modulated by Ca^{2+} ions together with calmodulin (CaM) [6,7,8]. The CaM binding region on the C-terminus was described in detail [6,8]. The domain contains several consensus CaM binding motifs with hydrophobic residues in specific positions and was also shown to interact with the IP3 receptor (IP3R) and described as the so-called CaM and IP3R binding domain (CIRB) conserved among all TRPC members [6].

S100A proteins are a large family of calcium-binding proteins found in *Vertebrates*. It was assumed that these proteins simply function as cellular calcium buffers, but they have been later reported to take part in the regulation of many cellular processes [9].

S100A1 is a small dimeric protein that is highly expressed in cardiomyocytes, and also in fast and slow twitch muscles, brain and hippocampal neurons [10]. It contains two EF-hand motifs that are able to bind Ca^{2+} ions, causing a conformational change by moving one helix and exposing a broad hydrophobic surface that enables the protein to interact with a variety of target proteins and ion channels [11,12]. In contrast to CaM, the first EF hand motif binds Ca^{2+} with a lower affinity than the second EF hand [13,14].

The TRPC6 channel modulates the calcium levels in eukaryotic cells, including sensory receptor cells in response to external signals. Its activity is modulated by multiple factors. It was recently shown that CaM, a Ca^{2+} binding protein, acts as an important mediator of Ca^{2+}-dependent regulation [6,8] and the interaction site was characterized [7,8]. S100A1 behaves similarly in terms of mediating the activity of other ion channels [15,16]. For this reason we tested the binding of the S100A1 protein to TRPC6 C-terminus (CT) (801–878), which interacts directly with CaM [7,8]. Using site-directed mutagenesis of the predicted basic amino acid residues of TPRC6 CT combined with steady-state fluorescence anisotropy measurements, we found that the S100A1 protein is able to bind to the TRPC6 C-terminus. Moreover, this binding site overlaps with the previously reported CIRB binding site on the same receptor.

Materials and Methods

TRPC6 Cloning, Expression and Purification

The coding region for the C-terminal part of rat TRPC6 (amino acids 801–878) was cloned into the pET42b expression vector (Novagen). Point mutations of several basic amino acids, namely Arg852, Arg864, Lys 856 and Ile 857, as well as the triple substitutions Arg852/Lys859/Arg860 and Lys859/Arg860/Arg864 were performed by site-directed mutagenesis according to the manufacturer's protocol (Stratagene). All the constructs were confirmed by DNA sequencing.

The proteins were expressed as fusion proteins with a His-tag on their C-termini in *E. coli* Rosetta cells (Novagen). The expression of the proteins was induced by 0.5 mM isopropyl-1-thio-β-D-galactopyranoside for 16 hours at 20°C. The proteins were purified by Chelating Sepharose Fast Flow (Amersham Biosciences) according to the manufacturer's protocol. Gel permeation chromatography on Superdex 75 (Amersham Biosciences) was used as a final purification step. A 25 mM Tris-HCl buffer (pH 7.5) containing 500 mM NaCl and 2 mM $CaCl_2$ was used for the elution. The protein samples were concentrated using spin columns (Millipore) and the purity was verified by 15% SDS-PAGE (Fig. S1). The concentration of the constructs was estimated by measuring absorbance at 280 nm. The integrity of the proteins was verified by MS-MS analysis. The expression and purification of the (His)6-tagged proteins was described in detail previously [17].

S100A1 Protein Cloning, Expression, Purification and Labeling

cDNA coding for human S100A1 was cloned into the pET28b expression vector (Novagen). The protein was expressed in E.coli BL21 cells. Its expression was induced by 0.5 mM isopropyl-1-thio-b-D-galactopyranoside for 12 hours at 25°C. The protein was purified using Phenyl Sepharose CL4B (Amersham Biosciences) equilibrated with 50 mM Tris-HCl (pH 7.5), 100 mM NaCl, 2 mM $CaCl_2$. Bound S100A1 was eluted with 50 mM Tris-HCl (pH 7.5), 100 mM NaCl, 1.5 mM EDTA and concentrated using a spin column for protein concentration (Millipore). Concentrated protein solution was loaded into a Superdex 75 column (Amersham Pharmacia Biotech) and eluted with 25 mM Tris-HCl (pH 7.5), 100 mM NaCl, 2 mM $CaCl_2$ as a final purification step. The purity of the protein was verified by 15% SDS-PAGE (Fig. S2). The concentration of the protein was assessed by BCA's assay using BSA as a standard protein [18].

The S100A1 protein was then dialyzed against 10 mM $NaHCO_3$ buffer (pH 10.0) and 100 mM NaCl for 8 hours at 4°C. The protein sample was mixed with 0.6 dansyl chloride (DNS) solution (Sigma) in a molar ratio of 1:1.5 and incubated at 4°C for 12 h. The sample was dialyzed for 8 hours against 25 mM Tris-HCl (pH 7.5), 150 mM NaCl and 2 mM EDTA to remove the free DNS-chloride and then against the same buffer containing 2 mM $CaCl_2$ instead of EDTA at 4°C overnight [19]. The incorporation stoichiometry was determined by comparing the peak protein absorbance at 280 nm with the absorbance of the bound DNS measured at 340 nm, using an extinction coefficient of 4,300 m^{-1} $cm^{-1}T$ [20].

Steady-state Fluorescence Anisotropy Measurements

Steady-state fluorescence anisotropy measurements were used as a binding assay to determine the binding affinity between fluorescently labeled S100A1 protein and the C-terminal part of TRPC6 and its mutants. The experiment was performed using an ISS PC1^{TM} photon-counting spectrofluorimeter The monochromator excitation and emission wavelengths were set to 340 nm and 520 nm for all measurements. The fraction of bound TRPC6 protein (FB) was calculated from the equation 1:

$$F_B = \frac{(r_{obs} - r_{min})}{(r_{max} - r_{obs})Q + (r_{obs} - r_{min})}$$

where r_{obs} is the observed anisotropy for any TRPC6 protein concentration, r_{max} is the anisotropy at saturation and r_{min} is the minimum observed anisotropy for the free DNS-S100A1. The parameter Q represents the quantum yield ratio of the bound to the free form, and was estimated by calculating the ratio of the intensities of the bound to the free fluorophore. To determine the equilibrium dissociation constant (K_D), the values of the bound fraction of the protein were plotted against the TRPC6 protein concentration and fitted using the equation 2:

$$F_B = \frac{K_D + [P_1] + [P_2] - \sqrt{(K_D + [P_1] + [P_2])^2 - 4[P_1][P_2]}}{2[P_1]}$$

where K_D is the equilibrium dissociation constant, [P1] is the DNS-S100A1 concentration, and [P2] is the concentration of the TRPC6 protein. Non-linear data fitting was performed using the program SigmaPlot10 [17]. All experiments were carried out in at least triplicate.

Mass Spectrometric Analysis

The excised protein band from SDS-PAGE, TRPC6, was digested with trypsin endoprotease (Promega) directly in the gel after destaining and cysteine modification by iodoacetamide [21]. The resulting peptide mixture was extracted, loaded onto the MALDI-TOF target with α-cyano-4-hydroxycinnamic acid as the matrix, and positively charged spectra or MS/MS were acquired using an UltraFLEX III mass spectrometer (Bruker-Daltonics, Bremen, Germany) with internal calibration (monoisotopic $[M+H]^+$ ions of the TRPC6 peptides with known sequences).

Circular Dichroism Spectroscopy

Circular dichroism (CD) experiments were carried out in a Jasco J-815 spectrometer (Tokyo, Japan). The protein concentration was kept constant for all measured samples and was 0.35 mg/ml. The spectra were collected from 200 to 300 nm using a 0.1 cm quartz cell at room temperature. A 0.5 nm step resolution, 20 nm/min speed, 8 s response time and 1 nm bandwidth were used. After baseline correction, the final spectra were expressed as a molar

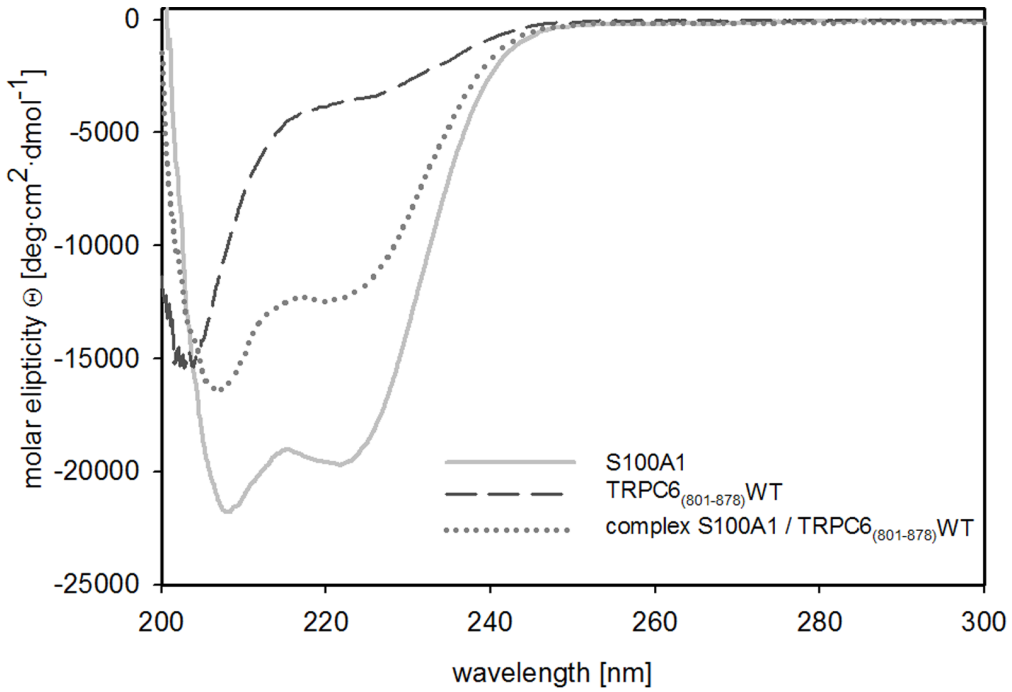

Figure 1. Circular dichroism spectroscopy measurement of TRPC6$_{(801–878)}$WT, S100A1 and the complex of S100A1 and TRPC6 $_{(801–878)}$WT. Examples of CD spectra of TRPC6$_{(801–878)}$WT, S100A1 and the complex of S100A1 and TRPC6 $_{(801–878)}$WT expressed as a molar elipticity Q (deg·cm^2·dmol^{-1}) per residue.
doi:10.1371/journal.pone.0062677.g001

elipticity Q (deg·cm^2·dmol^{-1}) per residue. Secondary structure content was estimated using Dichroweb software [22].

Results and Discussion

TRPC6 and S100A1 Expression and Purification

The TRPC6 C-terminal protein construct (801–878) and its mutants were expressed as fusion proteins with a 6x His-tag on their C-termini in E. coli Rosetta cells. The S100A1 protein was expressed in E.coli BL21 cells. All proteins were purified by a two-step purification process. The proteins were soluble and in sufficient amount to perform the binding experiments (Fig. S1 and S2). The integrity of the proteins was verified by circular dichroism spectroscopy measurement. Numerical analysis of the experimental spectra enabled estimation of the relative abundance of the various secondary structure elements. (Fig. 1, Tab. 1). The α-helical conformation (66%) was found to be the major component of the S100A1 protein, which is in good agreement with the conformation found in its native state. The structure of the TRPC6 C-terminus is unknown. According to the theoretical prediction of the secondary structural elements using computational tools, the region was predicted to be mostly unordered. The CD spectra analysis confirmed the theoretical prediction, suggesting that the TRPC6 protein construct was adopting its native form. The experiment was also used to observe changes in the secondary structural elements during the creation of the TRPC6/S100A1 complex (Fig 1, Tab 1). We compared the CD spectrum of the complex with the CD spectra of the proteins alone. Because the CD spectra of the mixture are the sum of the TRPC6 protein construct and S100A1 individually, we suggest that the changes in the secondary structure of TRPC6 (801–878) have no significant effect on its binding to S100A1.

S100A1 Binds to TRPC6 (801–878) C-terminus

S100 protein family is known to act as calcium-signaling molecules by converting changes in cellular calcium levels to a variety of biological responses. In this manner, many of the S100 proteins have been shown to modulate enzyme activities, oligomerization of cytoskeletal protein components (tubulin, desmin, glial fibrillary acidic protein), modulate ubiquitination,

Table 1. Calculated incidence (%) of secondary structures of S100A1 and TRPC6$_{(801–878)}$ WT and TRPC6 single mutant R852A and complex of TRPC6$_{(801–878)}$ WT/S100A1.

Protein	Helix	Antiparallel	Parallel	Beta Turn	Random Coil
TRPC6$_{(801–878)}$WT	0,18	0,15	0,12	0,20	0,36
TRPC6$_{(801–878)}$ R852A	0,22	0,14	0,11	0,20	0,34
S100A1	0,66	0,03	0,03	0,12	0,15
S100A1+ TRPC6$_{(801–878)}$WT	0,43	0,07	0,07	0,17	0,25

doi:10.1371/journal.pone.0062677.t001

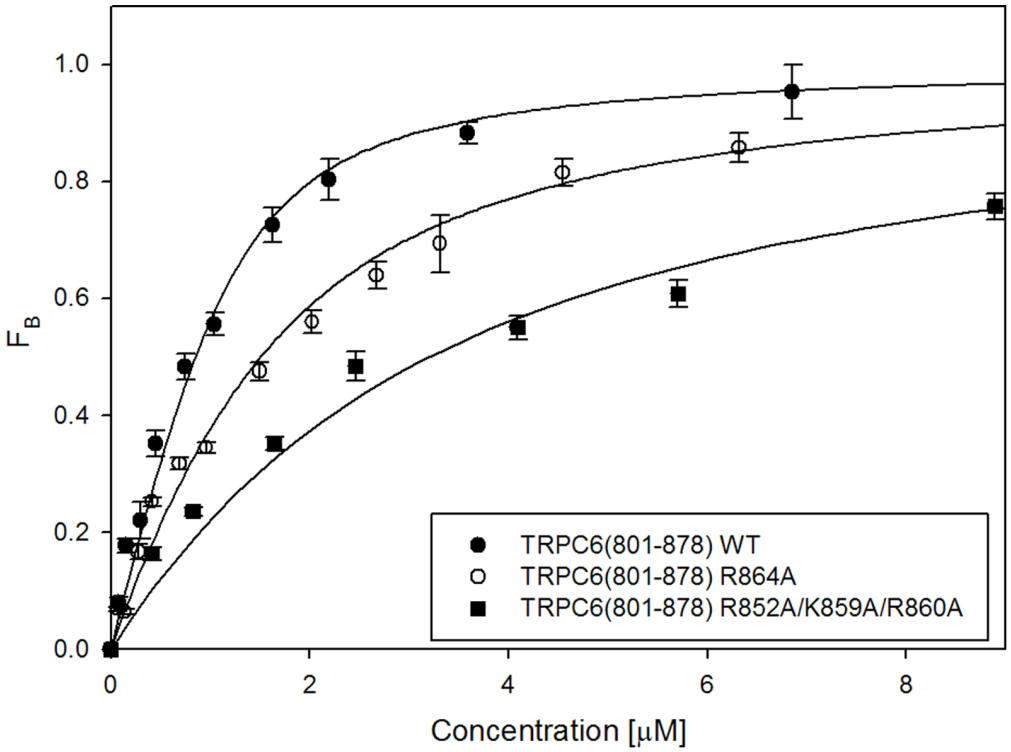

Figure 2. Steady-state fluorescence anisotropy measurement of TRPC6$_{(801–878)}$ WT and selected mutants to fluorescently labeled S100A1 protein. DNS- S100A1 protein (232 μM) was titrated with TRPC6 fusion protein and the Fb was calculated using equation 1 as was described in material and methods.Binding isotherms and dissociatin constants were calculated by fitting the data to the equation 2 as was described in material and methods. Values are expressed as the mean ± standard deviation (SD) measured from at least from three independent experiments. Binding isotherms of wild-type TRPC6 $_{(801–878)}$ is represented as black circles, single mutant is TRPC6$_{(801–878)}$ R864A as white circles and triple mutant TRPC6$_{(801–878)}$ K859A/R860A/R864A as black squares.
doi:10.1371/journal.pone.0062677.g002

control membrane vesicle formation and participate in trafficking of proteins to the inner surface of the plasma membrane [11]. The interaction between the transient receptor potential cation channel proteins TRPV5 and TRPV6 with S100A10 has been shown using two-hybrid and co-immunoprecipitation experiments [23,24]. In this role, the S100A10-annexin A2 complex is thought mediate trafficking of the TRV5 and TRV6 proteins to the plasma membrane where they act as calcium-selective channels. Recently our research group has also shown a direct interaction between S100A1 protein and TRPM3 ion channel, where this protein was able to compete with CaM for the overlapping binding site [25].

The protein samples were used for steady-state fluorescence anisotropy measurement to characterize the binding ability of the S100A1 protein to TRPC6 C-terminal region 801–878. Increasing amounts of the TRPC6 protein construct were titrated into the DNS-S100A1 solution. The equilibrium dissociation constant of the TRPC6$_{(801–878)}$/Ca^{2+}-S100A1 complex was estimated to be 0.31+/−0.04 μM (Fig. 2). The value of the equilibrium dissociation constant is nearly the same as was estimated for CaM binding to be 0.320+/−0.019 μM [8]. As the amino acid residues important for CaM binding are known (Fig. 3), we tested their role in S100A1 binding (Fig. 2). The single substitution of R852A and triple substitution of K859A/R860A/R864A had almost no effect on its binding. (Fig. 2, Tab. 2). Interestingly, in comparison to the CaM binding, where the neutralization of this residue had the most striking effect [8], the R852 residue did not influence the interaction with S100A1 at all. Although the TRPC6 WT binding affinities to both ligands CaM and S100A1 are almost the same, according to the results we obtained it seems that different residues are involved in the binding. The mutations of K856A and R864A

NKRNEEKKFG ISGSHEDLSK FSLDKNQLAH NKQSSTRSSE

DYHLNSFSNP PRQYQKIMKR LIKRYVLQAQ IDKESDEV

Figure 3. Amino acid senquence of TRPC6 fusion protein. Native rat TRPC6 801–878 amino acid sequence containing integrative binding site was investigated. Predicted important basic amino acids that were replaced by alanine are in red.
doi:10.1371/journal.pone.0062677.g003

Table 2. Summary of estimated equilibrium dissociation constants of the complex of TRPC6$_{(801–878)}$WT and its mutants with S100A1.

Protein	$K_{D/\mu}M$
TRPC6$_{(801–878)}$*WT*	0.31+−0.04
TRPC6$_{(801–878)}$ R852A	0.48+−0.11
TRPC6$_{(801–878)}$ K856A	0.76+−0.09
TRPC6$_{(801–878)}$ R864A	0.92+−0.08
TRPC6$_{(801–878)}$R852A/K859A/R860A	2.62+−0.22
TRPC6$_{(801–878)}$K859A/R860A/R864A	0.40+−0.05

doi:10.1371/journal.pone.0062677.t002

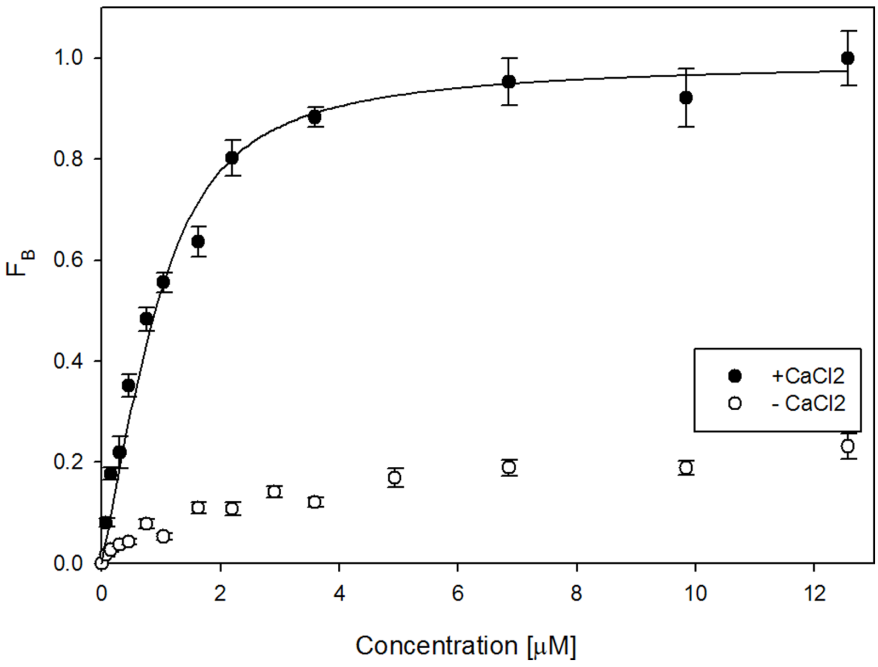

Figure 4. Steady-state fluorescence anisotropy measurement of interaction between TRPC6$_{(801–878)}$ WT and DNS- S100A1 protein in presence and absence of calcium ions. Titration of DNS-S100A1 protein (232 μM) with TRPC6 fusion protein in presence of calcium ions resulted in an increase of bound fraction (Fb) (white dots) compared to when the DNS-S100A1 protein was titrated with TRPC6 fusion protein in absence of of calcium ions (black dots). Values are expressed as the mean ± standard deviation (SD) measured from at least three independent experiments.
doi:10.1371/journal.pone.0062677.g004

lead to an up to 3-fold decrease in the binding affinity to S100A1. These results are in a good agreement with TRPC6/CaM binding data. The R852A/K859A/R860A triple mutation caused the most significant decrease in binding ability (Tab. 2).

Binding of TRPC6 801–878 to S100A1 is Calcium-dependent

Since S100A1 is a Ca^{2+}-binding protein and Ca^{2+} ions play a crucial role in TRPC6 activity regulation, the role of calcium ions in S100A1 binding to TRPC6 (801–878) was assessed. The experiment was performed in a solution without calcium. There was no increase in fluorescence anisotropy when calcium was absent (Fig. 4), suggesting that the binding is calcium-dependent. The same behavior has been detected for the CaM/TRPC6– CT (801–878) interaction [8].

In this report the interaction of the Ca^{2+}-binding protein S100A1 with the conserved region (801–878) of the TRPC6-CT was investigated. We found that these proteins bind with high affinity and the binding is Ca^{2+}-dependent, analogous to that of CaM. According to our results, the interaction is similar but not exactly the same, because different residues are essential for the interaction. Here we show the role of some basic amino acid residues from the so-called CIRB region of TRPC6 affecting its binding to S100A1. These results could suggest potential physiological consequences which will need further investigation.

Supporting Information

Figure S2 Final purification step of the S100A1 protein. Chromatogram and SDS-PAGE of fractions 1-6 after gel chromatography on Sephadex 75.
(DOCX)

Figure S1 Final purification step of the protein construct TRPC6 (801–878). Chromatogram and SDS-PAGE of fractions 1–9 after the gel chromatography on Sephadex 75.
(DOCX)

Acknowledgments

We would like to thank Dr. L. Bednarova from the Institute of Organic Chemistry and Biochemistry of the Academy of Sciences of the Czech Republic for her assistance with CD spectra measurements.

Author Contributions

Conceived and designed the experiments: JB LG BH MJ HJ KB JT. Performed the experiments: JB LG BH MJ HJ KB JT. Analyzed the data: JB LG BH MJ HJ KB JT. Contributed reagents/materials/analysis tools: JB LG BH MJ HJ KB JT. Wrote the paper: JB LG BH JT.

References

1. Ramsey IS, Delling M, Clapham DE (2006) AN INTRODUCTION TO TRP CHANNELS. Annual Review of Physiology 68: 619–647.
2. Minke B (2006) TRP channels and Ca2+ signaling. Cell Calcium 40: 261–275.
3. Pedersen S, Owsianik G, Nilius B (2005) TRP channels: An overview. Cell Calcium 38: 233–252.
4. Clapham DE, Runnels LW, Strubing C (2001) The TRP ion channel family. Nature Reviews Neuroscience 2: 387–396.
5. Nilius B, Owsianik G, Voets T, Peters JA (2007) Transient Receptor Potential Cation Channels in Disease. Physiological Reviews 87: 165–217.
6. Zhu MX (2005) Multiple roles of calmodulin and other Ca(2+)-binding proteins in the functional regulation of TRP channels. Pflugers Arch 451: 105–115.
7. Kwon Y, Hofmann T, Montell C (2007) Integration of phosphoinositide- and calmodulin-mediated regulation of TRPC6. Molecular Cell 25: 491–503.

8. Friedlova E, Grycova L, Holakovska B, Silhan J, Janouskova H, et al. (2010) The interactions of the C-terminal region of the TRPC6 channel with calmodulin. Neurochemistry International 56: 363–366.
9. Wright NT, Cannon BR, Zimmer DB, Weber DJ (2009) S100A1: Structure, Function, and Therapeutic Potential. Curr Chem Biol 3: 138–145.
10. Zimmer DB, Chaplin J, Baldwin A, Rast M (2005) S100-mediated signal transduction in the nervous system and neurological diseases. Cell Mol Biol (Noisy-le-grand) 51: 201–214.
11. Santamaria-Kisiel L, Rintala-Dempsey AC, Shaw GS (2006) Calcium-dependent and -independent interactions of the S100 protein family. Biochemical Journal 396: 201–214.
12. Zimmer DB, Landar A (1995) Analysis of S100A1 expression during skeletal muscle and neuronal cell differentiation. J Neurochem 64: 2727–2736.
13. Rustandi RR, Baldisseri DM, Inman KG, Nizner P, Hamilton SM, et al. (2001) Three-Dimensional Solution Structure of the Calcium-Signaling Protein Apo-S100A1 As Determined by NMR†,‡. Biochemistry 41: 788–796.
14. Wright NT, Varney KM, Ellis KC, Markowitz J, Gitti RK, et al. (2005) The Three-dimensional Solution Structure of Ca2+-bound S100A1 as Determined by NMR Spectroscopy. Journal of Molecular Biology 353: 410–426.
15. Wright NT, Prosser BL, Varney KM, Zimmer DB, Schneider MF, et al. (2008) S100A1 and calmodulin compete for the same binding site on ryanodine receptor. J Biol Chem 283: 26676–26683.
16. Treves S, Scutari E, Robert M, Groh S, Ottolia M, et al. (1997) Interaction of S100A1 with the Ca2+ Release Channel (Ryanodine Receptor) of Skeletal Muscle†. Biochemistry 36: 11496–11503.
17. Grycova L, Lansky Z, Friedlova E, Obsilova V, Janouskova H, et al. (2008) Ionic interactions are essential for TRPV1 C-terminus binding to calmodulin. Biochemical and Biophysical Research Communications 375: 680–683.
18. Smith PK, Krohn RI, Hermanson GT, Mallia AK, Gartner FH, et al. (1985) Measurement of protein using bicinchoninic acid. Analytical Biochemistry 150: 76–85.
19. Kincaid RL, Vaughan M, Osborne JC, Tkachuk VA (1982) Ca2+-dependent interaction of 5-dimethylaminonaphthalene-1-sulfonyl-calmodulin with cyclic nucleotide phosphodiesterase, calcineurin, and troponin I. Journal of Biological Chemistry 257: 10638–10643.
20. Johnson JD, Collins JH, Potter JD (1978) Dansylaziridine-labeled troponin C. A fluorescent probe of Ca2+ binding to the Ca2+-specific regulatory sites. Journal of Biological Chemistry 253: 6451–6458.
21. Prochazkova K, Osicka R, Linhartova I, Halada P, Sulc M, et al. (2005) The Neisseria meningitidis outer membrane lipoprotein FrpD binds the RTX protein FrpC. J Biol Chem 280: 3251–3258.
22. Holakovska B, Grycova L, Bily J, Teisinger J (2011) Characterization of calmodulin binding domains in TRPV2 and TRPV5 C-tails. Amino Acids 40: 741–748.
23. Borthwick LA, Neal A, Hobson L, Gerke V, Robson L, et al. (2008) The annexin 2-S100A10 complex and its association with TRPV6 is regulated by cAMP/PKA/CnA in airway and gut epithelia. Cell Calcium 44: 147–157.
24. van de Graaf SFJ, Hoenderop JGJ, Gkika D, Lamers D, Prenen J, et al. (2003) Functional expression of the epithelial Ca2+ channels (TRPV5 and TRPV6) requires association of the S100A10-annexin 2 complex. EMBO J 22: 1478–1487.
25. Holakovska B, Grycova L, Jirku M, Sulc M, Bumba L, et al. (2012) Calmodulin and S100A1 Protein Interact with N Terminus of TRPM3 Channel. Journal of Biological Chemistry 287: 16645–16655.

APPENDIX 2

Grycova L, Holendova B, Lansky Z, Bumba L, Jirku M, **Bousova K**, Teisinger J., Ca(2+) binding protein S100A1 competes with calmodulin and PIP2 for binding site on the C-terminus of the TPRV1 receptor. ACS Chem Neurosci. 2015, 18;6(3):386-92. doi: 10.1021/cn500250r.

ACS Chemical Neuroscience

Letter

pubs.acs.org/chemneuro

Ca^{2+} Binding Protein S100A1 Competes with Calmodulin and PIP2 for Binding Site on the C-Terminus of the TPRV1 Receptor

Lenka Grycova,*[,†] Blanka Holendova,[†] Zdenek Lansky,[‡,∥] Ladislav Bumba,[§] Michaela Jirku,[†] Kristyna Bousova,[†] and Jan Teisinger*[,†]

[†]Institute of Physiology, [‡]Institute of Biotechnology, and [§]Institute of Microbiology, AS CR, v.v.i., Videnska 1083, 142 20 Prague 4, Czech Republic

[∥]B CUBE - Center for Molecular Bioengineering, Technische Universität Dresden, Arnoldstrasse 18, 01307 Dresden, Germany

ABSTRACT: Transient receptor potential vanilloid 1 ion channel (TRPV1) belongs to the TRP family of ion channels. These channels play a role in many important biological processes such as thermosensation and pain transduction. The TRPV1 channel was reported to be also involved in nociception. Ca^{2+} ions are described to participate in the regulation of TRP channels through the interaction with Ca^{2+}-binding proteins, such as calmodulin or S100A1. Calmodulin is involved in the Ca^{2+}-dependent regulation of TRPV1 via its binding to the TRPV1 C-terminal region. However, the role of the Ca^{2+}-binding protein S100A1 in the process of TRP channel regulation remains elusive. Here we characterized a region on the TRPV1 C-terminus responsible for the interaction with S100A1 using biochemical and biophysical tools. We found that this region overlaps with previously identified calmodulin and PIP2 binding sites and that S100A1 competes with calmodulin and PIP2 for this binding site. We identified several positively charged residues within this region, which have crucial impact on S100A1 binding, and we show that the reported S100A1−TRPV1 interaction is calcium-dependent. Taken together, our data suggest a mechanism for the mutual regulation of PIP2 and the Ca^{2+}-binding proteins S100A1 and calmodulin to TRPV1.

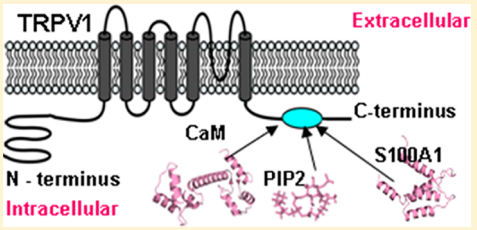

KEYWORDS: *TRPV1, vanilloid receptor, calmodulin, S100A1, calcium binding protein, surface plasmon resonance, fluorescence anisotropy*

The TRPV1 receptor is a member of the TRP channel family. This channel functions as a polymodal signal transducer of noxious stimuli. Recently, its predicted tetrameric structure and the membrane topology of its subunits have been confirmed: TRPV1 consists of six transmembrane helixes with a central pore region located between the fifth and the sixth transmembrane domain.[1] These structural features were verified by cryo-microscopy with sufficient resolution to reveal the principles of its gating mechanisms.[2] The intracellular termini contain important interaction sites for its agonists and regulatory molecules such as adenosine triphosphate (ATP), calmodulin, (CaM) and phosphatidyl inositol-4,5-bisphosphate (PIP2);[3−9] however, the structure of the intracellular regions has been solved only partially. The crystal structure of the isolated TRPV1 ankyrin repeat domain on the N-tail is the only known intracellular part.[3]

The activity of TRP channels is modulated by a wide range of stimuli. Usually the Ca^{2+} ions play an important role in these processes.[10] Calcium cellular level ranges from resting levels near 100 nM to signaling levels near 1 mM,[11] and regulates diverse amount of cellular processes through the interaction with a large number of calcium-sensor proteins such as CaM and S100A1. As reported previously, calcium takes part in the process of desensitizing TRPV1 receptors. This type of regulation is commonly tightly connected with Ca^{2+} binding proteins, such as CaM or S100A1 protein.[12] TRPV1 is inactivated via interactions with Ca^{2+}−CaM.[3,6,13] Similarly, Ca^{2+}-dependent cleavage of PIP2 and depletion of PIP2 is thought to play a major role in desensitization.[14−17] In contrast, the role of S100A1 in the process of TRP channel regulation remains elusive.

CaM is a small ubiquitously expressed protein, and its expression level ranges from nanomolar to micromolar levels.[18,19] Its structure in complex with various fragments derived from CaM-regulated proteins, both with and without Ca^{2+} ions (apocalmodulin), has been solved many times using NMR and X-ray diffraction. CaM has been described to interact with its targets in several ways. CaM contains four so-called EF hand motifs and undergoes large conformational changes upon Ca^{2+} binding. Two domains which participate in CaM binding in a Ca^{2+}-dependent manner have been identified within the intracellular termini of the TRPV1 receptor.[3,4] Nevertheless, the structure of TRPV1 in complex with CaM has not been determined yet.

S100 proteins are calcium-signaling molecules, which convert changes in cellular calcium levels to a variety of biological responses such as protein phosphorylation, cell growth and motility, cell-cycle regulation, transcription, differentiation and cell survival. S100A1 is one of the first proteins of this family to be characterized. It is a small (10.5 kDa) protein that forms

DOI: 10.1021/cn500250r
ACS Chem. Neurosci. XXXX, XXX, XXX−XXX

dimers. Along with CaM, S100A1 is a member of a large group of EF hand signaling proteins. CaM is present in all cells, and it is highly conserved among species. In contrast, S100 proteins are specific for vertebrates and have diverse tissue distributions.[20] S100A1 contains two EF-hand domains that bind Ca^{2+} ions with different affinities (500 μM and 1−50 μM),[21,22] and the S100A1 protein binds calcium and undergoes a conformational change by moving one helix and exposing a broad hydrophobic surface.[23] Several interactions of S100A1 protein with target molecules in Ca^{2+}dependent manner were described. Similarly to CaM, the dissociation constants of the S100A1 for its target range from nanomolar to micromolar levels.[24−26] Recently, some members of the TRP family were identified as biological targets of the S100 proteins. TRPV5 and TRPV6 interaction with the S100A10−annexin A2 complex is thought to mediate its trafficking to the plasma membrane.[27] Moreover, intracellular tails of TRPC6 and TRPM3 possess overlapping binding sites for S100A1 protein and CaM.[25,26] CaM and S100A1 also compete for binding sites within RyR1 receptor where they play a regulatory role.[22]

S100A1 and CaM have similar structural features, but no structural-functional studies or known physiological consequences of S100A1 binding to TRPV1 have been published yet. Here we utilize site-directed mutagenesis in combination with biophysical tools (steady-state fluorescence anisotropy, surface plasmon resonance (SPR)) to characterize the interaction of S100A1 with TRPV1. We show that S100A1 binds to TRPV1 and competes directly with CaM for the overlapping binding site on the C-terminus of TRPV1 (TRPV1-CT). Furthermore, we show that the interaction is calcium-dependent and that TRPV1 undergoes conformational changes upon binding to S100A1. In addition, we identified important basic residues of TRPV1 that actively participate in S100A1 binding.

RESULTS AND DISCUSSION

S100A1 Binds to TRPV1-CT. The C-terminus of TRPV1 contains a CaM binding site.[4,13,28] CaM typically recognizes motifs of hydrophobic and basic amino acid residues.[29] According to the CaM Target Database, the TRPV1-CT binding site has an atypical sequence but matches the so-called 1-8-14 conserved motif.[30] In previous reports, we found that the C-terminal region of TRPV1 (TRPV1-CT) harbors the integrative binding sites for CaM and PIP2.[4,31] Since a family of the Ca^{2+}-binding S100 proteins was shown to interact with similar binding motifs like CaM,[29,32] we sought to examine whether TRPV1-CT also shares binding site for the S100A1 protein. Ca^{2+} ions bind to two canonical EF hand motifs of S100A1 triggering a conformational switch of the S100A1 molecule and allowing the interaction between target protein and S100A1.[33] Hence, only the Ca^{2+}-bound conformation of S100A1 is able to recognize TRPV1 binding site. Thus, the experiments were done in Ca^{2+} excess to ensure only one population of S100A1 conformation occurs. First, steady-state fluorescence anisotropy measurements were employed to determine the role of Ca^{2+} in the interaction between TRPV1-CT and S100A1. As shown in Figure 1, titration of TRPV1-CT with fluorescently labeled S100A1 in the presence of 2 mM Ca^{2+} ions revealed an increase in fluorescence anisotropy indicating the formation of the TRPV1-CT/S100A1 complex with an estimated equilibrium dissociation constant of 169 ± 21 nM (mean ± SD, n = 3). In contrast, no changes in fluorescence anisotropy were observed during the titration experiments in the absence of Ca^{2+} ions suggesting that calcium

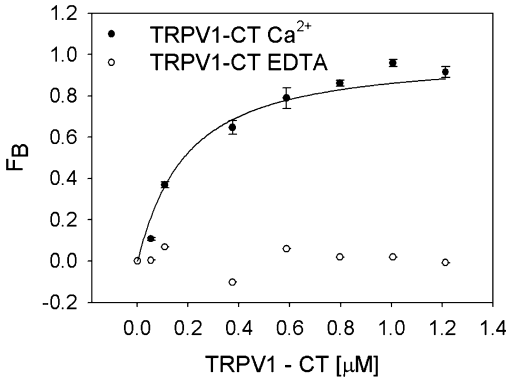

Figure 1. S100A1 binds TRPV1-CT in Ca^{2+}-dependent manner. Fluorescently labeled S100A1 was titrated with TRPV1-CT in the absence (○) and presence of 2 mM calcium ions (●), and the formation of the TRPV1-CT/S100A1 complex was followed by steady-state fluorescence anisotropy measurement. Fluorescence anisotropy was expressed as the bound fraction (FB) calculated according to eq 1 in the Methods. The solid line represents the binding isotherm determined by fitting the experimental data using a nonlinear least-squares analysis (see eq 2 in the Methods). The results are means ± SD from three independent experiments.

ions are strictly required for interaction between TRPV1-CT and S100A1. The kinetics of interaction between TRPV1-CT and S100A1 was further assessed by surface plasmon resonance (SPR). S100A1 was immobilized to a GLC chip at coupling level of 300 RU and washed in parallel by serially diluted TRPV1-CT at a flow rate of 30 μL/mL. Interaction of TRPV1-CT with S100A1 was specific, since negligible binding of thioredoxin alone was detected to the chip coated with S100A1 (Figure 2). Kinetic parameters of the interaction were calculated from global fitting of concentration-dependent binding curves (Figure 2A). The data were fitted to both a simple 1:1 Langmuir-type binding model and a conformational change model. We found that the interaction between S100A1 and TRPV1-CT is better described (in terms of reduced χ^2 and residual statistics) by the conformational change model indicating that formation of the complex occurs in two phases; a transient interaction of the TRPV1-CT and S100A1 subunits followed by a conformational transition of TRPV1-CT within the bound complex. Similar binding kinetics was also observed during the interaction of TRPV1-CT with CaM. As shown in Figure 2, the binding curves fit well to the conformational change model indicating that the formation of the TRPV1-CT/CaM complex is associated with a structural rearrangement of TRPV1-CT upon binding to CaM. The kinetic parameters of the interactions revealed that the rates of complex formation (represented here as association rate constants, k_{a1}) are similar for both S100A1 and CaM, but the stability of the complexes (represented by dissociation rate constant, k_{d1}) is significantly higher for S100A1. Thus, the binding affinity (K_{d1}) of TRPV1-CT to S100A1 is about two times higher for S100A1 than for CaM. (Table 1).

Alanine Scanning Mutagenesis of Basic Amino Acid Residues Engaged in Binding Site of TRPV1-CT. The importance of specific residues involved in binding of TRPV1-CT to CaM has been already investigated.[4,34] Based on the contact residues identified in the TRPV1-CT/CaM complex, alanine scanning mutagenesis of TRPV1-CT was performed followed by SPR analysis to assess the contribution of individual residues in kinetics of interaction and stability of

DOI: 10.1021/cn500250r
ACS Chem. Neurosci. XXXX, XXX, XXX−XXX

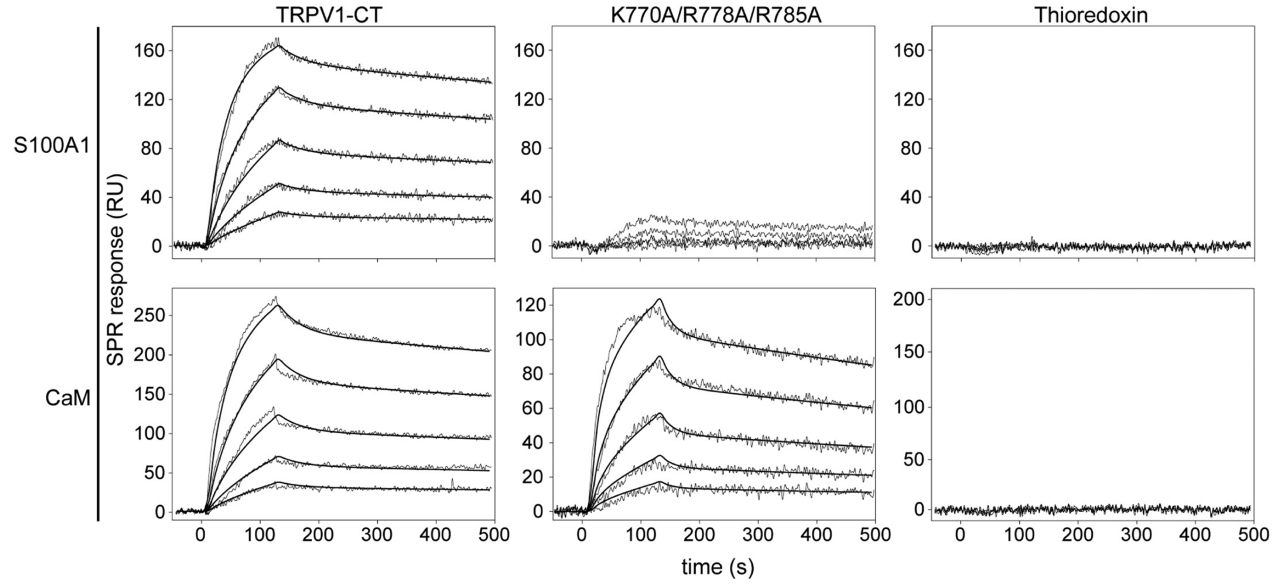

Figure 2. SPR kinetic binding analysis of the TRPV1-CT interaction with S100A1 and CaM. One-shot kinetics data of the wild-type TRPV1-CT (left column), the K770A/R778A/R785A mutant (middle column), and thioredoxin (right column) interacting with the Ca^{2+}-binding S100A1 protein (upper row) and CaM (lower row). The proteins were serially diluted (500, 250, 125, 62.5, and 31.25 nM) and injected in parallel over the sensor chip at flow rate of 30 μL/min. The kinetic data were globally fitted by using a conformational change model (see Methods). The fitted curves are superimposed as thin black line on top of the sensograms.

Table 1. Kinetic and Binding Affinity Constants for the Interactions of the C-Terminal Region of TRPV1 (TRPV1-CT) with the Ca^{2+}-Binding S100A1 Protein and Calmodulin (CaM)

		k_{a1} ($\times 10^4$ M^{-1} s^{-1})[a]	k_{d1} ($\times 10^{-2}$ s^{-1})[a]	K_{d1} ($\times 10^{-7}$ M)[ab]	k_{a2} ($\times 10^{-2}$ s^{-1})[a]	k_{d2} ($\times 10^{-4}$ s^{-1})[a]
WT	S100A	4.3 ± 0.8	0.7 ± 0.4	1.6 ± 0.4	1.5 ± 0.3	7.3 ± 0.9
	CaM	3.0 ± 0.4	12.3 ± 3.1	4.1 ± 0.9	1.7 ± 0.2	6.4 ± 0.2
K770A/R781A/R785A	S100A	4.7 ± 1.1	0.6 ± 0.2	1.3 ± 0.3	1.3 ± 0.4	7.4 ± 1.5
	CaM	2.0 ± 0.5	2.4 ± 0.5	1.2 ± 0.2	2.2 ± 0.3	5.1 ± 1.1
K770A/R785A	S100A	4.8 ± 1.1	1.8 ± 0.9	3.8 ± 0.3	1.3 ± 0.5	8.4 ± 2.1
	CaM	16.3 ± 0.5	1.5 ± 0.6	0.9 ± 0.4	1.9 ± 0.3	9.0 ± 1.0
K770A/R778A/R785A	S100A	ND	ND	ND	ND	ND
	CaM	4.2 ± 0.5	0.3 ± 0.1	0.7 ± 0.6	0.5 ± 0.3	3.1 ± 0.7
R771A/R781A	S100A	4.8 ± 0.5	8.8 ± 0.4	18.0 ± 0.6	1.1 ± 0.3	7.3 ± 0.5
	CaM	25.8 ± 2.5	0.9 ± 0.3	3.5 ± 0.8	1.1 ± 0.3	7.9 ± 3.8
R771A/R778A	S100A	2.2 ± 0.3	1.1 ± 0.7	5.0 ± 0.7	1.2 ± 0.4	7.6 ± 0. 5
	CaM	11.9 ± 2.4	1.9 ± 0.9	1.6 ± 0.4	1.7 ± 0.5	6.0 ± 1.2
R881A	S100A	1.5 ± 0.1	1.1 ± 0.4	7.3 ± 2.4	2.2 ± 0.3	4.3 ± 2.5
	CaM	5.3 ± 0.2	0.5 ± 0.2	0.9 ± 0.3	1.1 ± 0.3	5.1 ± 4.5

[a]The results are means ± SD from the SPR analysis of two independent experiments carried out in triplicate. [b]The equilibrium dissociation constant of the initial phase of the interaction, K_{d1}, was determined as k_{d1}/k_{a1}.

the TRPV1-CT/S100A1complex. Overall comparison of K_{d1} values revealed significant decrease in the binding affinity (increase in K_{d1}) for the TRPV1-CT mutants (Table 1). The predominant mechanism that contributed to the decreased binding affinity of the mutants to S100A1 was the faster dissociation rate of the encounter complex (represented by k_{d1}) indicating a lower stability of the complex as compared to the wild-type. On the other hand, a significant decrease in the association rates of the encounter complex (k_{a1}) was detected for the R771A/R778A and R881A mutations suggesting that the formation of the complex is also affected in these mutants. The mutation K770A/R781A/R785A did not affect the binding of TRPV1-CT to S100A1. The double mutation (K770A/R785A, R771A/R778A) and the single substitution (R881A) caused up to 5-fold decrease in the binding affinity, while the affinity of S100A1 for the R771A/R781A mutant was about 1 order of magnitude lower than for the wild-type. In contrast, the binding of the K770A/R778A/R785A triple mutant to S100A1 was completely inhibited indicating that these three residues play an important role in formation of the TRPV1-CT/S100A1 complex. The identical triple mutant has been previously shown to block interaction of TRPV1-CT with PIP2 embedded in the membrane of liposome.[31] However, the triple mutant K770/R778/R785 was still able to interact with CaM, even with a higher binding affinity than for the wild-type. It should be also emphasize that several TRPV1-CT mutants (namely K770A/R785A and R771A/R778A) had faster association rates (k_{a1}) for CaM resulting in higher tendency of these mutants to form the complexes with CaM. Such differences would be attributed to substantial divergences in the tertiary structures of S100A1 and CaM.[33] Taken together, these results showed that TRPV1-CT harbors the binding site for

DOI: 10.1021/cn500250r
ACS Chem. Neurosci. XXXX, XXX, XXX−XXX

both S100A1 and CaM; however, the binding of S100A1 is more specific than that of CaM, which is likely to influence an intimate regulation of the TRPV1 channel.

S100A1 Competes with CaM and PIP2 for Binding to TRPV1-CT. In order to determine whether S100A1 competes with CaM for the same binding site on the TRPV1-CT, CaM was mixed with TRPV1-CT in a molar ratio of 1:1 and the capacity of the prepared TRPV1-CT/CaM complex to bind S100A1 was analyzed by using SPR. As shown in Figure 3, the

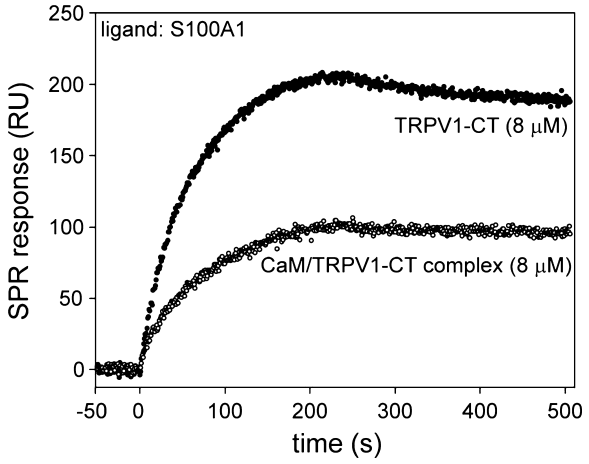

Figure 3. S100A1 and CaM share the binding site within the TRPV1-CT. TRPV1-CT (8 μM) and the TRPV1-CT/CaM complex (8 μM) were injected in parallel over the SPR sensor chip coated with S100A1 at flow rate of 30 μL/min. Inhibition of binding of the TRPV1-CT/CaM complex to S100A1 is represented by a decrease of SPR signal response.

binding of the TRPV1-CT/CaM complex was reduced to about 50% as compared to TRPV1-CT alone, indicating that S100A1 and CaM compete for the identical binding site within TRPV1-CT. In view of the fact that CaM shares the TRPV1-CT binding site with PIP2, we sought to examine whether S100A1 is also able to compete with PIP2 for binding to TRPV1-CT. The PIP2-enriched liposomes were immobilized to the sensor chip and the capacity of the preformed TRPV1-CT/S100A1 complex to interact with the membrane-bound PIP2 was probed by SPR. As shown in Figure 4A, the binding of the TRPV1-CT/S100A1 complex was almost completely inhibited as compared to TRPV1-CT alone suggesting that the binding site for S100A1 overlaps with the PIP2-binding site on TRPV1-CT. Reversely, only a very small portion (about 1/10) of the TRPV1-CT molecules attached to the PIP2-enriched liposomes were shown to interact with S100A1 (SPR response of 470 and 50 RU for TRPV1-CT and S100A1, respectively) indicating that S100A1 is not able to form a 1:1 complex with TRPV1-CT when bound to PIP2.(Figure 4B). Collectively, these data indicated that S100A1 competes with CaM and PIP2 for the binding site on TRPV1-CT.

TRPV1 is an important nociceptor. Regulation of its activity is proposed to be mediated via interactions with sensitizing agents as for example PIP2[3,14−17,35] or desensitizing agents as for example CaM.[3,4,6,13] Both of these ligands interact with the TRPV1-CT integrative binding site. We showed here that the third ligand, S100A1 protein, competes with CaM and PIP2 for identical binding site on TRPV1-CT and triggers the conformational changes of TRPV1 upon binding. The calcium sensor proteins CaM and S100A1 often interact with the same

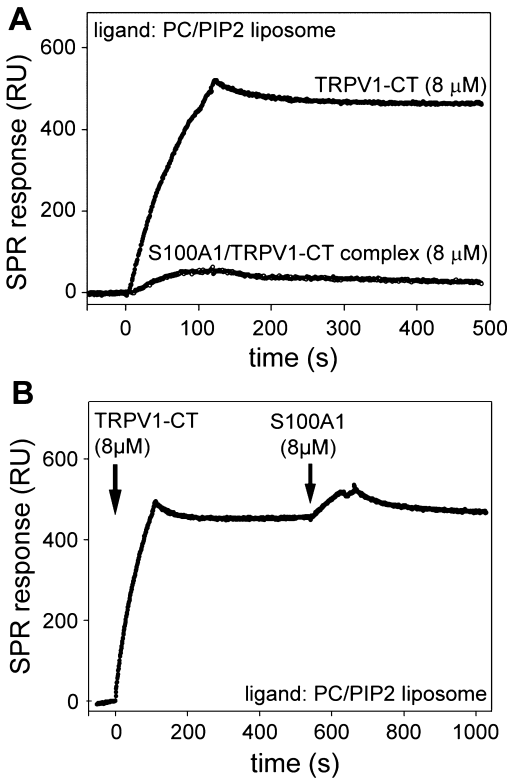

Figure 4. S100A1 and PIP2 share the binding site within the TRPV1-CT. (A) TRPV1-CT (8 μM) and the TRPV1-CT/S100A1 complex (8 μM) were injected in parallel over the SPR sensor chip coated with the PC/PIP2 (80:20) liposomes at flow rate of 30 μL/min. Inhibition of binding of the TRPV1-CT/S100A1 complex to the PIP2-enriched liposomes is represented by a decrease of SPR signal response. (B) SPR kinetic binding of S100A1 to TRPV1-CT bound to the PIP2-enriched liposome. TRPV1-CT (8 μM) was injected over the SPR sensor chip coated with PC/PIP2 (80:20) liposomes, left to dissociate, and immediately overlaid with subsequent injection of S100A1 (8 μM) onto the identical surface. The arrows represent injection of individual proteins. The flow rate was maintained at 30 mL/min during the whole experiment.

target proteins[22] and S100A has been shown to play a regulatory role.[36] While CaM participates in TRPV1 desensitization the physiological role of S1000A1 in TRPV1 activity modulation is elusive. The binding affinity of TRPV1-CT for S100A1 and CaM is comparable and ranges in submicromolar levels. Typical concentrations of S100A1 protein and CaM in the cell cytosol are estimated to be in a broad range (from nanomolar to micromolar levels),[37,38] but they are strictly tissue and cell specific. Whether the TRPV1/S100A1 interaction has a regulatory function thus remains to be tested as more electrophysiological information on S100 proteins in complex with TRP channels become available.

METHODS

TRPV1-CT Expression and Purification. The C-terminal part of rat TRPV1 (amino acids 712−838) (TRPV1-CT) was cloned into the bacterial expression vector pET32b (Novagen) as was described in detail previously.[31] Point mutations of several amino acid residues for alanine (R771A, R778A, K770A/R785A, R771A/R781A, R771A/R778A, K770A/R778A/R785A, K770A/R781A/R785A) were introduced by using PfuUltra high-fidelity DNA polymerase (Stratagene). The results of the mutagenesis were verified by sequencing. TRPV1-CT and all its mutant versions were expressed fused with the thioredoxin protein and a His-tag on the N-terminus in Rosetta

DOI: 10.1021/cn500250r
ACS Chem. Neurosci. XXXX, XXX, XXX−XXX

Escherichia coli cells. The protein expression was induced by isopropyl 1-thio-β-D-galactopyranoside (Roth) for 12 h at 20 °C. Proteins were purified using Chelating Sepharose Fast Flow (GE Healthcare) according to the standard protocol followed by gel permeation chromatography on a Superdex 75 column (GE Healthcare). Protein concentration was assessed by measuring the absorption at 280 nm. The purity was verified using 12% SDS-polyacrylamide gel electrophoresis (PAGE).

S100A1 Cloning, Expression, Purification, and Labeling. cDNA coding for the human S100A1 protein was cloned into the pET28b expression vector. The protein was expressed in BL21 *E. coli* cells. Protein expression was induced by isopropyl-1-thio-β-D-galactopyranoside (Roth) for 12 h at 25 °C. The cells were pelleted by centrifugation and resuspended in 50 mM Tris-HCl buffer (pH 7.5) containing 2 mM EDTA and 0.2 mM PMSF. The cells were disrupted by sonication and centrifuged. $CaCl_2$ was added to the supernatant (final concentration 5 mM). The protein was purified using affinity chromatography on Phenyl Sepharose CL4B (Amersham Biosciences), where 50 mM Tris-HCl buffer (pH 7.5) containing 1.5 mM EDTA and 100 mM NaCl was used for the elution. Gel permeation chromatography on a Superdex 75 column (Amersham Pharmacia Biotech) was used as a final purification step. The protein was eluted with 50 mM HEPES buffer (pH 7.0) containing 250 mM NaCl, 2 mM $CaCl_2$, 2 mM β-mercaptoethanol, and 10% glycerol. Protein samples were concentrated using spin columns for protein concentration (Millipore). Protein concentration was assessed by measuring absorption at 280 nm. The purity was verified using 15% SDS-polyacrylamide gel electrophoresis (PAGE).

The protein was then dialyzed overnight into 10 mM NaHCO3 (pH 10.0) at 4 °C. For fluorescent labeling, S100A1 was mixed with 0.6 M dansyl chloride (DNS) solution (Sigma) at a molar ratio of 1:1.5 and incubated at room temperature for 8 h. The mixture was dialyzed overnight at 4 °C against 20 mM Tris-HCl buffer (pH 8.0) containing 250 mM NaCl and 2 mM $CaCl_2$ to remove the free DNS. The level of protein labeling was checked by measuring the ratio of the fluorescence intensities of the unbound and bound states (excitation at 340 nm, emission at 500 nm).

CaM Expression, Purification, and Labeling. CaM was expressed and purified according to the protocol published in our previous work.[39] The protein was labeled with the fluorescent probe DNS, as described above for S100A1.

Preparation of the TRPV1-CT/CaM and TRPV1-CT/S100A1 Complexes. The proteins were mixed with a 1:1 molar ratio and incubated for 1 h at room temperature in the presence of 2 mM Ca^{2+} followed by gel permeation chromatography on a Superdex 75 column (GE Healthcare). The freshly prepared complexes were immediately used for the binding experiments.

Steady State Fluorescence Anisotropy Binding Assay. Fluorescence anisotropy was measured in an ISS photon counting steady-state spectrofluorimeter (ISS PC1TM) at room temperature in a buffer containing 20 mM Tris-HCl (pH 7.5), 6 mM $CaCl_2$, and 2.66 mM DNS-S100A1. The final concentration of the fluorescently labeled protein in the measuring buffer in the cuvette was 10 nM. Increasing amounts of the solution of TRPV1-CT protein were titrated into the cuvette. DNS-S100A1 was excited at 340 nm, and fluorescence was collected at 500 nm. Steady-state fluorescence anisotropy was recorded at each protein concentration. The fraction of TRPV1-CT bound to the fluorescent probe, F_B, was determined from the anisotropy changes using eq 1:

$$F_B = \frac{(r_{obs} - r_{min})}{(r_{max} - r_{obs})Q + (r_{obs} - r_{min})} \quad (1)$$

where r_{min} and r_{max} are the anisotropies of the free and bound DNS-S100A1, respectively, r_{obs} is the observed anisotropy, and Q is the ratio of the fluorescence intensities of the free and bound protein (f_{max}/f_{min}).[40] All experiments were carried out at least in triplicate. F_B was plotted against TRPV1 protein concentration and fitted using equation

$$F_B = \frac{K_D + [P_1] + [P_2] - \sqrt{(K_D + [P_1] + [P_2])^2 - 4[P_1][P_2]}}{2[P_1]} \quad (2)$$

to determine the equilibrium dissociation constant (K_D) for TRPV1/S100A1 complex formation.[40] Nonlinear data fitting was performed using the package SigmaPlot 2000 (6.1) SPSS Inc. P_1 is the concentration of DNS-S100A1, and P_2 is the concentration of TRPV1 fusion protein.

Surface Plasmon Resonance (SPR). All SPR measurements were performed at 25 °C using CaM- and S100A1-coated GLC sensor chip mounted on a ProteOn XPR36 protein interaction array system (Bio-Rad, Hercules, CA). CaM and S100A1 proteins were diluted to a final concentrations of 10 μg/mL in 10 mM acetate buffer (pH 3.5) and washed over the sensor chip using a ProteOn amine coupling kit (Bio-Rad) at a flow rate of 30 μL/min followed by the injection of 1 M ethanolamine (pH 8.5) to block nonreacted groups. The subsequent SPR measurements were carried out in 10 mM HEPES (pH 7.4), 150 mM NaCl, 2 mM $CaCl_2$, and 0.005% Tween 20 at a flow rate of 30 μL/min. The proteins were serially diluted in running buffer to the indicated concentrations, and injected in parallel ("one-shot kinetics") over the CaM and S100A1 surface. Surfaces were typically regenerated with 100 μL of 50 mM EDTA, 1 M NaCl. The binding curves were processed by using a ProteOn Manager software (Bio-Rad) and corrected for sensor background by interspot referencing (the sites within the 6 × 6 array which are not exposed to ligand immobilization but are exposed to analyte flow), and double referenced by subtraction of analyte (channels 1−5) using a "blank" injection (channel 6). The data were analyzed globally by fitting both the association and the dissociation phases simultaneously for five different protein concentrations using both a 1:1 Langmuir-type binding model and the two-state (conformational change) model to determine the kinetics association and dissociation rate constants. The Langmuir-type model assumes the interaction between protein A and B resulting in a direct formation of the final complex (AB):

$$A + B \underset{k_d}{\overset{k_a}{\rightleftarrows}} AB$$

where k_a and k_d are the association and the dissociation rate constants, respectively. The two-state (conformational change) model assumes the two-step association process:

$$A + B \underset{k_{d1}}{\overset{k_{a1}}{\rightleftarrows}} [AB]^* \underset{k_{d2}}{\overset{k_{a2}}{\rightleftarrows}} AB$$

where [AB]* and AB represent encounter complex (transition state) and final docked state, respectively. Parameters k_{a1} and k_{d1} are the association and the dissociation rate constants for the first step (encounter complex formation), while k_{a2} and k_{d2} are forward and reverse rate constants for the second step (conformational change).

Interaction of TRPV1-CT and the TRPV1-CT/S100A1 complex with the PIP2-enriched liposomes was performed as previously described.[31] In brief, the liposomes (100 nm in diameter) made from 1,2-dimyristoyl-*sn*-glycero-3-phosphocholine (PC) and L-α-phosphatidylinositol-4,5-bisphosphate (PIP2) (Avanti Lipids, Alabaster, AL) were immobilized to a neutravidin-coated NLC chip (Biorad, Hercules, CA) using a pair of two complementary oligonucleotides, modified at their 5′ ends by biotin and cholesterol, respectively. The proteins were injected at identical concentrations (8 μM) at a flow rate of 30 μL/min.

AUTHOR INFORMATION

Corresponding Authors

*E-mail: l.grycova@biomed.cas.cz.

*E-mail: teisingr@biomed.cas.cz.

Author Contributions

L.G. designed the experiments, performed the experiments, analyzed the data, contributed reagents/materials/analysis

DOI: 10.1021/cn500250r
ACS Chem. Neurosci. XXXX, XXX, XXX−XXX

tools, and wrote the paper. B.H. performed the experiments and wrote the paper. Z.L. analyzed the data, contributed reagents/materials/analysis tools, and wrote the paper. L.B. designed the experiments, performed the experiments, analyzed the data, and wrote paper. M.J. and K.B. performed the experiments. J.T. designed the experiments, contributed reagents/materials/analysis tools, and wrote the paper.

Funding

This study was supported by the Grant Agency of the Czech Republic (Grant Nos. 301/10/1159, 207/11/0717, 15-11851S), Grant Agency of Charles University (842314, 238214), the Grant Agency of the Czech Republic Project of Excellence in the Field of Neuroscience (P304/12/G069), BIOCEV CZ.1.05/1.1.00/02.0109 from the ERDF and by institutional support by RVO 86 652 036.

Notes

The authors declare no competing financial interest.

REFERENCES

(1) Liao, M., Cao, E., Julius, D., and Cheng, Y. (2013) Structure of the TRPV1 ion channel determined by electron cryo-microscopy. *Nature 504*, 107−112.

(2) Cao, E., Liao, M., Cheng, Y., and Julius, D. (2013) TRPV1 structures in distinct conformations reveal activation mechanisms. *Nature 504*, 113−118.

(3) Lishko, P. V., Procko, E., Jin, X., Phelps, C. B., and Gaudet, R. (2007) The ankyrin repeats of TRPV1 bind multiple ligands and modulate channel sensitivity. *Neuron 54*, 905−918.

(4) Grycova, L., Lansky, Z., Friedlova, E., Obsilova, V., Janouskova, H., Obsil, T., and Teisinger, J. (2008) Ionic interactions are essential for TRPV1 C-terminus binding to calmodulin. *Biochem. Biophys. Res. Commun. 375*, 680−683.

(5) Brauchi, S., Orta, G., Mascayano, C., Salazar, M., Raddatz, N., Urbina, H., Rosenmann, E., Gonzalez-Nilo, F., and Latorre, R. (2007) Dissection of the components for PIP2 activation and thermosensation in TRP channels. *Proc. Natl. Acad. Sci. U. S. A. 104*, 10246−10251.

(6) Rosenbaum, T., Gordon-Shaag, A., Munari, M., and Gordon, S. E. (2004) Ca^{2+}/calmodulin modulates TRPV1 activation by capsaicin. *J. Gen. Physiol. 123*, 53−62.

(7) Prescott, E. D., and Julius, D. (2003) A modular PIP2 binding site as a determinant of capsaicin receptor sensitivity. *Science 300*, 1284−1288.

(8) Zhu, M. X. (2005) Multiple roles of calmodulin and other Ca^{2+}-binding proteins in the functional regulation of TRP channels. *Pfluegers Arch. 451*, 105−115.

(9) Grycova, L., Lansky, Z., Friedlova, E., Vlachova, V., Kubala, M., Obsilova, V., Obsil, T., and Teisinger, J. (2007) ATP binding site on the C-terminus of the vanilloid receptor. *Arch. Biochem. Biophys. 465*, 389−398.

(10) Pedersen, S. F., Owsianik, G., and Nilius, B. (2005) TRP channels: An overview. *Cell Calcium 38*, 233−252.

(11) Yamniuk, A. P., and Vogel, H. J. (2004) Calmodulin's flexibility allows for promiscuity in its interactions with target proteins and peptides. *Mol. Biotechnol. 27*, 33−57.

(12) Vetter, S. W., and Leclerc, E. (2003) Novel aspects of calmodulin target recognition and activation. *Eur. J. Biochem. 270*, 404−414.

(13) Numazaki, M., Tominaga, T., Takeuchi, K., Murayama, N., Toyooka, H., and Tominaga, M. (2003) Structural determinant of TRPV1 desensitization interacts with calmodulin. *Proc. Natl. Acad. Sci. U. S. A. 100*, 8002−8006.

(14) Liu, B., Zhang, C., and Qin, F. (2005) Functional recovery from desensitization of vanilloid receptor TRPV1 requires resynthesis of phosphatidylinositol 4,5-bisphosphate. *J. Neurosci. 25*, 4835−4843.

(15) Lukacs, V., Thyagarajan, B., Varnai, P., Balla, A., Balla, T., and Rohacs, T. (2007) Dual regulation of TRPV1 by phosphoinositides. *J. Neurosci. 27*, 7070−7080.

(16) Mercado, J., Gordon-Shaag, A., Zagotta, W. N., and Gordon, S. E. (2010) Ca^{2+}-dependent desensitization of TRPV2 channels is mediated by hydrolysis of phosphatidylinositol 4,5-bisphosphate. *J. Neurosci. 30*, 13338−13347.

(17) Stein, A. T., Ufret-Vincenty, C. A., Hua, L., Santana, L. F., and Gordon, S. E. (2006) Phosphoinositide 3-kinase binds to TRPV1 and mediates NGF-stimulated TRPV1 trafficking to the plasma membrane. *J. Gen. Physiol. 128*, 509−522.

(18) Tran, Q. K., Black, D. J., and Persechini, A. (2003) Intracellular coupling via limiting calmodulin. *J. Biol. Chem. 278*, 24247−24250.

(19) Burgoyne, R. D., and Haynes, L. P. (2010) Neuronal calcium sensor proteins: Emerging roles in membrane traffic and synaptic plasticity. *F1000 Biol. Rep. 2*, 5 DOI: 10.3410/B2-5.

(20) Kato, K., Kimura, S., Haimoto, H., and Suzuki, F. (1986) S100a0 (alpha alpha) protein: Distribution in muscle tissues of various animals and purification from human pectoral muscle. *J. Neurochem. 46*, 1555−1560.

(21) Rustandi, R. R., Baldisseri, D. M., Inman, K. G., Nizner, P., Hamilton, S. M., Landar, A., Zimmer, D. B., and Weber, D. J. (2002) Three-dimensional solution structure of the calcium-signaling protein apo-S100A1 as determined by NMR. *Biochemistry 41*, 788−796.

(22) Wright, N. T., Prosser, B. L., Varney, K. M., Zimmer, D. B., Schneider, M. F., and Weber, D. J. (2008) S100A1 and calmodulin compete for the same binding site on ryanodine receptor. *J. Biol. Chem. 283*, 26676−26683.

(23) Rezvanpour, A., and Shaw, G. S. (2009) Unique S100 target protein interactions. *Gen. Physiol. Biophys. 28*, F39−46.

(24) Treves, S., Scutari, E., Robert, M., Groh, S., Ottolia, M., Prestipino, G., Ronjat, M., and Zorzato, F. (1997) Interaction of S100A1 with the Ca^{2+} release channel (ryanodine receptor) of skeletal muscle. *Biochemistry 36*, 11496−11503.

(25) Bily, J., Grycova, L., Holendova, B., Jirku, M., Janouskova, H., Bousova, K., and Teisinger, J. (2013) Characterization of the S100A1 protein binding site on TRPC6 C-terminus. *PLoS One 8*, e62677.

(26) Holakovska, B., Grycova, L., Jirku, M., Sulc, M., Bumba, L., and Teisinger, J. (2012) Calmodulin and S100A1 protein interact with N terminus of TRPM3 channel. *J. Biol. Chem. 287*, 16645−16655.

(27) van de Graaf, S. F., Hoenderop, J. G., Gkika, D., Lamers, D., Prenen, J., Rescher, U., Gerke, V., Staub, O., Nilius, B., and Bindels, R. J. (2003) Functional expression of the epithelial Ca^{2+} channels (TRPV5 and TRPV6) requires association of the S100A10-annexin 2 complex. *EMBO J. 22*, 1478−1487.

(28) Lau, S. Y., Procko, E., and Gaudet, R. (2012) Distinct properties of Ca^{2+}-calmodulin binding to N- and C-terminal regulatory regions of the TRPV1 channel. *J. Gen Physiol 140*, 541−555.

(29) Rhoads, A. R., and Friedberg, F. (1997) Sequence motifs for calmodulin recognition. *FASEB J. 11*, 331−340.

(30) Yap, K. L., Kim, J., Truong, K., Sherman, M., Yuan, T., and Ikura, M. (2000) Calmodulin target database. *J. Struct. Funct. Genomics 1*, 8−14.

(31) Grycova, L., Holendova, B., Bumba, L., Bily, J., Jirku, M., Lansky, Z., and Teisinger, J. (2012) Integrative binding sites within intracellular termini of TRPV1 receptor. *PLoS One 7*, e48437.

(32) Wilder, P. T., Lin, J., Bair, C. L., Charpentier, T. H., Yang, D., Liriano, M., Varney, K. M., Lee, A., Oppenheim, A. B., Adhya, S., Carrier, F., and Weber, D. J. (2006) Recognition of the tumor suppressor protein p53 and other protein targets by the calcium-binding protein S100B. *Biochim. Biophys. Acta 1763*, 1284−1297.

(33) Bhattacharya, S., Bunick, C. G., and Chazin, W. J. (2004) Target selectivity in EF-hand calcium binding proteins. *Biochim. Biophys. Acta 1742*, 69−79.

(34) Lau, S. Y., Procko, E., and Gaudet, R. (2012) Distinct properties of Ca^{2+}-calmodulin binding to N- and C-terminal regulatory regions of the TRPV1 channel. *J. Gen. Physiol. 140*, 541−555.

(35) Yao, J., and Qin, F. (2009) Interaction with phosphoinositides confers adaptation onto the TRPV1 pain receptor. *PLoS Biol. 7*, e46.

(36) Prosser, B. L., Hernandez-Ochoa, E. O., and Schneider, M. F. (2011) S100A1 and calmodulin regulation of ryanodine receptor in striated muscle. *Cell Calcium 50*, 323−331.

DOI: 10.1021/cn500250r
ACS Chem. Neurosci. XXXX, XXX, XXX−XXX

(37) Su, A. I., Wiltshire, T., Batalov, S., Lapp, H., Ching, K. A., Block, D., Zhang, J., Soden, R., Hayakawa, M., Kreiman, G., Cooke, M. P., Walker, J. R., and Hogenesch, J. B. (2004) A gene atlas of the mouse and human protein-encoding transcriptomes. *Proc. Natl. Acad. Sci. U. S. A. 101*, 6062−6067.
(38) Chin, D., and Means, A. R. (2000) Calmodulin: a prototypical calcium sensor. *Trends Cell Biol. 10*, 322−328.
(39) Holakovska, B., Grycova, L., Bily, J., and Teisinger, J. (2011) Characterization of calmodulin binding domains in TRPV2 and TRPV5 C-tails. *Amino Acids 40*, 741−748.
(40) Lakowicz, J. r. (2006) *Principles of fluorescence spectroscopy*, 3rd ed., Springer, New York.

DOI: 10.1021/cn500250r
ACS Chem. Neurosci. XXXX, XXX, XXX−XXX

APPENDIX 3

Bousova K, Jirku M, Bumba L, Bednarova L, Sulc M, Franek M, Vyklicky L, Vondrasek J, Teisinger J., PIP2 and PIP3 interact with N-terminus region of TRPM4 channel. Biophys Chem. 2015, 205:24-32. doi: 10.1016/j.bpc.2015.06.004.

Biophysical Chemistry 205 (2015) 24–32

Contents lists available at ScienceDirect

Biophysical Chemistry

journal homepage: http://www.elsevier.com/locate/biophyschem

PIP2 and PIP3 interact with N-terminus region of TRPM4 channel

Kristyna Bousova [a,b], Michaela Jirku [b,c], Ladislav Bumba [d], Lucie Bednarova [e], Miroslav Sulc [d], Miloslav Franek [f], Ladislav Vyklicky [b], Jiri Vondrasek [e], Jan Teisinger [b,*]

[a] 2nd Faculty of Medicine, Charles University in Prague, 15006 Prague, Czech Republic
[b] Institute of Physiology, Academy of Sciences of the Czech Republic, 14220 Prague, Czech Republic
[c] Faculty of Science, Charles University in Prague, 12843 Prague, Czech Republic
[d] Institute of Microbiology, Academy of Sciences of the Czech Republic, 14220 Prague, Czech Republic
[e] Institute of Organic Chemistry and Biochemistry, Academy of Sciences of the Czech Republic, 16610 Prague, Czech Republic
[f] 3rd Faculty of Medicine, Charles University in Prague, 10000 Prague, Czech Republic

HIGHLIGHTS

- TRPM4 N- terminus channel contains binding site for potential regulatory molecules PIP2 and PIP3
- Basic R755 and R767 amino acids of TRPM4 N-terminal were determined to interact with the PIP2/PIP3 molecules directly
- TRPM4 fusion protein segments do not change its secondary structure content during complex formation with PIP2 or PIP3
- Molecular model of TRPM4 segment with PIP2 docking confirmed non-covalent binding mode

GRAPHICAL ABSTRACT

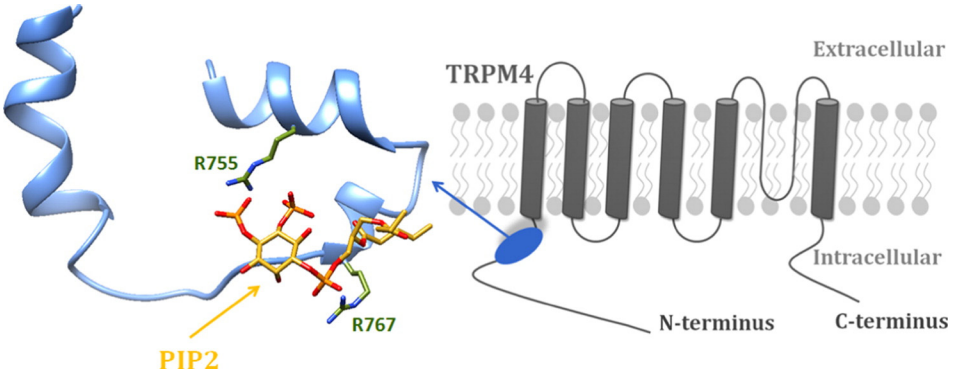

ARTICLE INFO

Article history:
Received 14 April 2015
Received in revised form 4 June 2015
Accepted 6 June 2015
Available online 09 June 2015

Keywords:
TRPM4 channel
PIP2
Binding site
Surface plasmon resonance
Molecular modeling
Circular dichroism

ABSTRACT

The transient receptor potential melastatin 4 (TRPM4) is a calcium-activated non-selective ion channel broadly expressed in a variety of tissues. Receptor has been identified as a crucial modulator of numerous calcium dependent mechanisms in the cell such as immune response, cardiac conduction, neurotransmission and insulin secretion. It is known that phosphoinositide lipids (PIPs) play a unique role in the regulation of TRP channel function. However the molecular mechanism of this process is still unknown. We characterized the binding site of PIP2 and its structural analogue PIP3 in the E733–W772 proximal region of the TRPM4 N-terminus via biophysical and molecular modeling methods. The specific positions R755 and R767 in this domain were identified as being important for interactions with PIP2/PIP3 ligands. Their mutations caused a partial loss of PIP2/PIP3 binding specificity. The interaction of PIP3 with TRPM4 channels has never been described before. These findings provide new insight into the ligand binding domains of the TRPM4 channel.

1. Introduction

Transient receptor potential channels (TRPs) are non-selective ion channels that play a unique role in cell sensor systems and are involved

* Corresponding author.
E-mail address: jan.teisinger@fgu.cas.cz (J. Teisinger).

http://dx.doi.org/10.1016/j.bpc.2015.06.004
0301-4622/

in many calcium-mediated cell functions [1,2]. TRPs are a diverse family of proteins expressed in many organisms, tissues and cell types. Their variety is demonstrated by proposed functions: transmission of painful stimuli, modulation of vascular tone, involvement in pathogenesis of diabetes mellitus, supply of intracellular calcium stores and modulation of cell cycle, [3,4]. In sensory neurons, TRPs contribute to many of activities including thermal sensation, homeostasis of body temperature and pain [5]. In the central nervous system (CNS), they have been associated with synaptic transmission, neurogenesis and brain development [6,7]. These special nociceptive receptors are transporters of mono and bivalent cations into the cell [3]. The structure of TRPs was unknown for a long time, despite numerous crystallization attempts to resolve their structure, recently almost the entire three-dimensional structure of the vanilloid 1 (TRPV1) and ankyrin 1 (TRPA1) receptor was determined by single-particle electron cryo-microscopy [8–10]. All members of the TRP superfamily share the same membrane topology. They have six transmembrane helices (TM) with a pore region between TM5–TM6 (Fig. 1A) and all of them have a homotetrameric structure [11–14]. Intracellularly located N- and C-tails are responsible for the regulation of TRP channels, which carry binding sites for signal ligands such as the intracellular calcium binding protein calmodulin [15,16] or plasma membrane lipid phosphatidylinositol-4,5-bisphosphate (PIP2) [17–20].

There is significant sequence similarity between TRPV, TRP canonical (TRPC) and TRP melastatin (TRPM), but no conservation between the N-terminal region of TRPM and those of TRPV and TRPC has been noted. On the other hand, the C-terminal domains of those three channels exhibit very high conservation in the proximal region (so-called TRP box) [21–24]. The TRPM family consists of eight members, which can be subdivided into four groups based on their sequence homology: M1 and M3, M4 and M5, M6 and M7, M2 and M8 [25]. TRPM4 is a calcium-activated non-selective ion channel that mediates the transport of monovalent cations (Fig. 1A). The activity of the encoded protein increases with increasing intracellular calcium concentration, but this channel does not transport calcium [26–28]. TRPM4 participates in ongoing processes in neurons [29,30], cardiomyocytes [31], pancreas cells [32], T-cells [33,34] and a link has been proven between defects in the TRPM4 receptor and progressive familial heart block type 1B [31].

Nowadays, more than 50 endogenous lipids and lipid-like molecules have been identified as direct activators or inhibitors of TRP channels. Regulators form lipids from a variety of metabolic pathways, including metabolites of the cyclooxygenase, lipooxygenase and cytochrome P450 pathways, phospholipids and lysophospholipids [35]. The most studied modulators of TRP channel function are phosphoinositides [18,38–40], which appear as the major regulators of this family ion channels. PIP2 and its structural analogue phosphatidylinositol-3,4,5-trisphosphate (PIP3) belong to the group of phosphoinositides that are low-abundant members of plasma membrane. These phospholipids function in a number of crucial cellular processes, such as plasma membrane-cytoskeleton linkages, second messenger signaling, regulation of proteins involved in phospholipid metabolism, cell adhesion and motility, and membrane trafficking [36,37]. PIP2 binding and regulation in TRPM receptors have also been studied extensively. It has been found that PIP2 activates TRPM3 [19], TRPM4 [41], TRPM5 [42], TRPM7 [43,44] and TRPM8 [45] channels. Analysis of the primary structure of the TRPM4 N-terminus revealed that PIP2 binding motif is conserved [46]. Under physiological conditions the phosphatidylinositols (PIPs) are negatively charged, the interactions of PIPs with the intracellular regions of ion channels, including TRPs, involve regions characterized by the presence of several positively charged residues [47–49]. Mutation of these positive residues has a critical role on PIP2 binding and this can lead to a PIP2-mediated channel regulation [39,50,51]. In some cases, binding is mediated by dedicated lipid-binding domains, one of the most known is the Pleckstrin Homology (PH) domain [52]. The elucidation of the crystal structure of K^+ channels with bound PIP2 provided the first atomistic description of a molecular mechanism by which PIP2 regulates channel activity and how it induces large conformation changes in the protein [53,54]. Whether or not the PIP2 modulation of TRPs involves similar conformational changes is still unknown. Moreover, some specific positively charged regions (e.g. PH domains) in TRPs could mediate the interaction with other PIPs with higher binding affinity — e.g. PIP3 [49,55,56].

In this study we addressed the localization of putative PIP2 and PIP3 binding site in the cytoplasmic domain of TRPM4 N-terminus using a combination of biophysical and molecular modeling tools. The proximal region E733–W772 of the N-terminus directly interacts with PIP2 and PIP3. According to the data presented, the binding affinity of PIP2 and PIP3 to studied N-terminus region of TRPM4 is approximately the same. The key residues R755 and R767 have been determined to be involved in PIP2/PIP3 binding. These findings provide new insight into the ligand binding domains of the TRPM4 channel.

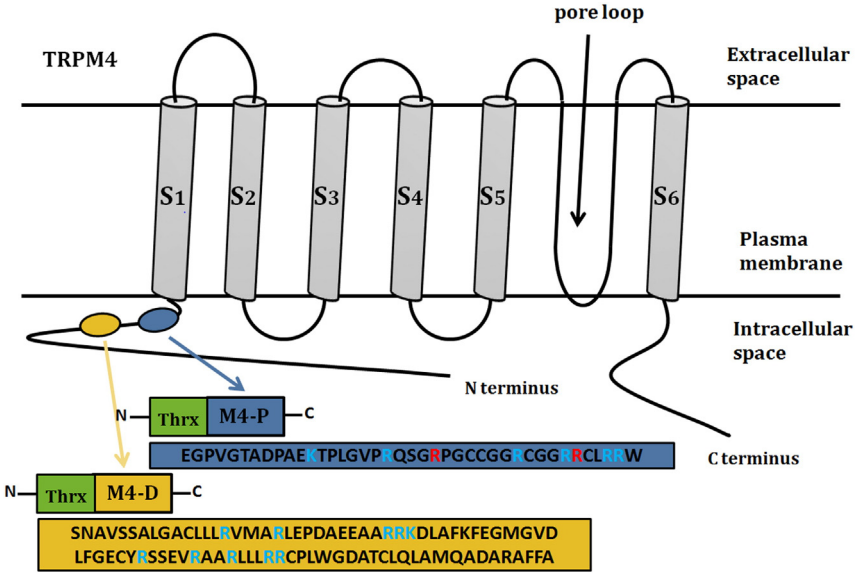

Fig. 1. Architecture of TRPM4 channel. The violet and yellow colored ovals show the location of the putative PIP2/PIP3 binding sites on N-terminus of TRPM4. The frames displayed proposed fusion (thioredoxin in green) protein constructs M4-D and M4-P. Their sequences displayed bellow show putative PH binding domains (blue letters). M4-P sequence shows amino acids involved in the interaction with PIP2 and PIP3 (red letters). (For interpretation of the references to color in this figure legend, the reader is referred to the web version of this article.)

2. Materials and methods

2.1. Cloning of expression vectors and site-directed mutagenesis

cDNA constructs coding the appropriate human TRPM4 (UniProtKB/Swiss-Prot: Q8TD43.1) N-termini distal (residues S583–A669, henceforth denoted as M4-D) and proximal (residues E733–W772, henceforth denoted as M4-P) regions. These were subcloned into the BamHI and NotI sites of the pET32b expression vector (Novagen). Mutagenesis was performed using Pfu Ultra High-fidelity DNA polymerase (Stratagene) according to the manufacturer's instructions. Selected positive amino acid residues were replaced with Ala. All clones were verified by DNA sequencing.

2.2. Fusion expression and purification of TRPM4 N-termini constructs

M4-D and M4-P constructs and double mutant were expressed fused with thioredoxin and 2× His-tag on the N- and C- termini in Rosetta cells. Bacteria were transformed with the indicated construct. Overnight starter cultures (5 ml) were used to inoculate cultures, these were grown at 37 °C until they reached $OD_{600} = 0.6$ Isopropyl-1-thio-β-D-galactopyranoside (0.5 mM) was then added and induction proceeded for 20 h at 25 °C. After pelleting the bacteria, cells were resuspended in solutions containing the following: 10 mM PBS, 1 M NaCl, 10 mM imidazole, 0,05% NP-40, 0.1 mM PMSF and 1 mM β-mercaptoethanol, (pH 7.7 for M4-D and pH 8.2 for M4-P). Large scale bacterial cultures were lysed with a sonicator (Misonix Sonicator 300, USA). Lysates were spun at 40,000 rpm for 40 min at 4 °C. The fusion proteins were purified in two step chromatography techniques. At first, affinity chromatography was used in a chelating Sepharose fast flow column (Amersham Biosciences). The fusion proteins were eluted with the following: 10 mM PBS, 500 mM NaCl, 2 mM β-Mercaptoethanol, and 400 mM imidazol, (pH 7.7 for M4-D and pH 8.2 for M4-P). Gel permeation chromatography in a Superdex 75 column (Amersham Biosciences) was used as a second purification step. The proteins were eluted with 25 mM HEPES, 250 mM NaCl, 2 mM β-MerkaptoEtOH, 0.1% Tween and 10% glycerol, (pH 7.7 for M4-D and pH 8.2 for M4-P). Protein samples were concentrated using spin columns for protein concentration (Millipore). The purity was verified using 15% SDS-polyacrylamide gel electrophoresis (PAGE).

2.3. Mass spectrometry

The integrity of purified fusion proteins was checked by MALDI-TOF, mass spectra were acquired using an UltraFLEX III mass spectrometer (Bruker-Daltonics, Bremen, Germany). Protein bands from M4-D and M4-P, were digested with trypsin endoprotease (Promega) directly in the gel after destaining and cysteine modification by iodoacetamide [57]. The resulting peptide mixtures were extracted and loaded onto the MALDI-TOF/TOF target with α-cyano-4-hydroxycinnamic acid as the matrix. Peptide identities were verified using MS/MS fragmentation of the molecules, determination of the molecular mass of the fragments, and comparison with predicted (UniProtKB/Swiss-Prot: Q8TD43.1) and experimentally obtained fragmentation patterns.

2.4. Liposome preparation

The lipids L-a-phosphatidylinositol-4,5-bisphosphate (PIP2), 1,2-dioleoyl-*sn*-glycero-3-phospho-(1′-myo-inositol-3′,4′,5′-trisphosphate) (PIP3) and 1,2-dimyristoyl-sn-glycero-3-phosphocholine (PC) were obtained from Avanti Polar Lipids, Inc. A stock solution of PIP2 and PIP3 was prepared in a chloroform: methanol: H_2O (20:9:1) mixture, a stock solution of PC only in chloroform. Liposomes of the following compositions were prepared: PC, PC/PIP2 50/50% and PC/PIP3 50/50% by mixing appropriate volumes of the stock solutions. After being dried under an N2 stream, lipid films were hydrated with Hanks' Balanced Salt Solution (HBSS) buffer (25 mM HEPES, 250 mM NaCl) followed by extrusion 21 times through a polycarbonate membrane with Nuclepore Track-Etched Membranes with 100 nm pore diameter (Avanti Lipids, USA). The liposomes obtained were then centrifuged (50,000 *g*) for 30 min at 4 °C. The vesicles were diluted to a final concentration of 100 μg/ml in HBSS.

2.5. Surface plasmon resonance

SPR measurements were performed at 25 °C using a liposome-coated NLC sensor chip (Bio-Rad, USA) mounted on a ProteOn XPR36 Protein Interaction Array System (Bio-Rad, USA). The liposomes were prepared as above besides that the hydrated lipids were incubated with 8 mM oligonucleotide 5′-TATTTCTGATGTCCACCCCC-3′, modified at the 3′ end with cholesterol (Generi Biotech, Czech Republic). The mixture was extruded through a 100-nm polycarbonate membrane (Avanti Lipids, USA) and the freshly-formed liposomes were incubated with 8 mM anti-sense oligonucleotide 5′-TGGACATCAGAAATACCCCC-3′, modified at the 3′ end with biotin (Generi-Biotech, Czech Republic). After 15 min of incubation, the non-bound biotinylated oligonucleotide was removed by centrifugation (50,000 *g* for 30 min at 4 °C). The pelleted vesicles were resuspended to a final concentration of 100 μg/ml in HBSS buffer and immediately immobilized on the streptavidin-coated NLC chip surface. All SPR experiments were carried out in HBSS buffer at a flow rate of 30 μl/min for both association and dissociation phases of the sensograms. The proteins were serially diluted in the running buffer and injected in parallel ("one-shot kinetics") over the immobilized liposome surfaces. Surfaces were typically regenerated with 100 μl of 50 mM NaOH and 150 mM NaCl. The sensograms were corrected for sensor background by interspot referencing (the sites within the 6 × 6 array which are not exposed to ligand immobilization but are exposed to analyte flow), and double referenced by subtraction of analyte (channels 1–5) using a "blank" injection (channel 6). The data were analyzed by using a ProteOn software (Bio-Rad, USA) and fitted with a 1:1 Langmuir-type and heterogeneous binding models to determine association (ka) and dissociation (kd) rate constants. The Langmuir-type model assumes the interaction between liposomes (L) and protein (P) resulting in a direct formation of the final complex (LP)

$$L + P \underset{kd}{\overset{ka}{\rightleftharpoons}} LP$$

where ka and kd are the association and the dissociation rate constants, respectively. The heterogeneous binding models assumes two binding sites on the ligand

$$L1 + P \underset{kd1}{\overset{ka1}{\rightleftharpoons}} L1P; \quad L2 + P \underset{kd1}{\overset{ka2}{\rightleftharpoons}} L2P$$

where L1 and L2 are two separate binding sites on the ligand and P is the analyte protein. Note that there are two separate sets of association and dissociation rate constants (ka1/kd1 and ka2/kd2) to describe each binding event. The binding response of a sensorgram from a heterogeneous ligand then, is the sum of the binding response of two separate binding events. An apparent equilibrium dissociation constant, KD was determined as KD = kd/ka.

2.6. Circular dichroism measurements

The electronic circular diochroism (ECD) spectra of M4-D and M4-P were collected with a Jasco J-815 CD spectrometer (Jasco Corporation, Tokyo, Japan) in spectral range 200–300 nm using 0.1 cm path length quartz cell at room temperature. The experimental setup was as follows: 0.5 nm step resolution, 10 nm/min speed, 16 s response time and 1 nm bandwidth. The sample concentration was kept constant 0.1 mg/ml in 25 mM HEPES (pH = 8.0) and 250 mM NaCl. The proteins were measured also with trifluorethanol (TFE) mixture (50% v/v TFE)

and in the presence of liposomes (final liposome concentration was 5 μM). After baseline correction, the final spectra were expressed as a molar ellipticity θ (deg·cm^2·dmol^{-1}) per residue. Secondary structure content was determined using an online circular dichroism analysis program Dichroweb software [58].

2.7. Molecular modeling

The 3D model of fusion construct — human TRPM4 N-terminus (UniProtKB/Swiss-Prot: Q8TD43.1; positions E733–W772, M4-P) with thioredoxin was generated by the I-Tasser prediction server [59,60]. The final model for construct was carefully selected, satisfying the criteria of Arg residue exposure to the solvent and geometry constraints of the potential ligand binding site. Docking PIP2 (ligand in 3SPI) and PIP3 (ligand in 1W1G) ligands were performed in Molecular Operating Environment (MOE) with the Induced Fit protocol [61]. The optimal binding mode was selected by applying the lowest interaction energy and best geometry fit criteria. Two molecular representations were generated using Chimera [62].

3. Results

3.1. Design and purification of TRPM4 constructs

We localized arginine and lysine rich regions to search for potential PIP2/PIP3 binding motif present in the intracellular termini of human TRPM4. Two putative PIP2/PIP3 binding sites M4-D and M4-P (regions 583–669 and 733–772) were predicted (Fig. 1). We cloned cDNA of these regions into a pET32_b vector for protein expression in Rosetta cells. To improve the solubility and expression yield of the proteins (wild type and its site directed mutants), we expressed and purified all of them as fusion proteins with the thioredoxin-tag at the N-terminus and 6× His tag at both N-termini. All expressed fusion proteins were soluble and in sufficient amounts to perform the binding experiments.

3.2. Analysis of PIP2/PIP3 binding to M4-D and M4-P peptides by surface plasmon resonance

To gain insight into the interactions of M4-D and M4-P with PIP2 and PIP3, we utilized surface plasmon resonance (SPR) technology. PIP2 or PIP3 was incorporated into liposomes by extrusion of the hydrated lipid mixtures (PC, PC/PIP2 and PC/PIP3) through membranes with a 100-nm pore size and the freshly-prepared lipid vesicles were immobilized to a neutravidin-coated NLC sensor chip through a biotin/cholesterol-functionalized DNA linker. The DNA linker consists of a short DNA sequence that is bi-functionalized with cholesterol and biotin, which the former is embedded within the lipid bilayer of liposomes, while the latter associates with neutravidin on the sensor chip to couple the lipid vesicles to the sensor surface. To minimize mass transfer effect, several coupling concentrations of liposomes leading to refractive index changes of 500, 1000, and 1500 RU were tested. Initial experiments at each of these liposome-coating concentrations were conducted with the TRPM4 fusion proteins at concentrations ranging from 0 to 10 μM. Initial estimates of koff values showed concentration dependence at coupling levels of 1000 and 1500 RU indicating mass transfer effects. However, coupling level of 500 RU resulted in clear responses and concentration independence of koff at flow rates of 30 μl/ml (data not shown). Consequently, coupling level of about 500 RU and flow rate of 30 μl/ml were used for the remaining experiments.

Real time interaction of serially-diluted M4-D and M4-P proteins with lipid surfaces revealed typical concentration-dependent binding curves (Figs. 2 and 3). Binding of the thioredoxin fusions was exclusively mediated through the TRPM4 segments, since thioredoxin itself did not bind the lipid surface (Fig. 2A–C). Kinetic parameters of the interaction between M4-D and PC, PIP2 and PIP3 enriched vesicles were calculated from global fitting of concentration-dependent binding curves (Fig. 2D–F). The experimental binding curves for M4-D fitted well to a simple 1:1 Langmuir binding model, revealing that the interaction of M4-D with lipid membrane follows pseudo first order kinetics and the adsorption of M4-D on lipid surfaces is limited by a finite number of identical binding sites. Moreover, the interaction of M4-D with lipids appears to be transient, suggesting that the M4-D segment of the TRPM4 channel does not embed in the lipid bilayer. However, kinetic rate constants were of similar values regardless of the presence or absence of PIP2 or PIP3, indicating no specificity of the M4-D segment of TRPM4 for polar heads of PIP2 and PIP3 lipids protruding out of the lipid membranes (Table 1).

Fig. 3A shows the experimental binding curves for the interaction of M4-P with liposomes made from phosphatidylcholine (PC) alone. The extensive fitting of the binding curves showed that these data could not be fitted to either 1:1 Langmuir binding model or other binding models, such as, heterogeneous analyte, heterogeneous ligand, and conformation change models. Moreover, the intensities of the response (RU) at the end of the association phases (120 s) were found to be

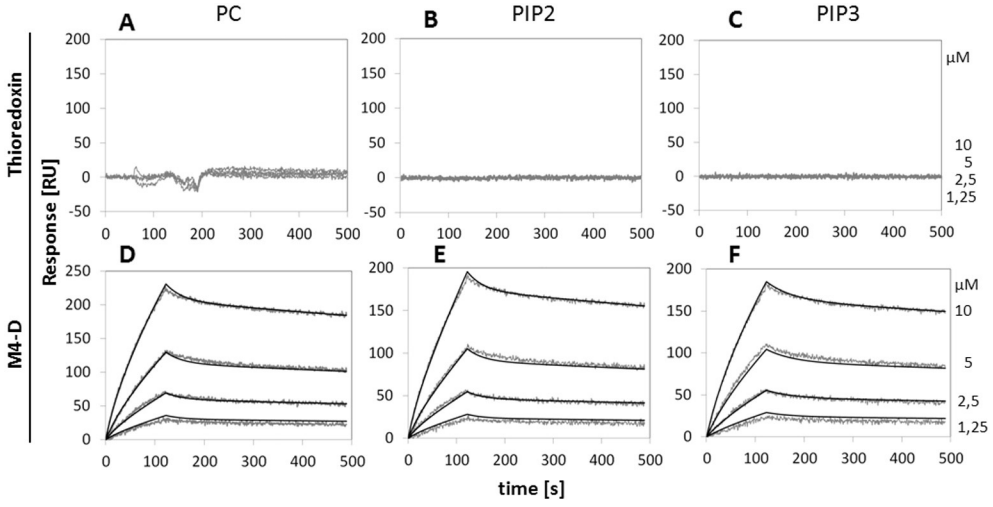

Fig. 2. SPR kinetic binding analysis of the interaction between M4-D and lipid vesicles. One-shot kinetic analysis of thioredoxin (A–C) and M4-D (D–F) interaction with liposomes containing phosphatidylcholine (PC) alone (A,D) or liposomes enriched with PIP2 (B,E) and PIP3 (C,F). Serially diluted proteins were injected in parallel over the sensor chip coated with 100-nm lipid vesicles and left to associate (120 s) and dissociate at constant flow rate of 30 μl/min. The kinetic data were globally fitted by using a heterogeneous ligand model (see Section 2). The fitted curves are superimposed as black lines on top of the sensograms.

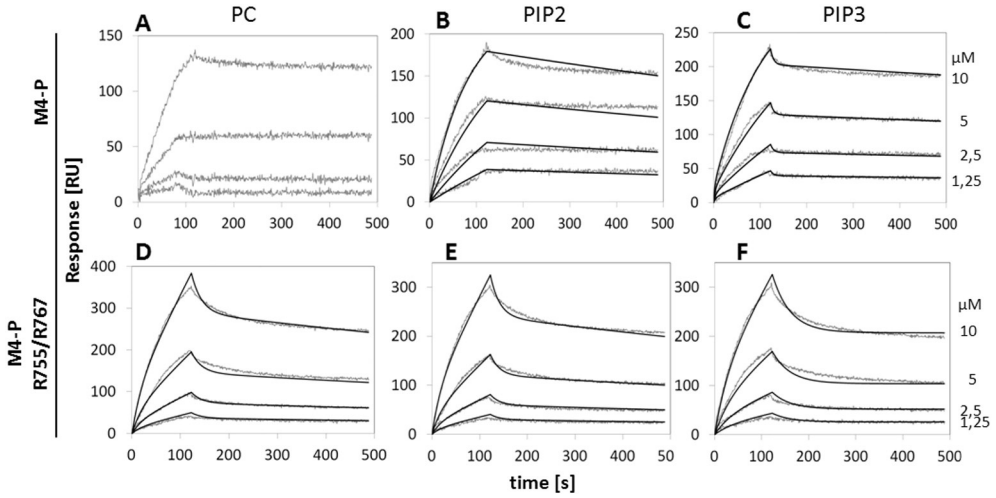

Fig. 3. SPR kinetic binding analysis of the interaction between M4-P and lipid vesicles. One-shot kinetic analysis of the interaction of M4-P (A–C) and its double mutant M4-P — R755A/R767A (D–F) with PC (A,D), PIP2 (B,E) and PIP3 enriched (C,F) lipid vesicles. Serially diluted proteins were injected in parallel over the sensor chip coated with 100-nm lipid vesicles and left to associate (120 s) and dissociate at constant flow rate of 30 μl/min. Apart from the interaction of M4-P with PC (A), which could not be fitted to any of the binding models, the kinetic data were globally fitted by using a heterogeneous ligand model (see Section 2). The fitted curves are superimposed as black lines on top of the sensograms.

linearly dependent on the concentration of the injected protein, indicating a non-specific interaction of M4-P with the lipid surface. In line with this observation, the data for the interaction of M4-P with PIP2 and PIP3 could not be fitted to a simple 1:1 binding model. Linear transformation of the association phase of the binding curves revealed nonlinear plots, demonstrating a more complex kinetics of the interactions. We then attempted to fit the binding curves to complex models to investigate the nature of these interactions. The data showed a close fit to a heterogeneous ligand model (Fig. 3B-C). The heterogeneous ligand model assumes that analyte (M4-P) binds two separate binding sites on the ligand (liposomes) and each ligand site binds the analyte independently with a different set of rate constants. The calculated association and dissociation rate constants (ka1, ka2, kd1, and kd2) as well as KD1 and KD2 for the interaction are listed in Table 2. The data analysis revealed that the affinities of M4-P to PIP2 and PIP3-enriched vesicles were comparable and found to be KD1 = 0.31 μM and KD2 = 5.5 μM for PIP2, and KD1 = 0.54 μM and KD2 = 5.4 μM for PIP3, respectively. In view of the fact that the heterogeneous ligand model assumes M4-P binding at two distinct sites with the binding affinity being approximately ten times higher for the first than the second site and simultaneously M4-P interacts non-specifically with liposome membranes made from PC alone, one can speculate that low-affinity KD2 values of the model corresponds to the non-specific interaction of M4-P with the PIP2- or PIP3-enriched vesicles, while high-affinity KD1 values could be attributed to the specific interaction of M4-P with polar heads of PIP2 or PIP3 on the lipid surfaces. Thus, the heterogeneous ligand model is the most likely model of the interaction of M4-P with PIP2- and PIP3-enriched vesicles.

Specificity of M4-P to PIP2 and PIP3 was further analyzed on a double mutant carrying substitution of two highly conserved arginine residues (R775 and R767) within a putative consensus motif (R/K-X12-14-R/K-X-R) that usually mediates high affinity binding of the PH domain to PIP3. In agreement with the wild-type construct, the binding curves for the interaction of the M4-P-R755A/R767A mutant with lipid vesicles were fitted to the heterogeneous ligand model (Fig. 3D–F). The calculated association and dissociation rate constants are listed in Table 2. Overall comparison of KD values revealed significant decrease in the binding affinity for the mutant. The main reason that contributes to the decreased binding affinity of the mutant was the faster dissociation (ka1) and slower association rates (kd1) of the arising complex. Moreover, the kinetics of interaction of the double mutant did not reveal any significant differences between binding to PC and PIP2- and PIP3-enriched vesicles indicating a complete loss of specificity for binding to PIP2 or PIP3. Thus, the M4-P segment of TrpM4 appears to interact specifically with PIP2 or PIP3 on the membrane surface and arginine residues R755 and R767 play an important role in this process.

3.3. Analysis of the secondary structure of M4-D and M4-P by circular dichroism

The secondary structure of the M4-D and M4-P fusion proteins was studied by ECD spectroscopy. Whereas the structure of cytosolic regions of TRPM4 is still unknown, the secondary structural composition of M4-D and M4-P fusion proteins with thioredoxin was determined as to be mostly disordered (Fig. 4 Table 2). ECD spectra of M4-D and M4-P fusion proteins confirmed that proteins are mostly unstructured, which is in a good agreement with the theoretical prediction based on their primary structure. According ECD spectra, both proteins M4-D and M4-P in the presence of liposomes formed by PC alone or PC containing PIP2/PIP3 (50/50%) do not change their secondary structure content (Fig. 4A, B and Table 2). This suggests that binding PIP2 or PIP3 to M4-D and M4-P proteins has no significant influence on their structure. According to our results based on 3D modeling of M4-P construct (Fig. 5), the model showed higher alpha helix content. While TFE is known as helix promoting solvent we also measured ECD spectra of M4-D and M4-P in the presence of TFE (Fig. 4C, D and Table 3) to estimate their ability to form α-helical structure [63–65]. The ECD spectra revealed that in the presence of TFE both proteins adopt helical structure more easily. A fraction of particular secondary structures obtained by analysis of ECD data corresponds to theoretical predictions from molecular modeling. This suggests that M4-D and M4-P in TFE environment could probably adopt a structure similar to their predicted fold. (See Table 4.)

Table 1
Kinetic and binding affinity constants for the interactions of M4-D with PC, PIP2 and PIP3 enriched lipid vesicles.

		ka × 10^2 [$M^{-1}\cdot s^{-1}$][a]	kd × 10^{-4} [s^{-1}]	KD [μM][b]
M4-D	PC	4.3 ± 1.2	6.5 ± 2.1	1.5 ± 0.6
	PIP2	2.5 ± 0.8	6.6 ± 2.4	2.6 ± 0.8
	PIP3	4.0 ± 1.3	6.5 ± 1.9	1.6 ± 0.7

[a] Results are means ± S.D. from the analysis of two independent measurements.
[b] The equilibrium dissociation constant (KD) was determined as ka/kd.

Table 2
Kinetic and binding affinity constants for the interactions of M4-P proteins with PC, PIP2 and PIP3 enriched lipid vesicles.

		ka1 × 10^3 [$M^{-1}\cdot s^{-1}$][a]	kd1 × 10^{-4} [s^{-1}]	KD1 [μM][b]	ka1 × 10^4 [$M^{-1}\cdot s^{-1}$]	kd2 × 10^{-1} [s^{-1}]	KD2 [μM]
M4-P	PC	–	–	–	–	–	–
	PIP2	1.5 ± 0.4	4.6 ± 1.1	0.3 ± 0.1	3.8 ± 0.8	2.1 ± 0.5	5.5 ± 1.4
	PIP3	1.2 ± 0.3	6.5 ± 2.1	0.5 ± 0.2	3.3 ± 0.7	1.8 ± 0.4	5.4 ± 1.3
R755/R767	PC	0.3 ± 0.1	9.8 ± 2.5	3.3 ± 0.9	4.1 ± 1.2	0.6 ± 0.2	1.5 ± 0.4
	PIP2	0.2 ± 0.1	10.1 ± 3.1	5.1 ± 1.4	5.2 ± 1.7	0.7 ± 0.2	1.3 ± 0.3
	PIP3	0.2 ± 0.1	9.9 ± 2.9	4.9 ± 1.5	3.2 ± 0.9	0.6 ± 0.2	1.9 ± 0.3

[a] Results are means ± S.D. from the analysis of two independent measurements.
[b] The equilibrium dissociation constants (KD1 and KD2) was determined as kd1/ka1 and kd1/ka1, respectively.

3.4. 3D modeling and PIP2/PIP3 docking of M4-P

To predict the interactions of the phospholipid binding site of TRPM4 N-termini with PIP2/PIP3 ligands, we created a 3D model of the corresponding M4-P N-terminus in fusion construct with thioredoxin (thioredoxin, 2× His-tags and TRPM4E733-W772 sequence). A model of human TRPM4 fusion protein was generated using the I-Tasser prediction server. The thioredoxin structure was deleted from the model and potential PIP2/PIP3 binding site was assigned by MOE. Eventually, PIP2 and PIP3 ligands were docked into the assigned binding site (Fig. 5). To orient PIP2/PIP3 ligands properly, we utilized structural information from the literature — in particular the interaction of PIP2 with the proximal region of the intracellular tails of potassium ion channels [53,54,66] which is well characterized. For the models of TRPM4-PIP2/PIP3 complexes we assumed that the interaction is accomplished by an arginine/lysine cluster interacting with the phosphate groups of PIP2 (PIP3). Positively charged amino acids are frequent in the vicinity of the inner plasma membrane leaflet where binding sites for regulatory molecules such as phosphatidylinositol phosphates are expected to be abundant. Their mutation to alanine residues causes a replacement of their charged-side chains in the binding site, which makes it less favorable for interaction with PIP2 [67–69]. According to this hypothesis, our in silico predictions support that R755A and R767A mutations result in the loss of non-covalent interactions with the phosphate groups of PIP2/PIP3 which is in agreement with our experimental data.

4. Discussion

PIP2 and PIP3 are short-lived phospholipids found on the cytosolic side of eukaryotic cell membranes and act as regulators of signaling proteins in the plasma membrane that induce a TRP channels [46,67]. It has been shown that many ion receptors — inward-rectifier and voltage-gated K^+ channels, Ca^{2+} channels, cyclic nucleotide gated channels, epithelial Na^+ and Cl^- channels are regulated by PIP2 [70]. Of the many described phospholipid-binding proteins, a number of different domain structures have been defined that exhibit stereospecific recognition of specific phosphoinositide head groups in the context of cellular membrane surfaces these include the pleckstrin homology (PH) and Phox-homology (PX) domains. The common hypothesis to explain the binding of PIP2 is that positively charged residues present in the domain are responsible for the ligand-dependent modulation of the TRP's activity. Similarly, TRP channels also contain intracellular domain clusters which have been identified as PIP2 binding pockets [49,71]. The regulation of TRPs by phosphoinositides, especially by PIP2 and PIP3, has only been described for the TRPC subfamily [55]. It was found that PIP3 bound TRPC6 directly with the highest potency. Biophysical and bioinformatics methods were used to improve our

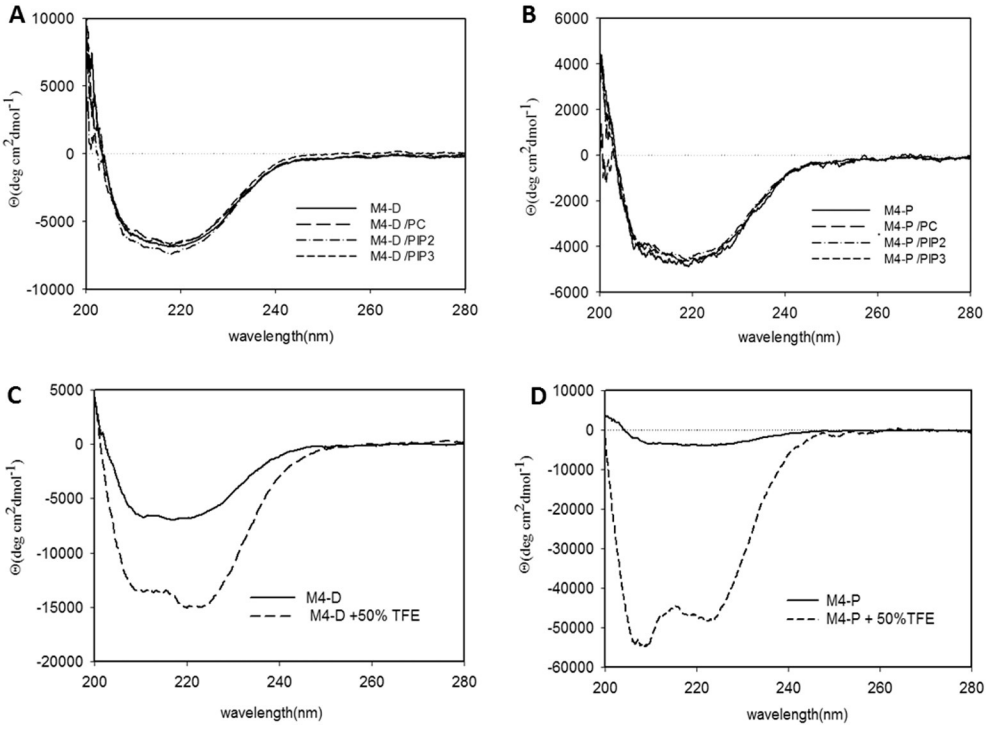

Fig. 4. ECD spectra of peptide M4-D and M4-P in presence of liposomes and TFE. Peptide M4-D (A) and M4-P (B) in the interaction with PC, PIP2 and PIP3 enriched lipid vesicles. Peptides M4-D (C) and M4-P (D) in the presence of 50% (v/v) TFE. CD spectra were expressed as molar ellipticity Q ($deg\cdot cm^2\cdot dmol^{-1}$) per residue.

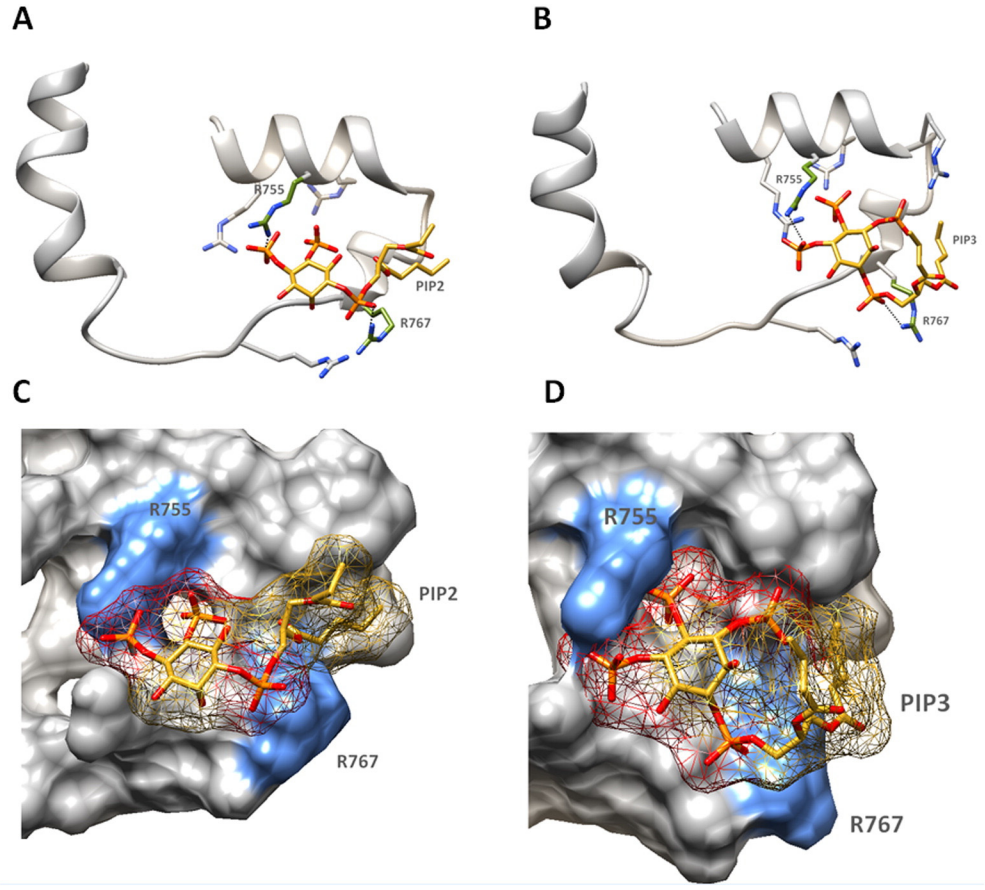

Fig. 5. M4-P domain binds PIP2 and PIP3. (A) Schematic view of the interactions of M4-P/PIP2 and (B) M4-P/PIP3. All arginines exhibit similar binding to the PIP2 and PIP3. Important arginine residues bonded (dashed lines) to PIP2/PIP3 are colored green (R755 and R767). We used the following color convention: gray — protein backbone of the M4-P, yellow — carbon atoms of PIP2, oxygen (O_2) — red, nitrogen (N) — blue, phosphorus (P) — orange. (C) Solvent accessible surface representation of the M4-P/PIP2 and (D) M4-P/PIP3 complexes; surfaces of lysine and arginine R755, R767 colored blue. (For interpretation of the references to color in this figure legend, the reader is referred to the web version of this article.)

understanding of the regulation of the TRPM4 channel by two similar ligands (PIP2/PIP3) and identify the binding sites or actual potential gating sites on the N-termini.

The regulation of TRPM channels by PIP2 was demonstrated [72]. A binding site for PIP2, calmodulin and calcium-binding protein A1 protein (S100A1) was found in the TRPM3 N-terminus and these ligands can compete with each other [14]. As for TRPM5, PIP2 promotes the gating of this channel, which, after desensitization, was activated by lower concentrations of Ca^{2+} in the presence of PIP2 [42]. The hydrolysis of PIP2 by phospholipase C (PLC)-coupled hormones may constitute an important pathway for TRPM6 gating [37,40,73]. The importance of PIP2 has also been reported for TRPM7, in which PIP_2 hydrolysis by PLCs inhibits channel activation [43,44]. The breakdown of PIP2 also appears to underlie the desensitization of TRPM8 [45]. Because PIP2 is degraded by PLC, the action of PIP2 may underlie the response of some TRPs to the stimulation of PLC-coupled plasma membrane receptors, as mentioned above for TRPM7 [44]. In the intracellular C-terminus region of the TRPM4 channel, the PIP2 binding site in the TRP box domain was described by electrophysiology experiments. The group of Nilius et al. [41] investigated whether mutations in TRPM4-K1059, and R1062 in the TRP box domain affect the response to PIP2. It was demonstrated that PIP2 enhances the activity of TRPM4 Ca^{2+}-activated cation channels by decreasing Ca^{2+} sensitivity and shifting their voltage dependence, and provided evidence that these effects require an intact C-terminal PH domain. In contrast, the binding of PIP2 to the N-terminus of the TRPM4 channel has not been reported before.

Here we used surface plasmon resonance to directly study the specificity and binding affinity of TRPM4 constructs to liposomes containing PIP2/PIP3. We proposed the two putative binding sites M4-D and M4-P in close proximity to each other and rich in Arg/Lys residues, which can be important for interaction with PIP2 and PIP3. It was found out that M4-D could interact with lipid bilayer but without any specificity for PIP2 or PIP3 lipids, but M4-P fusion protein binds both ligands specifically. Dissociation constants for M4-P–PIP2/PIP3 complexes were very similar and were in the micro molar range. A similar binding affinity for PIP2 (PIP3) was observed previously with the TRP family members [19,20]. Two important residues in the N-termini PIP2/PIP3 binding domain were found, namely R755 and R767, their mutation caused complete loss of specificity for PIP2/PIP3 binding. Here it is shown that PIP3 binds the same region on the TRPM4 N-terminus with almost the same affinity as PIP2. Moreover, the mutations of positively charged

Table 3
Calculated incidence (%) of secondary structure content. M4-D and M4-P fusion protein constructs and their complexes with PIP2 and PIP3 determined by CD spectroscopy in 25 mM HEPES (pH = 8.0), 250 mM NaCl.

	Helix	Anti-parallel	Parallel	β-turn	Random coil
M4-D	22	11	11	17	38
M4-D/PC	22	11	11	17	39
M4-D/PIP2	21	11	11	17	38
M4-D/PIP3	22	11	12	17	38
M4-P	17	13	13	17	40
M4-P/PC	15	13	13	18	41
M4-P/PIP2	15	11	14	17	42
M4-P/PIP3	17	13	13	17	40

Table 4
Calculated incidence (%) of secondary structure content. M4-D and M4-P fusion protein constructs determined by CD spectroscopy in 25 mM HEPES (pH = 8.0), 250 mM NaCl and 1 mM $CaCl_2$, and in the same buffer with 50% TFE added.

	Helix	Anti-parallel	Parallel	β-turn	Random coil
M4-D	22	11	11	17	38
M4-D + TFE	44	6	7	15	27
M4-P	17	13	13	17	40
M4-P + TFE	95	0	0	4	1

residues within this domain affected the binding to PIP3, as was observed for PIP2.

Intracellular N- and C-termini are highly heterologous for every subfamily of the whole superfamily of TRPs. Circular dichroism measurements were used to obtain knowledge of the secondary structure of TRPM4 N-termini fusion proteins — individually, in complexes with ligands PIP2/PIP3 and in the TFE environment. The secondary structure of TRPM4 N-termini fusion proteins was determined to be mostly unstructured. In complexes of TRPM4-PIP2/PIP3 no changes were detected in the secondary structure of proteins. According to these data we can assume that TRPM4 proteins do not undergo structural changes upon complex formation. Moreover, both M4-D and M4-P fusion proteins readily adopt a helical structure in TFE buffer, it follows that these regions may acquire more structural characteristics in the in vivo environment.

Molecular model of the TRPM4 N-termini proximal regions interacting with PIP2/PIP3 suggests that the phosphate head groups of PIP2 and PIP3 form ionic interactions with positively charged arginines R755 and R767. PIP2 binding pocket is present in the M4-P region. According to the data from SPR, the binding affinity for M4-P–PIP2/PIP3 complexes is very similar. The molecular model with PIP3 supports our data from SPR, because the one extra phosphate group of PIP3 does not have a particularly large influence on the strength of the interaction. Using methods of molecular modeling, we localized a possible interaction mode of the PIP2 binding pocket in the proximal M4-P of TRPM4 domain with PIP2/PIP3, but the structural basis of the action by lipids on TRP channel activity has not been determined yet.

In conclusion, we have identified proximal region E733–W772 TRPM4 N-terminus as PIP2 binding pocket using SPR measurements. The basic amino acid R755 and R767 residues are crucial in the interaction with PIP2 and PIP3, their mutation caused a total loss of binding specificity to ligands. This is the first report to show that PIP3 binds directly to TRPM4 family channel. M4-P domain can bind both PIP2 and PIP3 with a similar binding affinity to share the same binding site. It can be assumed that the binding site for PIP2 is always shared for PIP3. It was confirmed, from the in silico docking experiments, that R755 and R767 residues interact with the phosphates of the PIP2/PIP3 molecules directly, according to the same mode as was previously published [53,54,67]. During the interaction of fusion proteins with LUVs enriched by PIP2/PIP3, M4-D and M4-P do not change their secondary structure content. Surely, phosphatidylinositol phosphates are important regulators in TRP channels and it is very likely that they could regulate TRPM4 channel via binding to its intracellular N-terminus in the same way as was reported for other members of the TRPM family [19,42–44,72,73], nevertheless more functional studies will be required to elucidate the role of PIP2 and PIP3 in TRPM4 channel gating and regulation.

Acknowledgments

This study was supported by the Grant Agency of Charles University (grant no. 842313, 238214), the Grant Agency of the Czech Republic (grant no. 207/11/0717 and 15-11851S), the Grant Agency of the Czech Republic Project of Excellence in the Field of Neuroscience (grant no. P304/12/G069) and with institutional support RVO: 67985823.

References

[1] F. Yi, H. Han, New insights into the TRP channel: interaction with pattern recognition receptors, Channels 8 (2014) 13–19.
[2] J. Vriens, K. Held, A. Janssens, B.I. Thót, S. Kerselaers, B. Nilius, R. Vennekens, T. Voets, Opening of an alternative ion permeation pathway in a nociceptor TRP channel, Nat. Chem. Biol. 10 (2014) 188–195.
[3] T. Smani, G. Shapovalov, R. Skryma, N. Prevarskaya, J.A. Rosado, Functional and physiological implications of TRP channels, Biochim. Biophys. Acta 1853 (2015) 1772–1782.
[4] A. Gordon-Shaag, W.N. Zagotta, S.E. Gordon, Mechanism of Ca^{2+}-dependent desensitization in TRP channels, Channels 2 (2008) 125–129.
[5] D. Julius, TRP channels and pain, Annu. Rev. Cell Dev. Biol. 29 (2013) 355–384.
[6] R. Vennekens, A. Menigoz, B. Nilius, TRPs in the brain, Rev. Physiol. Biochem. Pharmacol. 163 (2012) 27–64.
[7] M.B. Morelli, C. Amantini, S. Liberati, M. Santoni, M. Nabissi, TRP channels: new potential therapeutic approaches in CNS neuropathies, CNS Neurol. Disord. Drug Targets 12 (2013) 274–293.
[8] M. Liao, E. Cao, D. Julius, Y. Cheng, Structure of the TRPV1 ion channel determined by electron cryo-microscopy, Nature 504 (2013) 107–112.
[9] K.W. Huynh, M.R. Cohen, S. Chakrapani, H.A. Holdaway, P.L. Stewart, V.Y. Moissenkova-Bell, Structural insight into the assembly of TRPV1 channels, Structure 22 (2014) 260–268.
[10] C.E. Paulsen, J.P. Armache, Y. Gao, Y. Cheng, D. Julius, Structure of the TRPA1 ion channel suggests regulatory mechanisms, Nature 520 (2015) 511–517.
[11] D.E. Clapham, TRP channels as cellular sensors, Nature 426 (2003) 517–524.
[12] C.L. Huang, The transient receptor potential superfamily of ion channels, J. Am. Soc. Nephrol. 15 (2004) 1690–1699.
[13] M.M. Moran, H. Xu, D.E. Clapham, TRP ion channles in nervous system, Curr. Opin. Neurobiol. 14 (2004) 362–369.
[14] R. Padinjat, S. Andrews, TRP channels at a glance, J. Cell Sci. 117 (2004) 5707–5709.
[15] L. Grycova, Z. Lansky, E. Friedlova, V. Obsilova, T. Obsil, J. Teisinger, Ionic interactions are essential for TRPV1 C-terminus binding to calmodulin, Biochem. Biophys. Res. Commun. 375 (2008) 680–683.
[16] B. Holakovska, L. Grycova, M. Jirku, M. Sulc, L. Bumba, J. Teisinger, Calmodulin and S100A1 interact with N terminus of TRPM3 channel, J. Biol. Chem. 287 (2012) 16645–16655.
[17] T. Voets, B. Nilius, Modulation TRPs by PIPs, J. Physiol. 582 (2007) 939–944.
[18] B. Nilius, G. Owsianik, T. Voets, Transient receptor potential channels meet phosphoinositides, EMBO J. 27 (2008) 2809–2816.
[19] B. Holendova, L. Grycova, M. Jirku, J. Teisinger, PtdIns(4,5)P2 interacts with CaM binding domains on TRPM3 N-terminus, Channels 6 (2012) 479–482.
[20] L. Grycova, B. Holendova, L. Bumba, J. Bily, M. Jirku, Z. Lansky, J. Teisinger, Integrative binding sites within intracellular termini of TRPV1 receptor, PLoS ONE 7 (2012) e48437.
[21] T. Voets, B. Nilius, TRPs make sense, J. Membr. Biol. 192 (2003) 1–8.
[22] X. Jin, J. Touhey, R. Gaudet, Structure of the N-terminal ankyrin repeat domain of the TRPV2 ion channel, J. Biol. Chem. 281 (2006) 25006–25010.
[23] P.V. Lishko, E. Procko, X. Jin, C.B. Phelps, R. Gaudet, The ankyrin repeats of TRPV1 bind multiple ligands and modulate channel sensitivity, Neuron 54 (2007) 905–918.
[24] C.B. Phelps, R.J. Huang, P.V. Lishko, R.R. Wang, R. Gaudet, Structural analyses of the ankyrin repeat domain of TRPV6 and related TRPV ion channels, Biochemistry 47 (2008) 2476–2484.
[25] C. Harteneck, Function and pharmacology of TRPM cation channels, Naunyn Schmiedeberg's Arch. Pharmacol. 371 (2005) 307–314.
[26] P. Launay, A. Fleig, A.L. Perraud, A.M. Scharenberg, R. Penner, J.P. Kinet, TRPM4 is a Ca^{2+} activated nonselective cation channel mediating cell membrane depolarization, Cell 109 (2002) 397–407.
[27] M. Murakami, F. Xu, I. Miyoshi, E. Sato, K. Ono, T. Iijima, Identification and characterization of the murine TRPM4, Biochem. Biophys. Res. Commun. 307 (2003) 522–528.
[28] J.C. Yoo, O.V. Yarishkin, E.M. Hwang, E. Kim, D.G. Kim, N. Park, S.G. Hong, J.Y. Park, Cloning and characterization of rat transient receptor potential-melastatin 4 (TRPM4), Biochem. Biophys. Res. Commun. 391 (2010) 806–811.
[29] B. Schattling, K. Steinbach, E. Thies, M. Kruse, A. Menigoz, F. Ufer, V. Flockerzi, W. Bruck, O. Pongs, R. Vennekens, M. Kneussel, M. Freichel, D. Merkler, M.A. Friese, TRPM4 cation channel mediates axonal and neuronal degeneration in experimental autoimmune encephalomyelitis and multiple sclerosis, Nat. Med. 18 (2012) 1805–1811.
[30] Y.S. Kim, E. Kang, Y. Makino, S. Park, J.H. Shin, H. Song, P. Launay, D.J. Linden, Characterizing the conductance underlying depolarization-induced slow current in cerebellar Purkinje cells, J. Neurophysiol. 109 (2013) 1174–1181.
[31] M. Krause, E. Schulze-Bahr, V. Corfield, A. Beckmann, B. Stallmeyer, G. Kurtbay, I. Ohmert, E. Shultze-Bahr, P. Brink, O. Pongs, Impaired endocytosis of the ion channel TRPM4 is associated with human progressive familial heart block type I, J. Clin. Invest. 119 (2009) 2737–2744.
[32] H. Cheng, A. Beck, P. Launay, S.A. Gross, A.J. Stokes, J.P. Kinet, A. Fleig, R. Penner, TRPM4 controls insulin secretion in pancreatic beta-cells, Cell Calcium 41 (2007) 51–61.
[33] G. Barbet, M. Demion, I.C. Moura, N. Serafini, T. Léger, F. Vrtovsnik, R.C. Monteiro, R. Guinamard, J.P. Kinet, P. Launay, The calcium activated nonselective cation channel TRPM4 is essential for the migration but not the maturation of dendritic cells, Nat. Immunol. 9 (2008) 1148–1156.
[34] T. Shimizu, G. Owsianik, M. Freichel, V. Flockerzi, B. Nilius, R. Vennekens, TRPM4 regulates migration of mast cells in mice, Cell Calcium 45 (2009) 226–232.
[35] F.J. Taberner, G. Fernandéz-Ballester, A. Fernandéz-Carvajal, A. Ferrer-Montiel, TRP channels interaction with lipids and its implications in disease, Biochim. Biophys. Acta Biomembr. S0005–2736 (2015) 00101–00107.

[36] B. Hille, E.J. Dickson, M. Kruse, O. Vivas, B.C. Sush, Phosphoinositides regulate ion channels, Biochim. Biophys. Acta Mol. Cell Biol. Lipids 1851 (2014) 844–856.
[37] T. Rohacs, Phosphoinositide regulation of TRP Channels, Handb. Exp. Pharmacol. 223 (2014) 1143–1176.
[38] P. Raghu, R.C. Hardie, Regulation of *Drosophila* TRPC channels by lipid messengers, Cell Calcium 45 (2009) 566–573.
[39] E.D. Prescott, D. Julius, A modular PIP2 binding site as a determinant of capsaicin receptor sensitivity, Science 300 (2003) 1284–1288.
[40] T. Rohacs, Phosphoinositide regulation of non-canonical transient receptor potential channels, Cell Calcium 45 (2009) 554–565.
[41] B. Nilius, F. Mahieu, J. Prenen, A. Janssens, G. Owsianik, R. Vennekens, T. Voets, The Ca^{2+}-activated cation channel TRPM4 is regulated by phosphatidylinositol 4,5-biphosphate, EMBO J. 25 (2006) 467–478.
[42] D. Liu, E.R. Liman, Intracellular Ca^{2+} and the phospholipid PIP2 regulate the taste transduction ion channel TRPM5, Proc. Natl. Acad. Sci. U. S. A. 100 (2003) 15160–15165.
[43] T. Rohacs, B. Nilius, Regulation of transient receptor potential (TRP) channels by phosphoinositides, Pflugers Arch. 455 (2007) 157–168.
[44] L.W. Runnels, L. Yue, D.E. Clapham, The TRPM7 channel is inactivated by PIP2 hydrolysis, Nat. Cell Biol. 4 (2002) 329–336.
[45] Y. Yudin, V. Lukacs, C. Cao, T. Rohacs, Decrease in phosphatidylinositol 4,5-bisphosphate levels mediates desensitization of the cold sensor TRPM8 channels, J. Physiol. 15 (2011) 6007–6027.
[46] S. Brauchi, G. Orta, C. Mascayano, M. Salazar, N. Raddatz, H. Urbina, E. Rosenmann, F. Gonzalez-Nilo, R. Latorre, Dissection of the components for PIP2 activation and thermosensation in TRP channels, Proc. Natl. Acad. Sci. U. S. A. 104 (2007) 10246–10251.
[47] A. Rezvanpour, G.S. Shaw, Unique S100 target protein interactions, Gen. Physiol. Biophys. 28 (2009) F39–F46.
[48] X. Steinberg, C. Lespay-Rebolledo, S. Brauchi, A structural view of ligand-dependent activation in thermo TRP channels, Front. Physiol. 5 (2014) (eCollection2014).
[49] A.E. Lemmon, K.M. Ferguson, R. O'Brien, P.B. Sigler, J. Schlessinger, Specific and high-affinity binding of inositol phosphates to an isolated pleckstrin homology domain, Proc. Natl. Acad. Sci. U. S. A. 92 (1995) 10472–10476.
[50] B. Nilius, J. Prenen, G. Droogmans, T. Voets, R. Vennekens, M. Freichel, U. Wissenbach, V. Flockerzi, Voltage dependence of the Ca^{2+}-activated cation channel TRPM4, J. Biol. Chem. 278 (2003) 30813–30820.
[51] V. Lukacs, B. Thyagarajan, P. Varnai, A. Balla, T. Balla, T. Rohacs, Dual regulation of TRPV1 by phosphoinositides, J. Neurosci. 27 (2007) 7070–7080.
[52] A. Gericke, N.R. Leslie, M. Losche, A.H. Ross, PI(4,5)P2-mediated cell signaling: emerging principles and PTEN as a paradigm for regulatory mechanism, Adv. Exp. Med. Biol. 991 (2013) 85–104.
[53] S.B. Hansen, X. Tao, R. MacKinnon, Structural basis of PIP2 activation of the classical inward rectifier K^+ channel Kir2.2, Nature 477 (2011) 495–498.
[54] M.R. Whorton, R. MacKinnon, Crystal structure of the mammalian GIRK2 K^+ channel and gating regulation by G proteins, PIP2, and sodium, Cell 147 (2011) 199–208.
[55] Y. Kwon, T. Hofmann, C. Montell, Integration of phosphoinositide- and calmodulin-mediated regulation of TRPC6, Mol. Cell 23 (2007) 491–503.
[56] A. Penna, V. Juvin, J. Chemin, V. Compan, M. Monet, F.A. Rassendren, PI3-kinase promotes TRPV2 activity independently of channel translocation to the plasma membrane, Cell Calcium 36 (2006) 495–507.
[57] K. Prochazkova, R. Osicka, I. Linhartova, P. Halada, M. Sulc, P. Sebo, The *Neisseria meningitidis* outer membrane lipoprotein FrpD binds the RTX protein FrpC, J. Biol. Chem. 280 (2005) 3251–3258.
[58] L. Whitmore, B.A. Wallace, Protein secondary structure analyses from circular dichroism spectroscopy: methods and reference databases, Biopolymers 89 (2008) 392–400.
[59] Y. Zhang, I-TASSER server for protein 3D structure prediction, BMC Bioinforma. 9 (2008) 1–8.
[60] A. Roy, A. Kucukural, Y. Zhang, I-TASSER: a unified platform for automated protein structure and function prediction, Nat. Protoc. 5 (2010) 725–738.
[61] Molecular Operating Environment (MOE), Chemical Computing Group Inc., 1010 Sherbooke St. West, Suite #910, Montreal, QC, Canada, H3A 2R7, 2013.
[62] E.F. Pettersen, T.D. Goddard, C.C. Huang, G.S. Couch, D.M. Greenblatt, E.C. Meng, T.E. Ferrin, UCSF Chimera—a visualization system for exploratory research and analysis, J. Comput. Chem. 25 (2004) 1605–1612.
[63] B. Filippi, G. Borin, V. Moretto, F. Marchiori, Conformational properties of the N-terminal residues of S-peptide. II. The guanidine hydrochloride–water–trifluoroethanol system, Biopolymers 17 (1978) 2545–2559.
[64] J.W. Nelson, N.R. Kallenbach, Stabilization of the ribonuclease S peptide α helix by trifluoroethanol, Proteins Struct. Funct. Genet. 1 (1986) 211–217.
[65] S.I. Segawa, N. Fukuno, K. Fujiwara, Y. Noda, Local structures in unfolded lysozyme and correlation with secondary structures in the native conformation: helix-forming or -breaking propensity of peptide segment, Biopolymers 31 (1991) 497–509.
[66] M.A. Zaydman, J. Cui, PIP2 regulation of KCNQ channels: biophysical and molecular mechanisms for lipid modulation of voltage-dependent gating, Front. Physiol. 5 (2014) (e).
[67] K. Bodhinathan, P.A. Slesinger, Alcohol modulation of G-protein-gated inwardly rectifying potassium channels: from binding to therapeutics, Front. Physiol. 5 (2014) eCollection 2014.
[68] B.R. Pattnaik, S. Tokarz, M.P. Asuma, T. Schroeder, A. Sharma, J.C. Mitchell, A.O. Edwards, D.A. Pillers, Snowflake vitreoretinal degeneration (SVD) mutation R162W provides new insights into Kir7.1 ion channel structure and function, PLoS ONE 8 (2013) e71744.
[69] G. Khelashvili, G. Galli, H. Weinstein, Phosphatidylinositol 4,5-biphosphate (PIP2) lipids regulate the phosphorylation of syntaxin N-terminus by modulating both its position and local structure, Biochemistry 51 (2012) 7685–7698.
[70] K.A. Morales, T.I. Igumenova, Synergistic effect of $Pb2^+$ and PIP2 on C2 domain-membrane interactions, Biochemistry 51 (2012) 3349–3360.
[71] B.C. Suh, B. Hille, Regulation of ion channels by phosphatidylinositol 4,5-bisphosphate, Curr. Opin. Neurobiol. 15 (2005) 370–378.
[72] S. Ximena, C. Lespay-Rebolledo, S. Brauchi, A structural view of ligand-dependent activation in thermo TRP channels, Front. Physiol. 5 (2014) 1–14.
[73] J. Xie, B. Sun, J. Du, W. Yang, H.C. Chen, L. Yue, Phosphatidylinositol 4,5-bisphosphate (PIP(2)) controls magnesium gatekeeper TRPM6 activity, Sci. Rep. 1 (2011) (Epub).

APPENDIX 4

Jirku M, Bumba L, Bednarova L, Kubala M, Sulc M, Franek M, Vyklicky L, Vondrasek J, Teisinger J, **Bousova K**, Characterization of the part of N-terminal PIP2 binding site of the TRPM1 channel. Biophys Chem. 2015, 207:135-42. doi: 10.1016/j.bpc.2015.10.005.

Biophysical Chemistry 207 (2015) 135–142

Contents lists available at ScienceDirect

Biophysical Chemistry

journal homepage: http://www.elsevier.com/locate/biophyschem

Characterization of the part of N-terminal PIP2 binding site of the TRPM1 channel

Michaela Jirku [a,b], Ladislav Bumba [c], Lucie Bednarova [d], Martin Kubala [e], Miroslav Sulc [a,c], Miloslav Franek [f], Ladislav Vyklicky [b], Jiri Vondrasek [d], Jan Teisinger [b], Kristyna Bousova [b,g,*]

[a] Faculty of Science, Charles University in Prague, 12843 Prague, Czech Republic
[b] Institute of Physiology, Academy of Sciences of the Czech Republic, 14220 Prague, Czech Republic
[c] Institute of Microbiology, Academy of Sciences of the Czech Republic, 14220 Prague, Czech Republic
[d] Institute of Organic Chemistry and Biochemistry, Academy of Sciences of the Czech Republic, 16610 Prague, Czech Republic
[e] Faculty of Science, Palacky University, 78341 Olomouc, Czech Republic
[f] 3rd Faculty of Medicine, Charles University in Prague, 10000 Prague, Czech Republic
[g] 2nd Faculty of Medicine, Charles University in Prague, 15006 Prague, Czech Republic

HIGHLIGHTS

- PIP2 binding site in the putative PH domain was determined in the TRPM1-NT
- Basic K464 residue present in the TRPM1-NT was suggested to interacts with PIP2
- The TRPM1-NT/PIP2 complex formation is associated with structural changes
- Molecular modeling confirmed non-covalent binding mode of the TRPM1-NT with PIP2

GRAPHICAL ABSTRACT

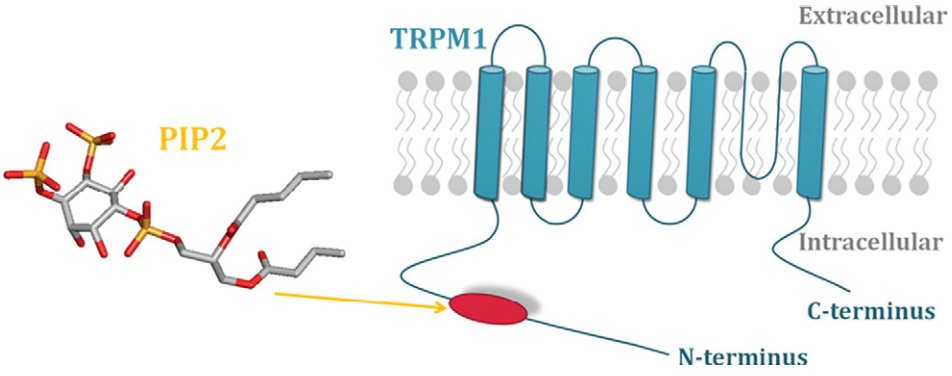

ARTICLE INFO

Article history:
Received 7 September 2015
Received in revised form 23 October 2015
Accepted 25 October 2015
Available online 27 October 2015

Keywords:
TRPM1 channel
Binding site
PIP2
Surface plasmon resonance
FRET
Circular dichroism

ABSTRACT

Transient receptor potential melastatin-1 (TRPM1) is a calcium channel that is essential for the depolarization of photo-responsive retinal bipolar cells, but most of the physiological functions and cellular roles of this channel are still poorly understood. Most transient receptor potential (TRP) channels are typically regulated by intracellular proteins and other signaling molecules. Phosphatidylinositol-4,5 bisphosphate (PIP2), a minor phospholipid component of cell membranes, has previously been shown to directly bind TRP channels and to play a unique role in modulating receptor function. To characterize the binding of PIP2 as a potential regulator of TRPM1, we utilized biophysical methods and molecular modeling to study the interactions of PIP2 with an N-terminal fragment of TRPM1 (residues A451–N566). The basic N-terminal residue K464 of TRPM1 suggests that it is part of putative pleckstrin homology (PH) domain and is involved in the interactions with PIP2. This is the first report detailing the binding of PIP2 at the N-terminus of the TRPM1 receptor.

* Corresponding author at: Institute of Physiology, Academy of Sciences of the Czech Republic, 14220 Prague, Czech Republic.
E-mail address: kristyna.bousova@fgu.cas.cz (K. Bousova).

http://dx.doi.org/10.1016/j.bpc.2015.10.005
0301-4622/

1. Introduction

Transient receptor potential channels (TRPs) are special nociceptive membrane proteins that are responsible for the entry of mono- and bivalent cations into the cell [1]. These proteins are a group of unique ion channels that play many critical roles in cellular processes such as calcium oscillations after T cell activation, mechanotransduction, thermosensation and the regulation of cell adhesion [2–4]. The three-dimensional structure of the membrane portion of vanilloid 1 (TRPV1) and ankyrin 1 (TRPA1) receptors was recently described [5,6]. However, structural information on the intracellular regions of TRPs is still lacking. According to structural analyses, TRP channels are tetramers assembled with four-fold symmetry from individual subunits that contain six putative transmembrane (TM) domains. The region between the fifth and sixth TM domains, which includes a putative pore loop, forms the ion permeation pathway [7–9]. The intracellular amino and carboxy termini of TRPs vary greatly in their lengths and amino acid sequences. These cytoplasmic regions contain various well-known domains and motifs that are likely to be involved in channel assembly, activation and regulation through protein–protein and/or protein–ligand interactions [10].

TRPM1, a non-selective cation channel, belongs to the transient receptor potential melastatin family [11]. This ion channel plays important roles in the depolarizing photo-response of retinal bipolar cells [12]. TRPM1 is capable of forming ion-conducting channels in the plasma membrane and can form ion channels outside of retinal bipolar cells [13]. Additionally, TRPM1 localized to the tip of melanocytic dendrites probably regulates the release of melanin from melanosomes [14]. Whereas the functions of most melastatin channels have been described [15–22], the properties and cellular roles of the TRPM1 channel remain to be explored. TRPM channels are regulated by a variety of different stimuli, and in many cases, involves interactions between channel proteins and intracellular signaling molecules such as phospholipids and Ca^{2+}-binding proteins [23–27]. Direct interaction and regulation by phosphatidylinositol-4, 5 bisphosphate (PIP2) has been observed for most TRPM channels [23–33]. Rampino and Nawy [34] found that the depletion of PIP2 together with the inhibition of PLC depresses TRPM1 current, indicating that a metabolite downstream of PIP_2 modulates the channel ON-state. We focused on TRPM1, which shows sequence similarity to the third known member of the melastatin TRP family — TRPM3 [35].Multiple binding sites for Ca^{2+}-binding proteins and PIP2 have already been characterized on the N-terminus of TRPM3 [25,26].

Phosphatidylinositol phosphates (PIPs) are widely present in the inner leaflet of the plasma membrane and are frequently involved in intercellular signaling. PIP2 is the most abundant of these molecules and appears to participate in the regulation of many membrane receptors [36–38]. Through direct interactions, PIP2 modulates the functions of many ion channels (inward-rectifier and voltage-gated K^+ channels, voltage-gated Ca^{2+} channels, cyclic nucleotide-gated channels, etc.) [39–41], and PIP2 has also emerged as a versatile regulator of TRPs [22,23]. The atomic-level description of the molecular mechanism by which PIP2 regulates channel activity, as well as how PIP2 induces conformation changes in the protein, was determined from crystal structures of a K^+ channel/PIP2 complex [42,43]. Apart from the similar general architecture of TRPs, PIPs are likely to be the only common factor regulating these proteins. Modulation by PIP2 has been shown in detail for vanilloid [44–46], melastatin [47–49] and polycystin [50] TRPs, for a large number of which PIP2 acts as both an activator and an inhibitor [22,23]. Although great advances have been made regarding the modulation of TRP channels by PIP2, a detailed molecular understanding of the regulation of TRP channel gating is still needed.

Here, we have identified the N-terminal A451-N566 region of TRPM1 as a potential PIP2 binding domain. Generally, domains interacting with phosphatidylinositol phosphates are usually identified as PH regions which are abundant on clusters of lysine and/or arginine. Our preliminary analysis of primary sequence of A451-N566 part of TRPM1 N-terminus pointed out on occurrence of this important domain. Results from biophysical and molecular modeling approaches suggest that basic amino acid K464 participates on formation of putative PH domain, which can formnon-covalent bonds with the phosphate groups of the PIP2 ligand in TRPM1 channel. Whether PIP2 acts as activator and/or inhibitor of TRPM1 remains unclear and will require further investigation. This is the first report to address the direct binding of PIP2 to TRPM1.

2. Materials and methods

2.1. Protein sample preparation and purification

The coding region of rat TRPM1 (TRPM1-NT; UniProtKB/Swiss-Prot: Q2WEA5; residues A451-N566) was ligated into the pET32b expression vector (Novagen, Madison, WI, USA) using the BamHI and XhoI sites (New England BioLabs, Ipswich, MA, USA). The amino acids K457, K461, K463, K464, K471 and K479 were mutated to Ala using Pfu Ultra High-fidelity DNA polymerase according to the manufacturer's protocol (Stratagene, Santa Clara, CA, USA). All clones were verified by DNA sequencing.

The TRPM1-NT protein was expressed as a thioredoxin-fusion protein by induction with Isopropyl-1-thio-β-D-galactopyranoside (0.5 mM) for 20 h at 25 °C and then purified from Rosetta *Escherichia coli* using a chelating Sepharose fast flow column (GE Healthcare, Little Chalfont, UK). The fusion protein was eluted with the following buffer: 10 mM PBS, 500 mM NaCl, 2 mM β-Mercaptoethanol, and 400 mM imidazole (pH 8.0). Gel permeation chromatography in a Superdex 75 column (GE Healthcare, Little Chalfont, UK) was used as a second purification step, and the protein was eluted in buffer containing 25 mM HEPES, 250 mM NaCl, 2 mM β-MercaptoEtOH, 0.1% Tween and 10% glycerol (pH 8.0). The protein concentration of purified TRPM1-NT was determined from UV absorption at 280 nm using an extinction coefficient of 20,970 $M^{-1}\cdot cm^{-1}$. The purity was verified using 15% SDS-polyacrylamide gel electrophoresis (PAGE). All mutants were prepared in the same manner. All expressed proteins were soluble, and expression yields were sufficient to perform spectroscopic and biochemical studies.

2.2. Mass spectrometry

The integrity of the TRPM1-NT fusion protein was verified by MALDI-TOF. Mass spectra were acquired using an Ultra-FLEX III mass spectrometer (Bruker-Daltonics, Bremen, Germany). The TRPM1-NT protein band from SDS-PAGE was digested with trypsin endoprotease (Promega, Madison, WI, USA) in the gel after destaining and cysteine modification with iodoacetamide [51]. The resulting peptide mixture was extracted and loaded onto the MALDI-TOF/TOF target with a matrix of α-cyano-4-hydroxycinnamic acid. Peptide identities were verified using manual interpretation of MS/MS tandem mass spectra of the selected *m/z* signals.

2.3. Fluorescent measurements

A fluorescent PIP2 analogue labeled with BODIPY (TopFluor PI(4,5)P2, Avanti Polar Lipids Inc., Alabaster, AL, USA; here after referred to as BODIPY-PIP2), was used to monitor PIP2 interactions with the TRPM1-NT protein. The concentration of BODIPY-PIP2 was 5 μM, and the spectra were measured in buffer containing 20 mM Tris, pH 7.5, 250 mM NaCl, and 2 mM CaCl2 in the absence or presence of 5 μM TRPM1-NT. Corrected excitation and emission spectra for RH421 were measured on a Fluorolog-3 spectrofluorometer (Horiba? Kyoto, Japan) with both excitation and emission bandpass set at 3 nm, a 1-nm step size, an integration time of 0.5 s per point, and with the temperature set at 20 °C (Peltier controlled). For free BODIPY-PIP2, the excitation spectrum was collected at an emission wavelength of 510 nm, and the

emission spectrum with an excitation wavelength of 495 nm. For protein-bound BODIPY-PIP2, the excitation spectrum was collected at an emission wavelength of 465 nm, and the emission spectrum with an excitation wavelength of 355 nm. The signal from pure buffer or protein solution, respectively, was subtracted as the background. FRET between tryptophan residues in TRPM1-NT and BODIPY-PIP2 was evaluated from the emission spectrum collected with an excitation wavelength of 295 nm. All other experimental conditions were the same.

2.4. LUV preparation

The lipids 1, 2-dimyristoyl-sn-glycero-3-phosphocholine (PC) and L-α-phosphatidylinositol-4, 5-bisphosphate (PIP2) were purchased from Avanti Polar Lipids Inc. (Alabaster, AL, USA). PC and PIP2 were dissolved in chloroform and a mixture of chloroform/methanol/H_2O (20:9:1), respectively, and mixed at a molar ratio of 1:1 for the preparation of PIP2-enriched vesicles. The lipids were dried under a stream of nitrogen and hydrated with Hank's Balanced Salt Solution (HBSS) buffer followed by extrusion using an Avanti Mini-Extruder (Avanti Polar Lipids Inc., Alabaster, AL, USA) through a Nuclepore Track-Etched Membrane (Avanti Polar Lipids Inc., Alabaster, AL, USA) with 100-nm diameter pores. The 100-nm LUVs were centrifuged at 50,000 g for 30 min at 4 °C and diluted to the desired concentrations in HBSS. For surface plasmon resonance (SPR) experiments, the lipids were hydrated in the presence of 8 mM of the oligonucleotide 5′-TATTTCTGATGTCCAC CCCC-3′ modified at the 3′ end with cholesterol (Generi-Biotech, Hradec Kralove, Czech Republic), and the mixture was extruded as above. The lipid/DNA ratio was 1200:1. The vesicles were then incubated with 8 mM anti-sense oligonucleotide 5′-TGGACATCAGAAATACCCCC- 3′, modified at the 3′ end with biotin (Generi-Biotech, Hradec Kralove, Czech Republic), centrifuged (50,000 g) for 30 min at 4 °C and diluted to a final concentration of 100 μg/ml in HBSS.

2.5. Surface plasmon resonance

SPR analyses were performed at 25 °C using a ProteOn XPR36 Protein Interaction Array System (Bio-Rad, Hercules, CA, USA) equipped with a neutravidin-coated NLC chip (Bio-Rad, Hercules, CA, USA). LUVs were immobilized on a streptavidin-coated NLC chip at a flow rate of 30 μl/min for 120 s and washed in SPR running buffer containing HBSS supplemented with 0.005% Tween-20 for an additional 30 min. The TRPM1-NT proteins were serially diluted in the running buffer and injected in parallel over the lipid surface at a constant flow rate of 30 μl/min. The lipid surfaces were typically regenerated by injecting 5 mM NaOH and 150 mM NaCl for 2 min. The sensograms were corrected for sensor background by interspot referencing (the sites within the 6 × 6 array that were not exposed to ligand immobilization but were exposed to analyte flow) and double referenced by subtraction of the analyte using a "blank" injection. Assuming a Langmuir-type binding between the protein (P) and protein binding sites (S) on vesicles (i.e., $P + S \leftrightarrow PS$), R_{eq} values were then plotted versus protein concentration (P_0), and the K_D value was determined by nonlinear least-squares analysis of the binding isotherm using the equation $R_{eq} = R_{max} / (1 + K_D / P_0)$.

2.6. Electronic circular dichroism spectroscopy

Electronic circular dichroism (ECD) spectra were measured at room temperature in a quartz cell with a 0.1-cm path length using a Jasco J-815 CD spectrometer (Jasco Corporation, Tokyo, Japan). The experimental setup was as follows: step resolution, 0.5 nm; speed, 10 nm/min; response time, 16 s; and bandwidth, 1 nm. The TRPM1-NT fusion protein concentration was in the 0.3–1.0 mg/ml range, the thioredoxin concentration was 0.14 mg/ml, and both were kept in 25 mM HEPES (pH 8.0) and 250 mM NaCl. The final LUV concentration was 5 μM. The spectra were obtained in the 200–300 nm range. Three different samples were measured: TRPM1-NT fusion protein, TRPM1-NT in complexes with LUVs formed by PC or PC/PIP2, TRPM1-NT mutants (K471A/K479A, K463A/K461A/K457A/K464A and K463A/K461A/K457A/K464A/K471A) in the same arrangement and thioredoxin alone. After baseline correction, the final spectra (averages of three scans) were expressed as molar residue ellipticities θ ($deg \cdot cm^2 \cdot dmol^{-1} \cdot$number of $residues^{-1}$). Secondary structure content was determined using the software Dichroweb [52].

2.7. Molecular modeling and ligand docking

To determine the potential PIP2 binding site in the wild-type TRPM1-NT peptide we performed ligand docking in the program Molecular Operating Environment (MOE) using the Induced Fit Protocol [53,54]. The optimal binding mode was selected based on most favorite docking score interaction energy and geometry criteria being satisfied simultaneously. For the purpose of the docking procedure, the molecular model of TRPM1-NT (UniProtKB/Swiss-Prot: Q2WEA5; positions A451-N566) with thioredoxin was generated by the Robetta prediction server [55]. The final TRPM1-NT model was carefully selected based on the requirements for Lys residue placement (oriented towards the solvent) and the geometric parameters of the potential PIP2 binding site. The quality of the structure was assessed using STING Millennium [56] and ProSA-web [57,58]. We also used 3D refine [59] to optimize the hydrogen bonding network and for atomic-level energy minimization. Schematic and solvent-accessible-surface representations of the TRPM1-NT/PIP2 complex were generated using Chimera freeware [60].

3. Results and discussion

3.1. The TRPM1-NT domain interacts with PIP2

In this report, we characterized the capacity of an N-terminal segment of the TRPM1 channel (TRPM1-NT; purified peptide sequence verified by Mass Spectrometry Fig. S1), encompassing residues A451 to N566, to interact with PIP2. This segment is characterized by a cluster of positively charged residues that are predicted to constitute a PH domain. Similar protein regions are present in other TRPM members that interact with PIPs anchored within biological membranes [16–22]. Neutralizing the positive charges in these regions usually results in a reduction in the binding affinity of PH domains for PIP2, indicating a direct interaction between the cytoplasmic regions of TRPM channels with PIPs [61–63]. Specifically, the N-terminal segment of TRPM3 contains at least two PIP2 binding sites, which are also shared by calcium-binding proteins such as calmodulin (CaM) and S100A1; thus, these ligands compete with each other for binding to the TRPM3 cytoplasmic tail [25–27]. A similar PIP2 (and its structural analogue PIP3) binding site was recently described in the TRPM4 N-terminus [28]. Furthermore, the PIP2 binding site in the TRPM4 C-terminal TRP-box domain was described using electrophysiology experiments [29]. PIP2 also promotes the gating of the TRPM5 and TRPM7 channels [30,32]. Moreover, disrupting the putative PIP2-binding sites in TRPM6 completely abrogated channel function [31]. In contrast, PIP2 depletion in the vicinity of TRPM8 plays an important role in its adaptation to cold and the desensitization of menthol-induced currents [33]. Dissociation constants for the interaction of PIP2 with TRPM channels are almost always in the micromolar ranged [25,28]. However, the putative PIP2 binding site in the N-terminal segment of TRPM1 does not share any homology with those previously described in TRPM channels, which paves the way to our understanding of the regulation of TRPM1 activity.

We observed the interaction of TRPM1 with BODIPY-labeled PIP2 in fluorescence experiments. This interaction was manifested by large shifts in both the excitation and emission spectra of BODIPY-PIP2, as well as by Förster resonance energy transfer (FRET) between tryptophan residues and BODIPY-PIP2. The excitation and emission spectra

of free BODIPY-PIP2 in buffer showed maximum fluorescence (λ_{max}) at 495 nm and 505 nm, respectively (Fig. S2). In the presence of TRPM1-NT, both the excitation and emission spectra were substantially blue-shifted, peaking at 355 nm and 465 nm, indicating changes in the environment of the BODIPY moiety. The primary amino acid sequence of TRPM1-NT contains three tryptophan residues, which can be selectively excited at 295 nm, yielding an emission spectrum with a λ_{max} of 335 nm. The emission spectrum of tryptophan overlaps strongly with the excitation spectrum of protein-bound BODIPY-PIP2 (Fig. S3), suggesting that tryptophan and bound BODIPY-PIP2 can form a FRET pair. Indeed, FRET was evident in the emission spectrum of TRPM1-NT/BODIPY-PIP2 excited at 295 nm. Upon the formation of the complex between TRPM1-NT2 and BODIPY-PIP2, we observed both a decrease in donor (tryptophan) fluorescence and an increase in acceptor (BODIPY-PIP2) fluorescence, which are typical characteristics of FRET (Fig. 1). Thus, fluorescence measurements provide strong evidence for the interaction of TRPM1-NT with soluble PIP2.

The interaction of TRPM1-NT with membrane-bound PIP2 was quantified using a surface plasmon resonance (SPR) binding assay. Control (PC only) and PIP2-enriched LUVs (100 nm in diameter) were immobilized on neutravidin-coated (NLC) sensor chips using a biotin/cholesterol-functionalized DNA linker at a coupling level of 500–1000 RU. The SPR response is linearly proportional to the mass accumulated at the sensor surface, and the relative intensity of the SPR signal corresponds to the density of LUVs. Hence, the intensity of SPR binding curves is directly dictated by the density of LUVs, but it does not affect the binding affinity of the analyte to the ligand at low LUVs coupling levels (500–1000 RU) [28]. The kinetics of the interaction of TRPM1-NT with PC and PIP2-enriched lipid vesicles was further analyzed by parallel injection of serially diluted (10–5–2.5–1.25 μM) TRPM1-NT protein over the sensor chip surface at a constant flow rate of 30 μl/min. As shown in Fig. S4, the concentration-dependent binding curves revealed that TRPM1-NT bound to the lipid vesicles with typical association and dissociation phases of the sensograms. The binding of the TRPM1-NT-thioredoxin fusion protein was strictly mediated through the TRPM1-NT segment, as thioredoxin alone was not able to interact with the lipid surfaces (Fig. S4E–F). The experimental binding curves for the TRPM1-NT interaction were globally fitted to several kinetic binding models, such as a simple 1:1 L, heterologous ligand, bivalent analyte or conformational change (two-state) models, but none of these models provided satisfactory results in terms of χ^2 and residual statistics. Thus, the binding affinity of TRPM1-NT to PIP2-enriched LUVs was calculated from steady-state binding data. Near equilibrium values (Req) taken from the end of the association phase of individual binding curves were plotted as a function of the TRPM1 concentration and, the equilibrium dissociation constant (K_D) was determined via nonlinear least squares analysis of the binding isotherm. As shown in Fig. 2, the interaction of TRPM1-NT with LUVs exhibited concentration-dependent and saturable binding, with K_D values of 18.3 ± 11.4 μM and 7.4 ± 3.9 μM for PC and PIP2-enriched lipid vesicles, respectively. Thus, the binding affinity of TRPM1-NT is almost three-times higher for PIP2 than for PC, indicating a higher specificity of TRPM1-NT for PIP2 on the membrane surface. Moreover, the K_D value of TRPM1-NT for PIP2 is in the micromolar range, which corresponds well to previous observations using homologous PH domains from related TRP channels [25,28,42].

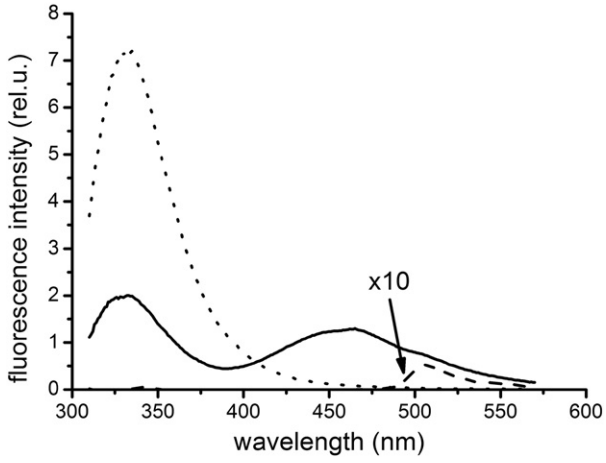

Fig. 1. FRET analysis of the TRPM1-NT/PIP2 interaction. The emission spectra of free TRPM1-NT (dotted line), free BODIPY-PIP2 (dashed line, magnified by a factor of 10) and the complex of TRPM1-NT and BODIPY-PIP2 (solid line).

3.2. Basic residue K464 of TRPM1-NT involved in the PIP2 interaction

PIP2 typically binds with protein domains containing a cluster of basic amino acid residues. To identify the TRPM1-NT residues that could be involved in the interaction with PIP2, lysine residues at positions 457, 461, 463, 464, 471 and 479 were substituted with alanine, and the capacity of the single (K463A and K471A), double (K463A/K461A and K471A/K479A), triple (K463A/K461A/K457A), quadruple (K463A/K461A/K457A/K464A) and quintuple (K463A/K461A/K457A/K464A/K471A) mutants to interact with the lipid surfaces was analyzed by SPR (Fig. 3, Suppl. Figs. S4C, D, S5). The binding affinities of TRPM1-NT proteins for PC and PIP2 are listed in Table 1. An overall comparison of the K_D values revealed that the binding affinity of the single (K463A), double (K463A/K461A) and triple (K463A/K461A/K457A) TRPM1-NT mutants remained nearly unaffected, indicating that these three proximal lysine residues (K457, K461, K463) do not play a major role in the interaction of TRPM1-NT with PIP2 (Fig. S5A–C).

The first significant changes in PIP2 binding affinity appears in the K463A/K461A/K457A/K464A TRPM1-NT mutant (Fig. S5D). The K_D of the interaction (16.2 μM) shows 2-fold decrease in binding affinity to PIP2-enriched LUVs compared with the wild type. Whereas this mutant shows a light decline in binding affinity for PC LUVs (K_D = 30.8 μM), which indicates to specificity for PIP2. The results suggest that K464 is involved in the interaction with PIP2.

Mutating five of the lysine residues (K463A/K461A/K457A/K464A/K471A) resulted in the complete loss of binding affinity to both types of LUVs (Fig. S5E). This could be explained by significant changes in

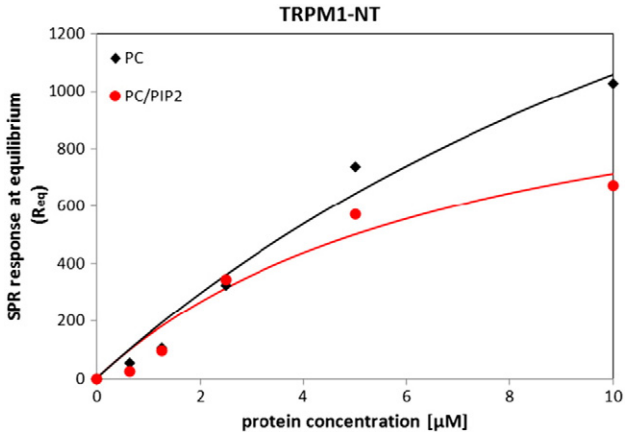

Fig. 2. TRPM1-NT specifically interacts with membrane-embedded PIP2. SPR equilibrium binding analysis of the TRPM1-NT interaction with PC (black diamonds) and PIP2-enriched lipid vesicles (red dots). The 100-nm LUVs were coupled to a neutravidin-coated (NLC) sensor chip using a biotin/cholesterol-functionalized DNA linker, and serially diluted TRPM1-NT was injected at a flow rate of 30 μl/min to allow the association phase of individual binding curves to reach near-equilibrium values (R_{eq}). The R_{eq} values were plotted as a function of the TRPM1-NT concentration, and K_D values were determined by nonlinear least-squares analysis of the binding isotherm (solid lines) using the equation $R_{eq} = R_{max} / 1 + K_D / P_0$), where R_{eq} stands for the SPR response value at equilibrium, R_{max} is the maximum response and P_0 is the protein concentration.

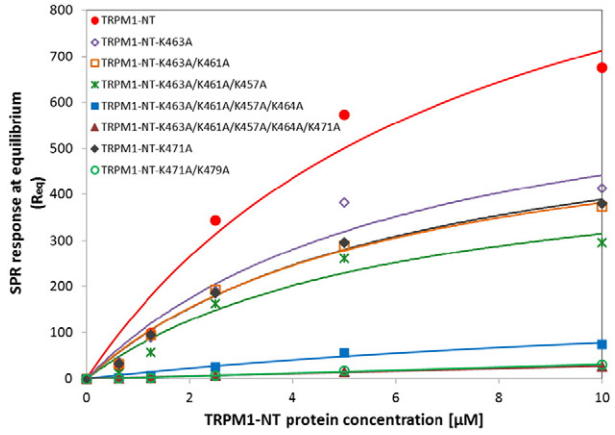

Fig. 3. Lysine residues at positions 464, 471 and 479 are involved in TRPM1-NT binding to PIP2. SPR equilibrium binding analysis of the interaction of wild-type TRPM1-NT, the single K463A and K471A, the double K463A/K461A and K471A/K479A, the triple K463A/K461A/K457A, the quadruple K463A/K461A/K457A/K464A and the quintuple K463A/K461A/K457A/K464A/K471A mutant constructs with PIP2-enriched LUVs. The proteins were injected at the indicated concentrations at flow rate of 30 μl/min over the lipid surface to reach near-equilibrium values (R_{eq}) in the association phase of the sensogram. The solid lines represent binding isotherms determined by nonlinear least-squares analysis as described above.

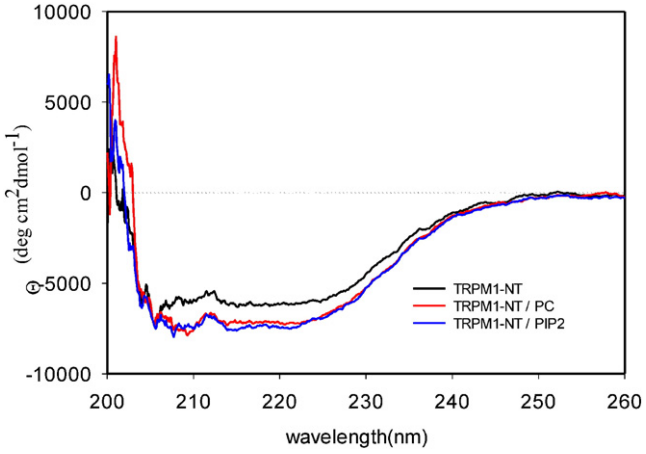

Fig. 4. Secondary structure of wild-type TRPM1-NT during complex formation with PIP2-enriched LUVs. ECD spectra of TRPM1-NT alone, in complex with LUVs formed by PC and in complex with LUVs formed by PC:PIP2 (1:1) in buffer containing 25 mM HEPES (pH 8.0) and 250 mM NaCl. CD spectra were expressed as molar residue ellipticities θ ($deg \cdot cm^2 \cdot dmol^{-1}$).

the secondary structure content of the quintuple mutant in LUVs environment. Using ECD was found out that the secondary structure of quintuple mutant alone showed no major changes against to the other prepared mutants, nevertheless the alpha helical content of quintuple mutant suddenly increase in LUVs (PC and PC/PIP2) environment (data from ECD are showed and discussed below). Based on this result we cannot say that K471 is involved in the interaction. In contrast, whereas almost no change in K_D was observed upon replacement of the single K471 residue (Fig. S5F), the double substitution of two distal lysine residues (K471 and K479) produced a notable decrease in the binding affinity of the K471A/K479A mutant for PIP2-enriched LUVs (Table 1). The interaction of this double mutant with PC LUVs as a positive control shows a decrease in binding affinity (Fig. S5G). As in the case of the quintuple mutant, there are no clear indicia whether K479 and K471 are involved in the PIP2 binding.

Collectively, these data suggested that the basic side chain of lysine residue at position 464 of TRPM1-NT mediates electrostatic interactions with the negatively charged phosphate group(s) of PIP2 at the membrane surface. Using SPR method, which was performed with multiple-lipid LUVs (PC + PIP2), it was not possible to determine the specificity of PIP2 to the K471 and K479. However, based on homology of putative PH domain of the TRPM1 and PH domain present in the Kir channel [64–66] can be assumed, that the K471 and K479 could at least partially interact with PIP2. Molecular modeling confirmed that the K464, K471 and K479 are closer to PIP2 ligand in predicted binding pocket than the other mutated amino acids (results see below in capitol: Modeling the TRPM1-NT/PIP2 interaction).

Table 1
Equilibrium dissociation constants (K_D) for the interactions of TRPM1-NT proteins with PC and PIP2-enriched LUVs.

TRPM1-NT	K_D (μM)	
	PC	PIP2
WT	18.3 ± 11.4	7.4 ± 3.9
K463A	15.2 ± 5.6	6.2 ± 3.1
K463A/K461A	26.5 ± 2.2	5.9 ± 1.3
K463A/K461A/K457A	22.5 ± 4.9	5.9 ± 2.9
K463A/K461A/K457A/K464A	30.8 ± 13.6	16.2 ± 11.3
K463A/K461A/K457A/K464A/K471A	>150	>150
K471A	11.7 ± 1.5	6.2 ± 1.3
K471A/K479A	>150	>150

The above results represent the means ± S.D. from two independent experiments.

3.3. The TRPM1-NT/PIP2 complex formation is associated with structural changes in TRPM1-NT

ECD spectroscopy was used to determine whether the TRPM1-NT protein undergoes changes in its secondary structure content during the formation of the TRPM1-NT/PIP2 complex. The ECD spectra of TRPM1-NT revealed a baseline conformation consisting of approximately 11.9% α-helix, 58.6% β-strands and 29.5% random coil (Fig. 4, Table 2). The formation of the TRPM1-NT/LUVs (enriched by PIP2) complex is accompanied by secondary structure changes, wherein the protein becomes more structured. The presence of helices increased the overall alpha-helical content of TRPM1-NT by 14.7% at the expense of a decrease in beta-strands by approximately 9.4%. The TRPM1-NT/LUVs (PC only) complex displayed only minor changes in secondary structure. Thus, according to the ECD study, the formation of the TRPM1-NT/PIP2 complex is accompanied by significant changes in secondary structure content.

Overall secondary structure content was also studied for the TRPM1-NT mutants in which residues that were found to participate or could be involved in the interaction with PIP2 (Figs. S6–S8, Table 2): K471A/K479A, K463A/K461A/K457A/K464A and K463A/K461A/K457A/K464A/K471A. All three alanine mutants showed greater alpha-helical content. For most of the interactions, the increase in secondary structure content came in the form of helices. Nevertheless, the interaction of the K463A/K461A/K457A/K464A mutant with LUVs formed by PC:PIP2 (1:1) showed an approximately 10% decrease in helical content, whereas the interaction of the quadruple mutant with PC alone showed a 12.5% increase in helicity. This supports our suggestion that the binding of the quadruple mutant to PIP2 is specific.

3.4. Modeling the TRPM1-NT/PIP2 interaction

Using molecular modeling, we were able to characterize the potential interaction interface of the N-terminal TRPM1 domain with PIP2. A de novo structural model of the rat TRPM1-NT peptide (A451-N566) was constructed based on the primary sequence, as described in the Methods. The final model was chosen from among the several Robetta server models generated. To determine the interaction mode of the PIP2-binding domain of TRPM1-NT, the PIP2 ligand was docked into the assigned binding pocket (Fig. 5). The orientation of PIP2 in the binding pocket was addressed based on information from structural

Table 2
Secondary structure content (%) of TRPM1-NT and its mutants after interaction with PC and PIP2-enriched LUVs.

TRPM1-NT	LUVs	α-Helix	β-Strand	β-Turn	Random coil
WT	–	11.9	41.4	17.2	29.5
WT	PC	22.6	34.0	16.4	27.0
WT	PIP2	26.6	28.7	20.5	24.2
K471A/K479A	–	25.6	34.1	22.4	17.9
K471A/K479A	PC	38.1	32.0	23.6	10.7
K471A/K479A	PIP2	14.8	27.5	20.5	37.2
K463A/K461A/K457A/K464A	–	27.8	23.3	22.5	26.4
K463A/K461A/K457A/K464A	PC	28.8	22.7	23.1	25.3
K463A/K461A/K457A/K464A	PIP2	34.3	20.4	19.4	25.8
K463A/K461A/K457A/K464A/K471A	–	20.3	23.8	21.1	34.9
K463A/K461A/K457A/K464A/K471A	PC	37.4	21.5	18.6	22.5
K463A/K461A/K457A/K464A/K471A	PIP2	34.3	20.4	19.4	25.8

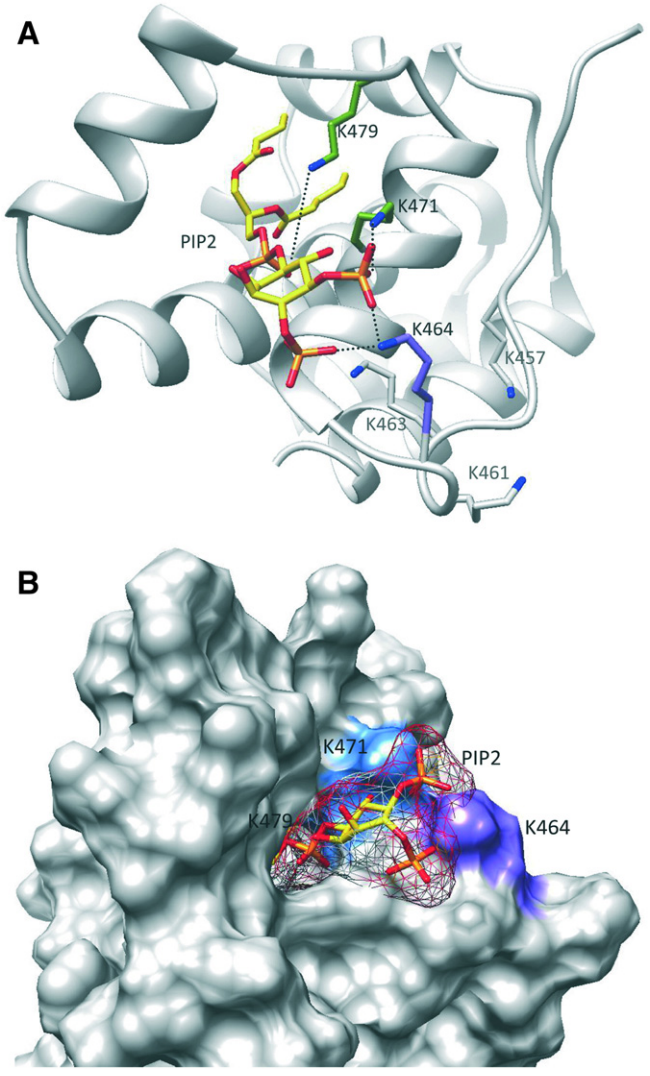

Fig. 5. Structural view of the putative PIP2-binding pocket of the TRPM1 channel. The 3D model of TRPM1-NT (A451-N566) was generated by the Robetta server. Ligand docking was performed in the MOE program using the Induced Fit protocol. (A) Schematic view of the interaction of TRPM1-NT with PIP2. The K464, K471 and K479 residues use a similar binding mechanism to PIP2. Although mutations at K457, K461, and K463 in the TRPM1 channel do not alter binding affinity, all three critical residues K464, K471 and K479 lie in close proximity to and directly interact with the phosphate groups of PIP_2. Important lysine residue bonded (dashed lines) to PIP2 is colored violet (K464), another suggested lysine are colored green (K471, K479). The following color convention was used: gray — protein backbone, yellow — carbon atoms of PIP2, oxygen (O_2) — red, nitrogen (N) — blue, phosphorus (P) — orange. (B) Solvent-accessible-surface representation of the TRPM1-NT/PIP2 complex. Surfaces of lysine residues bonded to PIP2 are colored violet (K464) and the suggested ones by blue (K471, K479).

studies of PIP2 with the intracellular regions of the K_{ir} channel [23,32,67]. Electrostatic potential surface maps of the K_{ir} model revealed patches of positively charged amino acids on the protein surface. These regions are known to be located proximal to the membrane, making them accessible to the negatively charged phosphate groups of PIP2. The 3D model confirmed that the interaction is mediated by the negatively charged phosphate groups of PIP2, which are coordinated by a patch of positively charged residues on the TRPM1 surface. The model shows amino acid residues K457, K461, K463, K464, K471 and K479 forming a hypothetical PIP2 binding site. According to the arrangement of amino acids in the 3D model, residues K464, K471 and K479 are predicted to be crucial for the interaction with the PIP2 phosphate groups. K457, K461, K463 do not participate directly in PIP2 binding, which is in agreement with the SPR studies. The criteria for a reasonable model were set based primarily on the accessibility of lysine residues.

Although we determined a possible PIP2 binding interface to the intracellular N-terminus of the TRPM1 fragment using both biophysical and molecular modeling approaches, the question of whether this interaction is mediated purely by the N-terminus of the TRPM1 fragment remains unanswered. It has been reported that potassium channels possess four PIP2 binding sites in the $K_{ir}6.2$ tetramer, one per subunit, with both the N- and C-terminal domains of the K_{ir} channels contributing to the PIP2 binding sites [42,43]. Specific intracellular portions of the channel are attracted to the plasma membrane due to direct interactions with the phospholipid. PIP2 exerts a tangential force on the N- and C-termini to open the channel. The PIP2-binding site for $K_{ir}6.2$, much like the ATP-binding site [68,69], lies at the interface between the N- and C-terminal regions, in close proximity to and between two neighboring subunits, as suggested by previous structural, functional and 3D molecular studies [69–72]. The position of the ligand-binding site at the subunit interface appears to be a common motif for ion channels and likely serves to precipitate a larger, coordinated conformational change in the whole channel upon ligand binding [69,73]. According to the tetramer assembly and with respect to the close proximity of the N- and C-terminal regions of TRP channels [5,6], we postulate that this pattern may also hold true for these receptors. However, structural findings concerning TRP channel intracellular regions, which are essential for understanding the mechanism of channel function, are still lacking.

Here, we have shown that the A451–N566 region of the TRPM1 N-terminus is involved in the interaction with the PIP2 ligand. The amino acid residue K464 takes part in the putative PIP2 binding pocket (PH domain) in the N-terminal part of the TRPM1. According to previous studies, the interaction domain is also accessible to other phosphatidylinositides [74]. The present study is the first report to show that PIP2 interacts with the TRPM1 channel. The structural basis for the effect of lipid binding on TRPM1 channel activity has yet to be determined, and unraveling the physiological significance of this binding will require further investigation.

Conflict of interest

The authors declare that the research was conducted in the absence of any commercial or financial relationships that could be construed as a potential conflict of interest.

Acknowledgments

We would like to thank Dr. Johannes Oberwinkler from Institut für Physiologie und Pathophysiologie, Philipps-Universität Marburg for providing us with the cDNA for rat TRPM1.

This study was supported by the Grant Agency of Charles University (238214, 842313), by the Grant Agency of the Czech Republic (grant no. 207/11/0717 and 15-11851S), by the Grant Agency of the Czech Republic Project of Excellence in the Field of Neuroscience (P304/12/G069), by the National Program of Sustainability I. (LO1204) and by the Institute of Physiology, Academy of Sciences of the Czech Republic (RVO: 67985823).

Appendix A. Supplementary data

Supplementary data to this article can be found online at http://dx.doi.org/10.1016/j.bpc.2015.10.005.

References

[1] A. Gordon-Shaag, W.N. Zagotta, S.E. Gordon, Mechanism of Ca^{2+}-dependent desensitization in TRP channels, Channels 2 (2008) 125–129.
[2] C. Montell, L. Birnbaumer, V. Flockerzi, The TRP channels, a remarkably functional family, Cell 108 (2002) 595–598.
[3] S.Y. Lin, D.P. Corey, TRP channels in mechanosensation, Curr. Opin. Neurol. 15 (2005) 350–357.
[4] M.J. Caterina, Transient receptor potential ion channels as participants in thermosensation and thermoregulation, Am. J. Physiol. Regul. Integr. Comp. Physiol. 292 (2007) R64–R76.
[5] M. Liao, E. Cao, D. Julius, Y. Cheng, Structure of the TRPV1 ion channel determined by electron cryo-microscopy, Nature 504 (2013) 107–112.
[6] C.E. Paulsen, J.P. Armache, Y. Gao, Y. Cheng, D. Julius, Structure of the TRPA1 ion channel suggests regulatory mechanisms, Nature 520 (2015) 511–517.
[7] K. Venkatachalam, C. Montell, TRP channels, Annu. Rev. Biochem. 9 (2007) 387–417.
[8] G. Owsianik, K. Talavera, T. Voets, B. Nilius, Permeation and selectivity of TRP channels, Annu. Rev. Physiol. 9 (2006) 685–717.
[9] M. Li, Y. Yu, J. Yang, Structural biology of TRP channels, Adv. Exp. Med. Biol. 9 (2011) 1–23.
[10] P.V. Lishko, E. Procko, X. Jin, C.B. Phelps, R. Gaudet, The ankyrin repeats of TRPV1 bind multiple ligands and modulate channel sensitivity, Neuron 54 (2007) 905–918.
[11] I. Audo, S. Kohl, B.P. Leroy, F.L. Munier, X. Guillonneau, et al., TRPM1 is mutated in patients with autosomal-recessive complete congenital stationary night blindness, Am. J. Hum. Genet. 85 (2009) 720–729.
[12] M. Nakamura, R. Sanuki, T.R. Yasuma, A. Onishi, K.M. Nishiguchi, C. Koike, M. Kadowaki, M. Kondo, Y. Miyake, T. Furukawa, TRPM1 mutations are associated with the complete form of congenital stationary night blindness, Mol. Vis. 16 (2010) 425–437.
[13] S. Lambert, A. Drews, O. Rizun, T. Wagner, A. Lis, S. Mannebach, S. Plant, M. Portz, M. Meissner, S. Phillip, J. Oberwinkler, Transient receptor potential melastatin 1 (TRPM1) is an ion-conducting plasma membrane channel inhibited by zinc ions, J. Biol. Chem. 286 (2011) 12221–12233.
[14] E. Oancea, J. Vriens, S. Brauchi, J. Jun, I. Splawski, D.E. Clapham, TRPM1 forms ion channels associated with melanin content in melanocytes, Sci. Signal. 2 (2009) ra21.
[15] D.E. Clapham, TRP channels as cellular sensors, Nature 426 (2003) 517–524.
[16] M. Faouzi, R. Penner, TRPM2, Handb. Exp. Pharmacol. 222 (2014) 403–426.
[17] J. Oberwinkler, S.E. Phillip, TRPM3, Handb. Exp. Pharmacol. 222 (2014) 427–459.
[18] I. Mathar, G. Jacobs, M. Kecskes, A. Menigoz, K. Philippaert, R. Vennekens, TRPM4, Handb. Exp. Pharmacol. 222 (2014) 460–488.
[19] E.R. Liman, TRPM5, Handb. Exp. Pharmacol. 222 (2014) 489–502.
[20] V. Chubanov, T. Gudermann, TRPM6, Handb. Exp. Pharmacol. 222 (2014) 503–520.
[21] A. Fleig, V. Chubanov, TRPM7, Handb. Exp. Pharmacol. 222 (2014) 521–546.
[22] L. Almaraz, J.A. Manenschijn, E. de la Peña, F. Viana, TRPM8, Handb. Exp. Pharmacol. 222 (2014) 522–579.
[23] T. Rohacs, B. Nilius, Regulation of transient receptor potential (TRP) channels by phosphoinositides, Pflugers Arch. 455 (2007) 157–168.
[24] T. Rohacs, Phosphoinositide regulation of TRP channels, Handb. Exp. Pharmacol. 223 (2014) 1143–1176.
[25] B. Holendova, L. Grycova, M. Jirku, J. Teisinger, PtdIns(4,5)P2 interacts with CaM binding domains on TRPM3 N-terminus, Channels 6 (2012) 479–482.
[26] B. Holakovska, L. Grycova, M. Jirku, M. Sulc, L. Bumba, J. Teisinger, Calmodulin and S100A1 protein interact with N terminus of TRPM3 channel, J. Biol. Chem. 287 (2012) 16645–16655.
[27] L. Grycova, B. Holendova, Z. Lansky, L. Bumba, M. Jirku, K. Bousova, J. Teisinger, Ca^{2+} binding protein S100A1 competes with calmodulin and PIP2 for binding site on the C-terminus of the TPRV1 receptor, ACS Chem. Neurosci. 6 (2015) 386–392.
[28] K. Bousova, M. Jirku, L. Bumba, L. Bednarova, M. Sulc, M. Franek, L. Vyklicky, J. Vondrasek, J. Teisinger, PIP2 and PIP3 interact with N-terminus region of TRPM4 channel, Biophys. Chem. 205 (2015) 24–32.
[29] B. Nilius, F. Mahieu, J. Prenen, A. Janssens, G. Owsianik, T. Vennekens, T. Voets, The Ca^{2+}-activated cation channel TRPM4 is regulated by phosphatidylinositol 4,5-biphosphate, EMBO J. 25 (2006) 467–478.
[30] D. Liu, E.R. Liman, Intracellular Ca^{2+} and the phospholipid PIP2 regulate the taste transduction ion channel TRPM5, PNAS 100 (2003) 15160–15165.
[31] J. Xie, B. Sun, J. Du, W. Yang, H.C. Chen, L. Yue, Phosphatidylinositol 4,5-bisphosphate (PIP(2)) controls magnesium gatekeeper TRPM6 activity, Sci. Rep. 1 (2011) 146.
[32] L.W. Runnels, L. Yue, D.E. Clapham, The TRPM7 channel is inactivated by PIP(2) hydrolysis, Nat. Cell Biol. 4 (2002) 329–336.
[33] Y. Yudin, V. Lukacs, C. Cao, T. Rohacs, Decrease in phosphatidylinositol 4,5-bisphosphate levels mediates desensitization of the cold sensor TRPM8 channels, J. Physiol. 15 (2011) 6007–6027.
[34] M. Rampino, S. Nawy, Relief of Mg^{2+}-dependent inhibition of TRPM1 by PKCα at the rod bipolar cell synapse, J. Neurosci. 31 (2011) 13596–13603.
[35] C. Harteneck, Function and pharmacology of TRPM cation channels, Naunyn Schmiedeberg's Arch. Pharmacol. 371 (2005) 307–314.
[36] S.J. Ashcroft, Intracellular second messengers, Adv. Exp. Med. Biol. 426 (1997) 73–80.
[37] M. Liscovitch, L.C. Cantley, Lipid second messengers, Cell 77 (1994) 329–334.
[38] A.F. Quest, S. Ghosh, W.Q. Xie, R.M. Bell, Adv. Exp. Med. Biol. 400A (1997) 297–303.
[39] B.C. Suh, B. Hille, DAG second messengers: molecular switches and growth control, Curr. Opin. Neurobiol. 15 (2005) 370–378.
[40] P. Delmas, B. Coste, N. Gamper, M.S. Shapiro, Phosphoinositide lipid second messengers: new paradigms for calcium channel modulation, Neuron 47 (2005) 179–182.
[41] S. McLaughlin, D. Murray, Plasma membrane phosphoinositide organization by protein electrostatics, Nature 438 (2005) 605–611.
[42] S.B. Hansen, X. Tao, R. MacKinnon, Structural basis of PIP2 activation of the classical inward rectifier K+ channel Kir2.2, Nature 477 (2011) 495–498.
[43] M.R. Whorton, R. MacKinnon, Crystal structure of the mammalian GIRK2 K+ channel and gating regulation by G proteins, PIP2, and sodium, Cell 147 (2011) 199–208.
[44] E.D. Prescott, D. Julius, A modular PIP2 binding site as a determinant of capsaicin receptor sensitivity, Science 23 (2003) 1284–1288.
[45] V. Lukacs, B. Thyagarajan, P. Varnai, A. Balla, T. Balla, T. Rohacs, Dual regulation of TRPV1 by phosphoinositides, J. Neurosci. 27 (2007) 7070–7080.
[46] J. Lee, S.K. Cha, T.J. Sun, C.L. Huang, PIP2 activates TRPV5 and releases its inhibition by intracellular Mg^{2+}, J. Gen. Physiol. 126 (2005) 439–451.
[47] B. Nilius, F. Mahieu, J. Prenen, A. Janssens, G. Owsianik, R. Vennekens, T. Voets, The Ca^{2+}-activated cation channel TRPM4 is regulated by phosphatidylinositol 4,5-biphosphate, EMBO J. 25 (2006) 467–478.
[48] A. Gwanyanya, K.R. Sipido, J. Vereecke, K. Mubagwa, ATP and PIP2 dependence of the magnesium-inhibited, TRPM7-like cation channel in cardiac myocytes, Am. J. Physiol. Cell Physiol. 291 (2006) 627–635.
[49] J. Benedikt, J. Teisinger, L. Vyklicky, V. Vlachova, Ethanol inhibits cold-menthol receptor TRPM8 by modulating its interaction with membrane phosphatidylinositol 4,5-bisphosphate, J. Neurochem. 100 (2007) 211–224.
[50] R. Ma, W.P. Li, D. Rundle, J. Kong, H.I. Akbarali, L. Tsiokas, PKD2 functions as an epidermal growth factor-activated plasma membrane channel, Mol. Cell. Biol. 25 (2005) 8285–8298.
[51] K. Prochazkova, R. Osicka, I. Linhartova, P. Halada, M. Sulc, P. Sebo, The *Neisseria meningitidis* outer membrane lipoprotein FrpD binds the RTX protein FrpC, J. Biol. Chem. 280 (2005) 3251–3258.
[52] L. Whitmore, B.A. Wallace, Protein secondary structure analyses from circular dichroism spectroscopy: methods and reference databases, Biopolymers 89 (2008) 392–400.
[53] Molecular Operating Environment (MOE). (2013) Chemical Computing Group Inc., 1010 Sherbooke St. West, Suite #910, Montreal, QC, Canada, H3A 2R7, 2013.
[54] A.L. Bowman, Z. Nikolovska-Coleska, H. Zhong, S. Wang, H.A. Carlson, Small molecule inhibitors of the MDM2-p53 interaction discovered by ensemble-based receptor models, J. Am. Chem. Soc. 129 (2007) 12809–12814.
[55] D.E. Kim, D. Chivian, D. Baker, Protein structure prediction and analysis using the Robetta server, Nucleic Acids Res. 32 (2004) W526–W531.
[56] G. Neshich, R.C. Togawa, A.L. Mancini, P.R. Kuser, M.E. Yamagishi, G. Pappas Jr., et al., STING Millennium: a web-based suite of programs for comprehensive and simultaneous analysis of protein structure and sequence, Nucleic Acids Res. 31 (2003) 3386–3392.
[57] M. Wiederstein, M.J. Sippl, ProSA-web: interactive web service for the recognition of errors in three-dimensional structures of proteins, Nucleic Acids Res. 35 (2007) W407–W410.
[58] M.J. Sippl, Recognition of errors in three-dimensional structures of proteins, Proteins 17 (1993) 355–362.
[59] D. Bhattacharya, J. Cheng, 3Drefine: consistent protein structure refinement by optimizing hydrogen bonding network and atomic-level energy minimization, Proteins 81 (2013) 119–131.
[60] E.F. Pettersen, T.D. Goddard, C.C. Huang, G.S. Couch, D.M. Greenblatt, E.C. Meng, T.E. Ferrin, UCSF Chimera—a visualization system for exploratory research and analysis, J. Comput. Chem. 25 (2004) 1605–1612.
[61] A.E. Lemmon, K.M. Ferguson, R. O'Brien, P.B. Sigler, J. Schlessinger, Specific and high-affinity binding of inositol phosphates to an isolated pleckstrin homology domain, Proc. Natl. Acad. Sci. U. S. A. 92 (1995) 10472–10476.

[62] B.C. Suh, B. Hille, Regulation of ion channels by phosphatidylinositol 4,5-bisphosphate, Curr. Opin. Neurobiol. 15 (2005) 370–378.
[63] L. Grycova, B. Holendova, L. Bumba, J. Bily, M. Jirku, Z. Lansky, J. Teisinger, Integrative binding sites within intracellular termini of TRPV1 receptor, PLoS One 7 (2012), e48437.
[64] C.C. Hernandez, O. Zaika, M.S. Shapiro, A carboxy-terminal inter-helix linker as the site of phosphatidylinositol 4,5-bisphosphate action on Kv7 (M-type) K+ channels, J. Gen. Physiol. 132 (2008) 361–381.
[65] V. Telezhkin, J.M. Reilly, A.M. Thomas, A. Tinker, D.A. Brown, Structural Requirements of Membrane Phospholipids for M-type Potassium Channel Activation and Binding, 287 (2012) 10001–10002.
[66] S.J. Alvis, I.M. Williamson, J.M. East, A.G. Lee, Interactions of Anionic Phospholipids and Phosphatidylethanolamine With the Potassium Channel KcsA, 85 (2003) 3828–3838.
[67] M.A. Zaydman, J. Cui, PIP2 regulation of KCNQ channels: biophysical and molecular mechanisms for lipid modulation of voltage-dependent gating, Front. Physiol. 5 (2014) 195.
[68] Z. Fan, J.C. Makielski, Anionic phospholipids activate ATP-sensitive potassium channels, J. Biol. Chem. 272 (1997) 5388–5395.
[69] J.F. Antcliff, S. Haider, P. Proks, M.S.P. Sansom, F.M. Ashcroft, Functional analysis of a structural model of the ATP-binding site of the KATP channel Kir6.2 subunit, EMBO J. 24 (2005) 229–239.
[70] S.L. Shyng, C.A. Cukras, J. Harwood, C.G. Nichols, Structural determinants of PIP(2) regulation of inward rectifier K(ATP) channels, J. Gen. Physiol. 116 (2000) 599–608.
[71] G.G. MacGregor, K. Dong, C.G. Vanoye, L. Tang, G. Giebisch, S.C. Hebert, Nucleotides and phospholipids compete for binding to the C terminus of KATP channels, Proc. Natl. Acad. Sci. U. S. A. 99 (2002) 2726–2731.
[72] D.E. Logothetis, D. Lupyan, A. Rosenthouse-Dantsker, Diverse Kir modulators act in close proximity to residues implicated in phosphoinositide binding, J. Physiol. 582 (2007) 953–965.
[73] F.M. Ashcroft, From molecule to malady, Nature 440 (2006) 440–447.
[74] Y. Kwon, T. Hofmann, C. Montell, Integration of phosphoinositide- and calmodulin-mediated regulation of TRPC6, Mol. Cell 23 (2007) 491–503.